Binary Evolution and its Applications

Zhanwen HAN

Yunnan Observatories of the CAS

Collaborators:

X. Chen, L. Li, F. Zhang, B. Wang, X. Meng, D. Jiang, H. Ge, Y. Han, H. Chen, Z. Liu, J. Liu, S. Yu

R. Webbink, Ph. Podsiadlowski, A. Lynas-Gray, L. Yungelson, M. Gilfanov, T.E. Wood, G. Stephan, ……

Outline

- Binary evolution
- Binary-related objects
- Evolutionary population synthesis
- Future perspectives

Outline

- Binary evolution
- Binary-related objects
- Evolutionary population synthesis
- Future perspectives

Stellar evolution

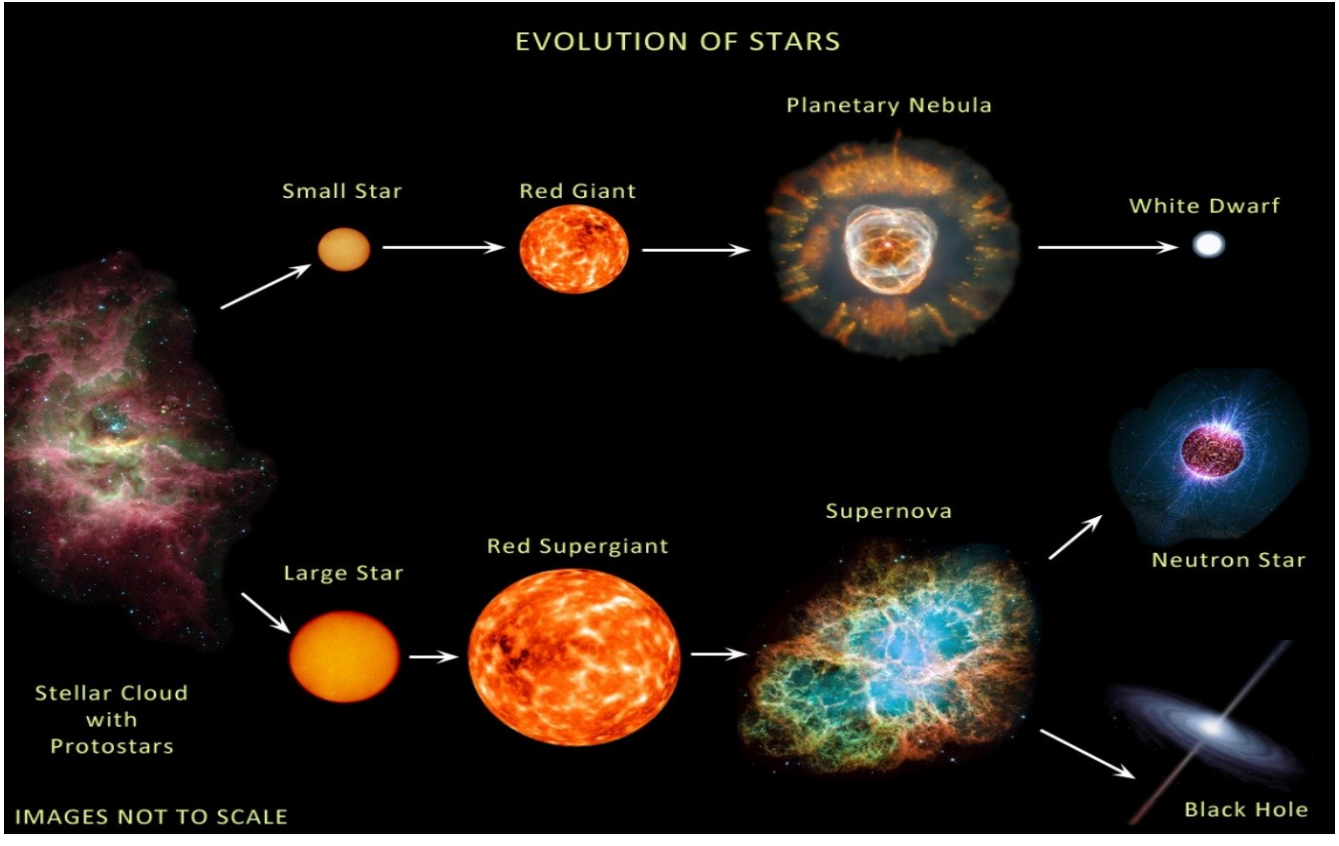

Half of the stars are in binaries

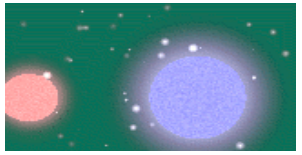

50% in binaries

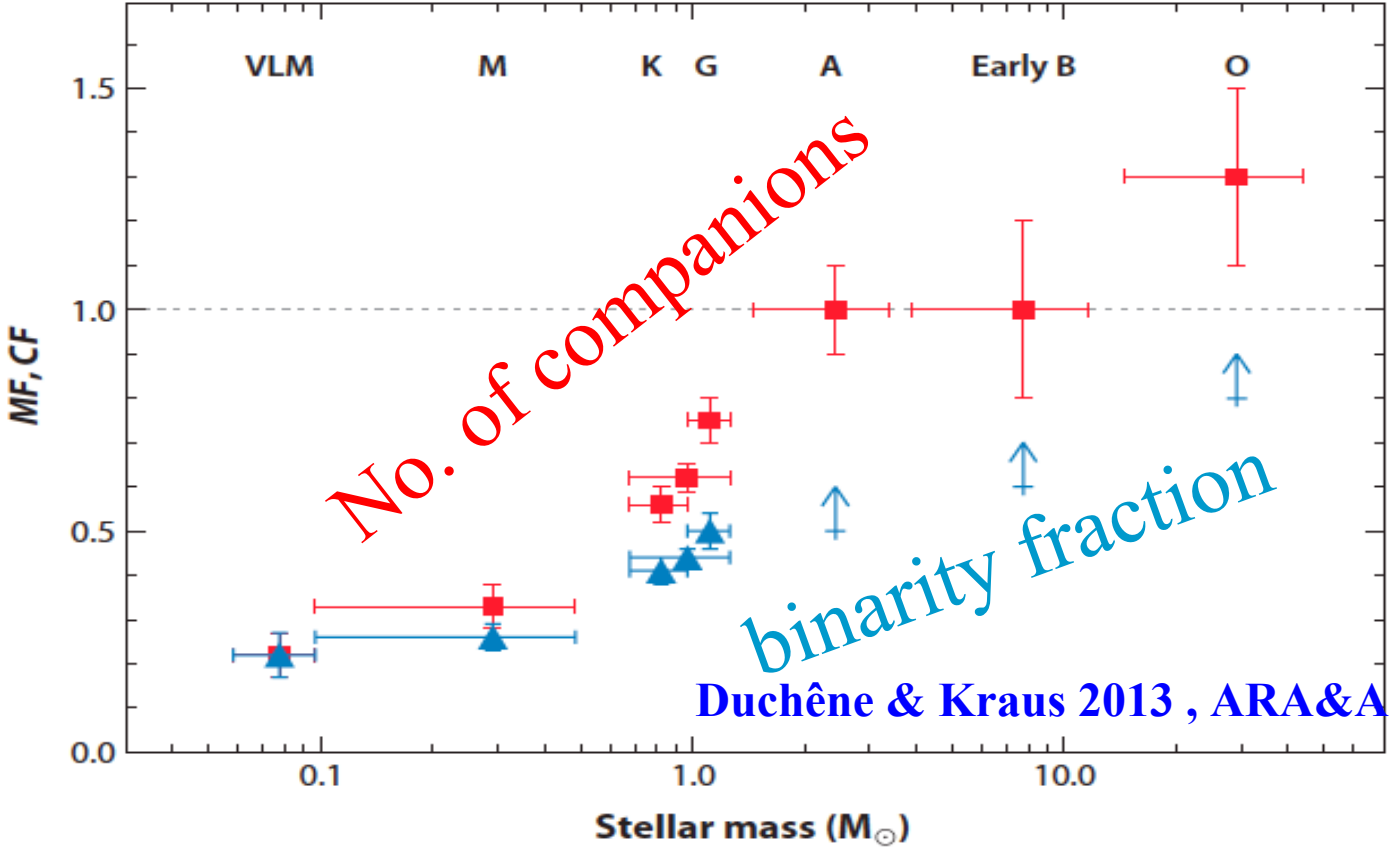

Duchêne & Kraus 2013 , ARA&A

Binary interaction dominates the evolution of massive stars

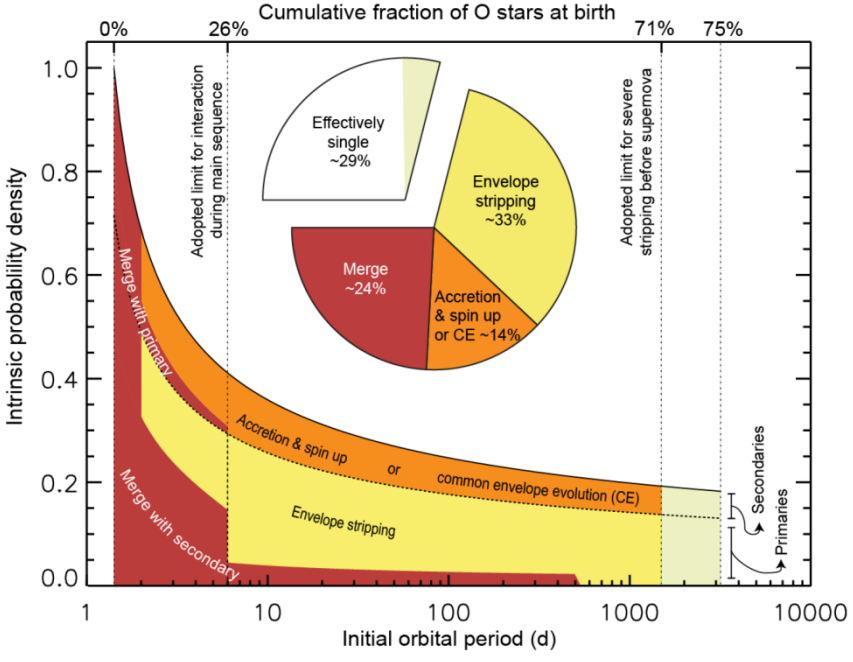

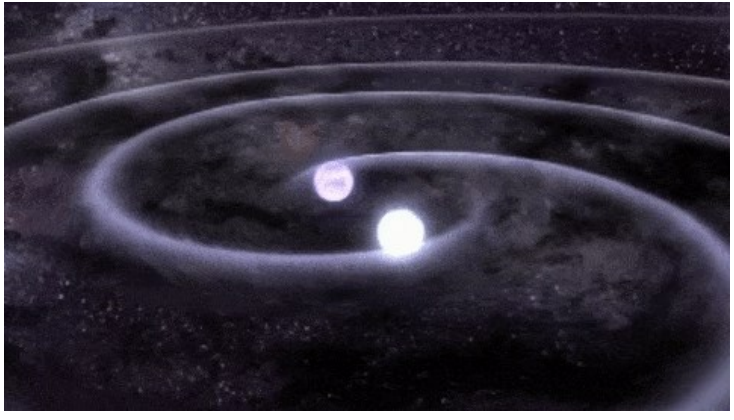

Sana et al 2012 Sci

Binary Evolution

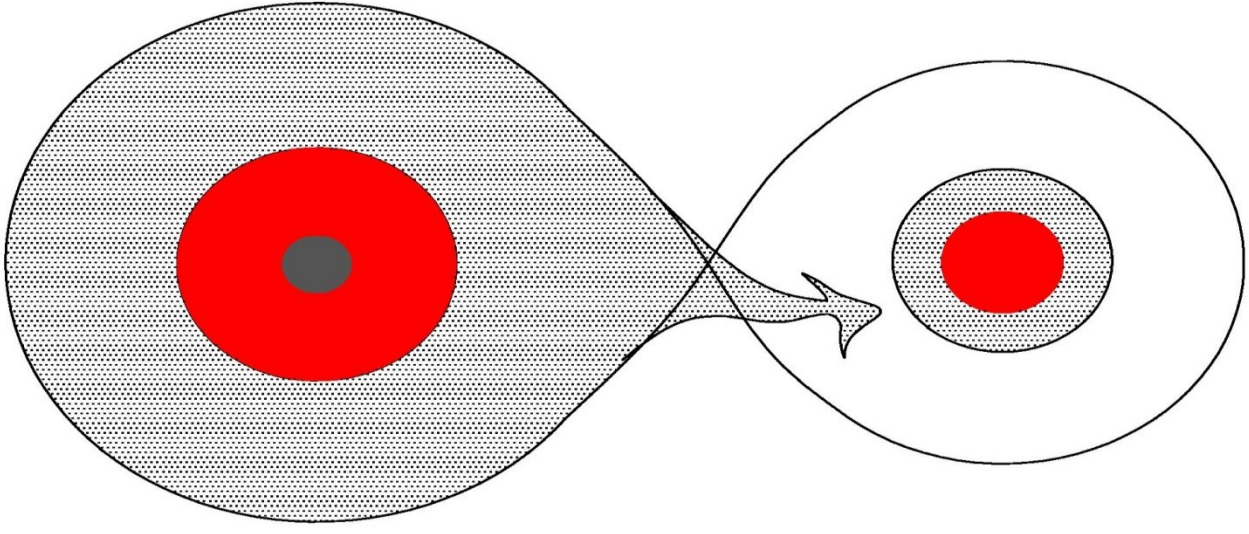

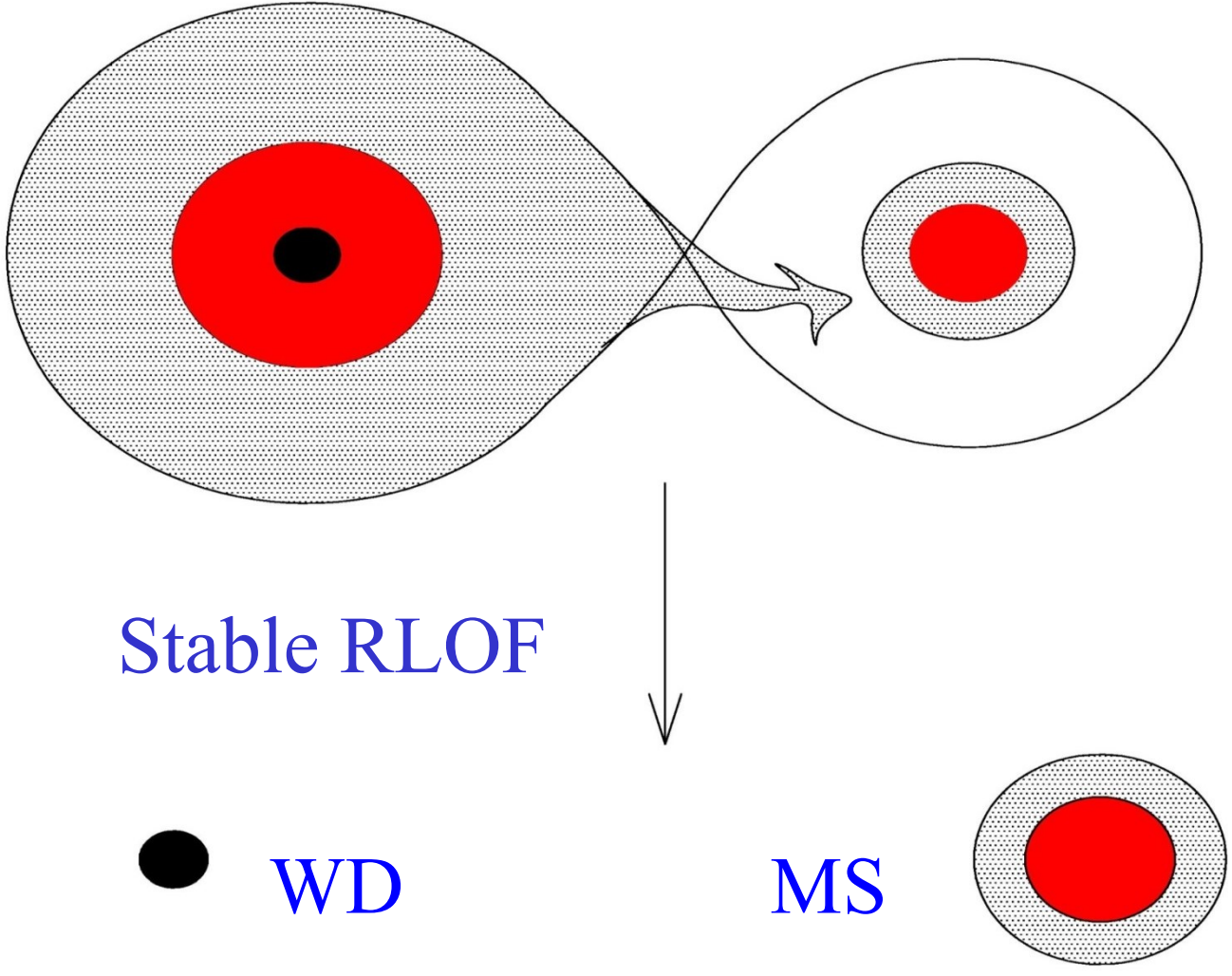
Stable RLOF
WD
MS

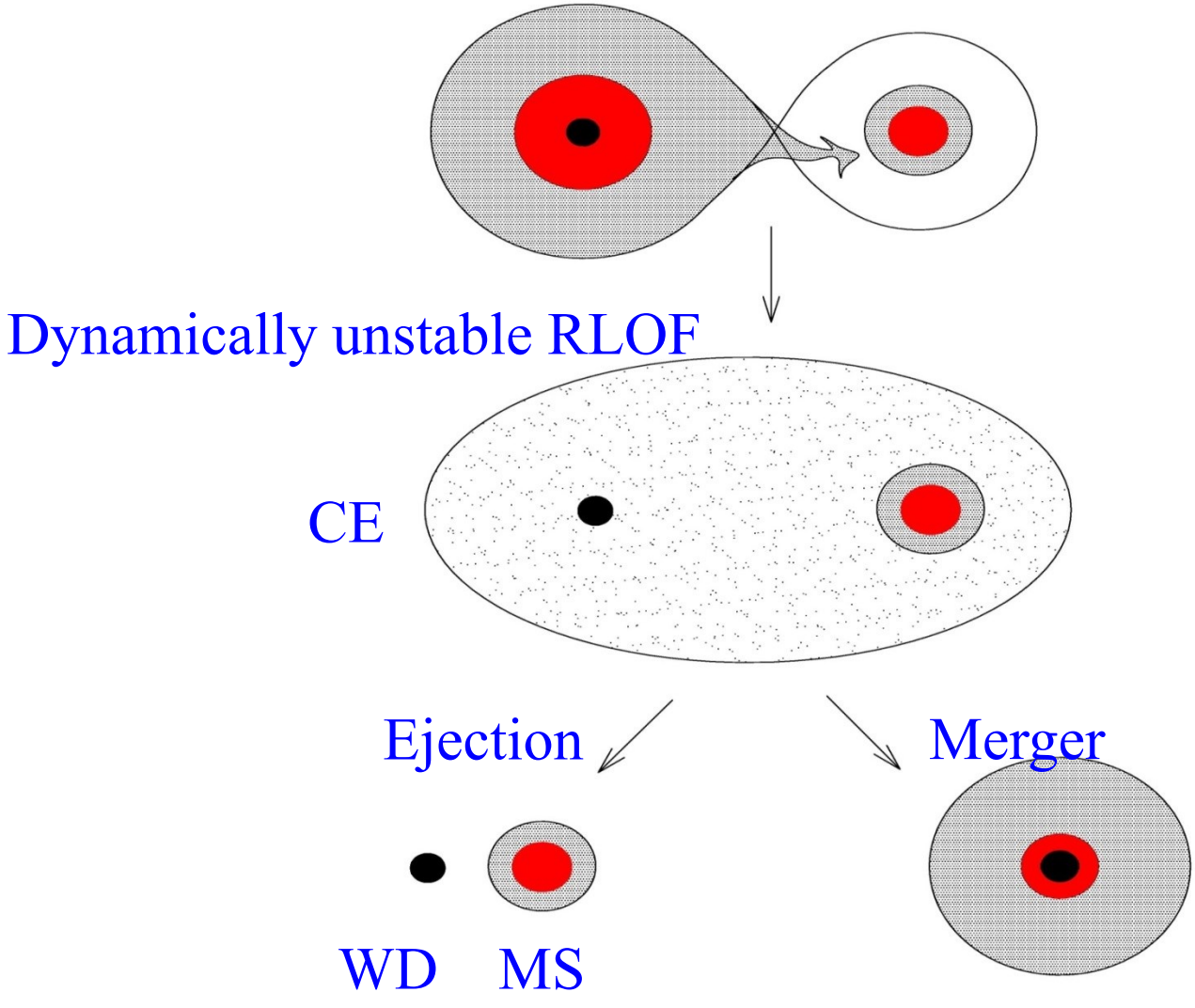
Dynamically unstable RLOF
CE
Ejection
Merger
WD
MS

Binary Evolution Flow Chart

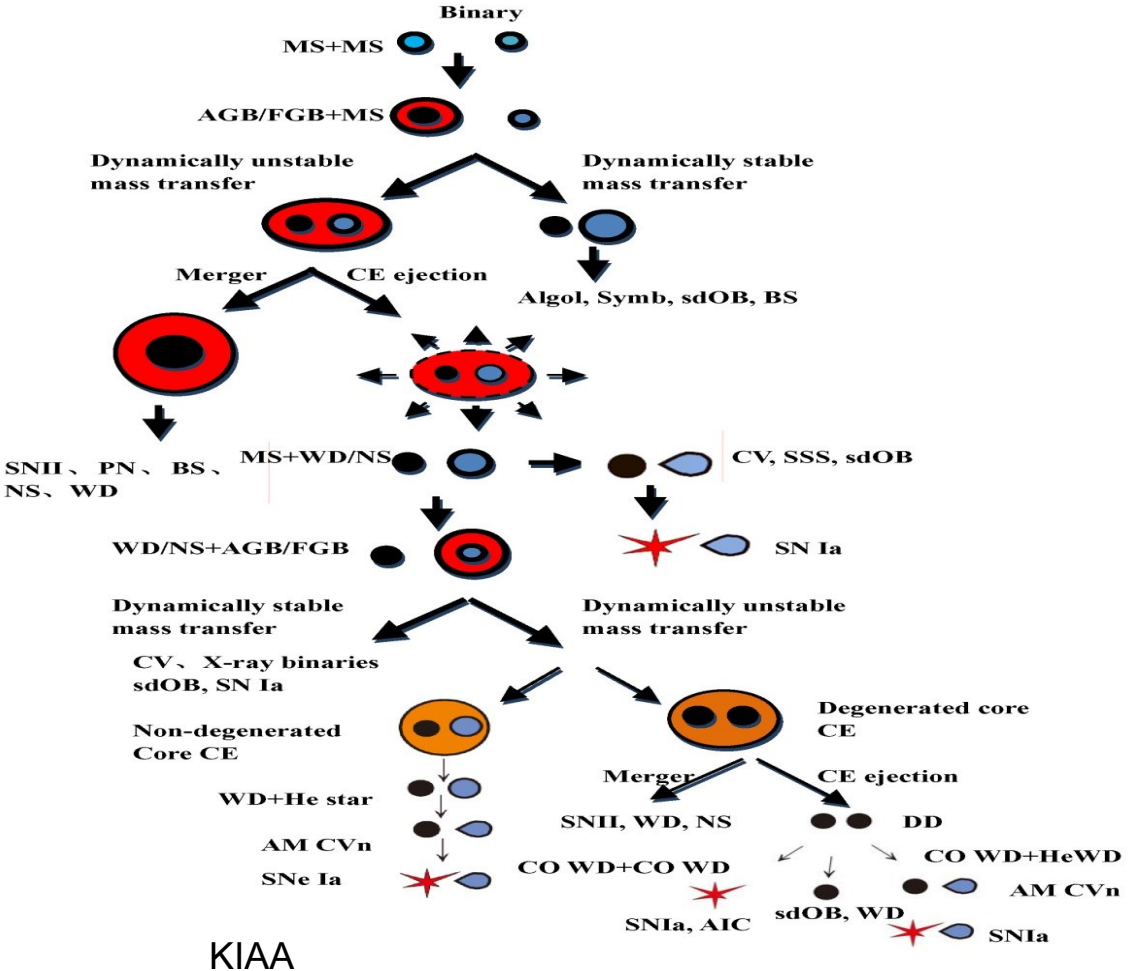

Binary evolution produces extotic objects

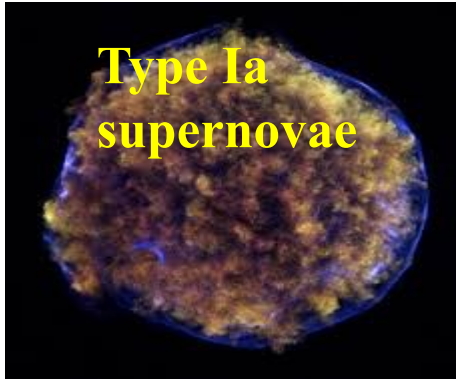

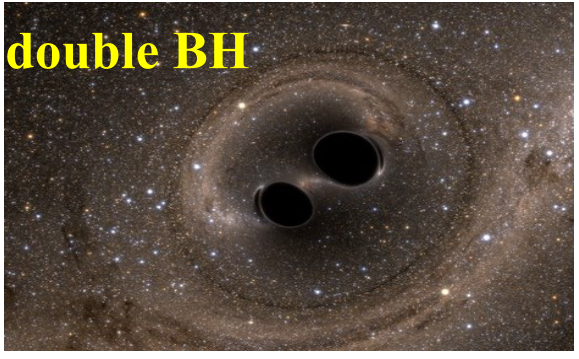

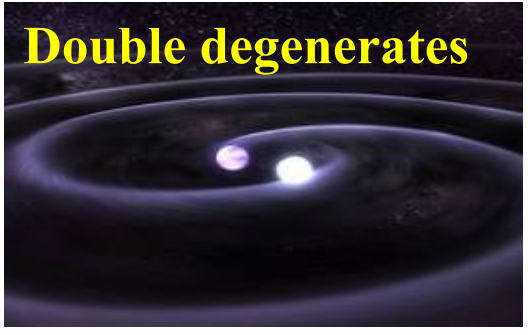

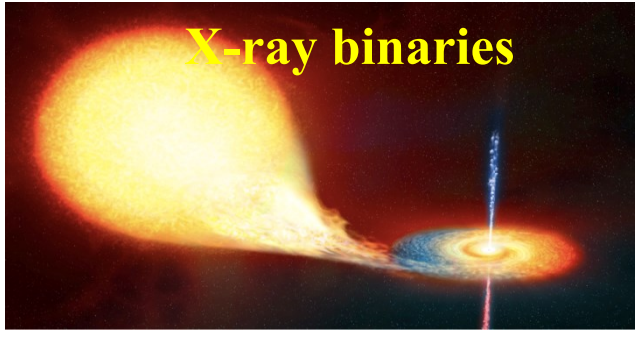

Basic problems:

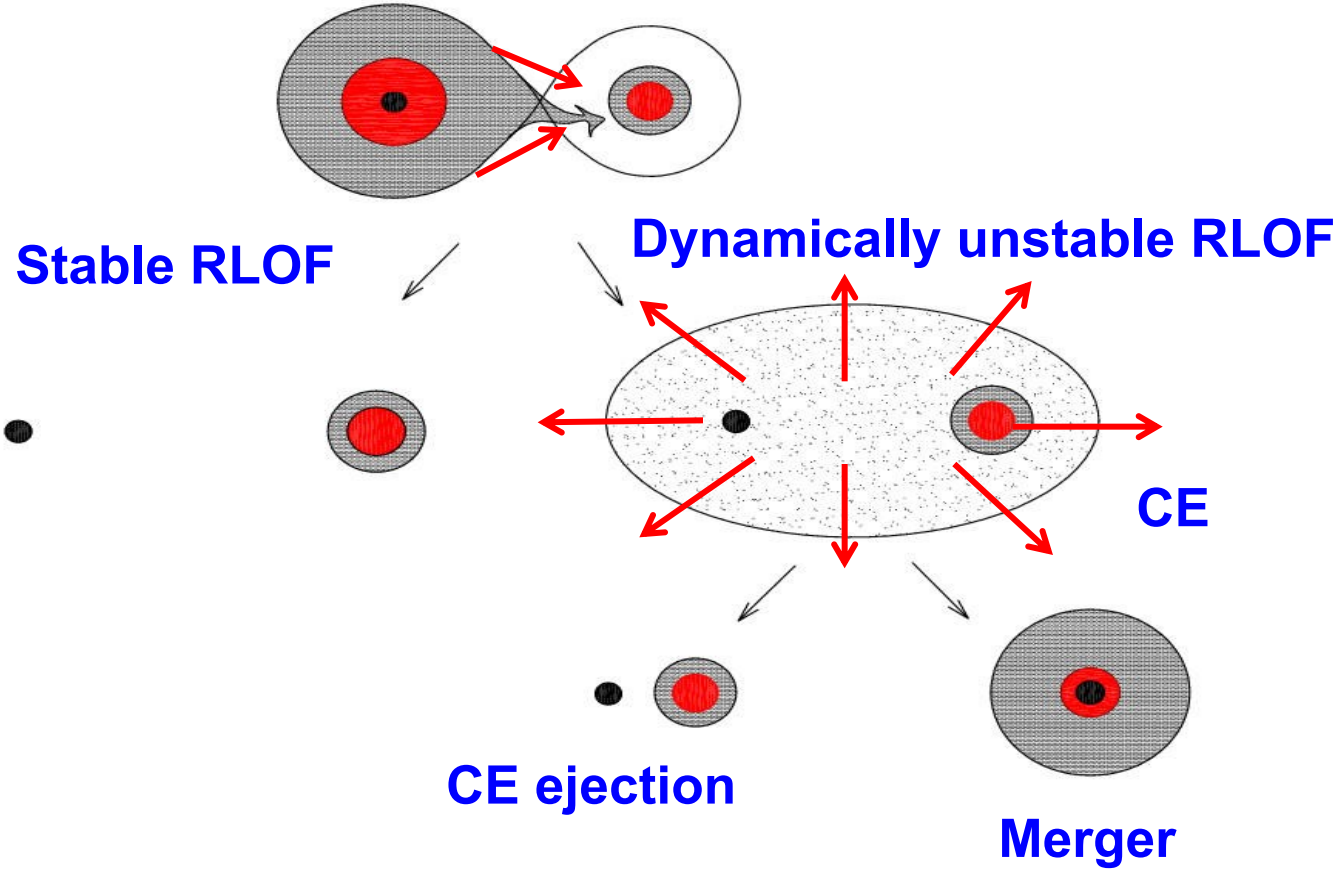

Basic problems:

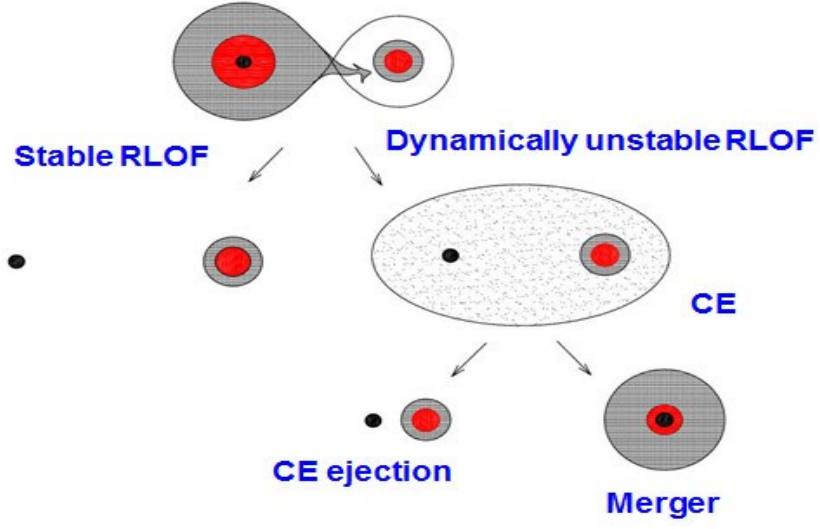

- mass transfer stability?
- CE evolution?

RLOF Stabilility criterion models

- Polytropic model
  (Hjellming+ 1987, Webbink 1988)

- detailed binary evolution calculation model (Pavlovskii+ 2015, 2017)

- Adiabatic mass loss model
  (Ge+ 2010, 2015)

Mass transfer in Binaries

Critical equipotential surface

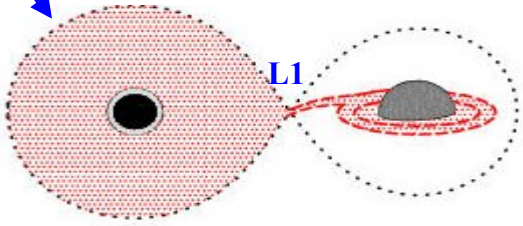

loser M_1 accretor M_2

Roche lobe radius:

$$\frac{R_{L1}}{a} = \frac{0.49q^{2/3}}{0.6q^{2/3} + \ln(1+q^{1/3})}$$

$q=M_1/M_2$ Eggleton, 1983, ApJ

Response of the loser **VS** **Response of the Roche lobe**

$$\zeta_{th} = \frac{\partial \ln R_1}{\partial \ln M_1}\Big|_{th} \qquad \zeta_{ad} = \frac{\partial \ln R_1}{\partial \ln M_1}\Big|_{ad} \qquad \zeta_L = \frac{\partial \ln R_L}{\partial \ln M_1}\Big|_{RLOF}$$

$(\zeta_{ad}, \zeta_{th}) > \zeta_L$ Nuclear Timescale MT（driven by nuclear burning）

$\zeta_{ad} > \zeta_L > \zeta_{th}$ Thermal timescale MT（driven by recovery of thermal equilibrium）

$\zeta_L > \zeta_{ad}$ Dynamical timescale MT（constrained by hydrostatic equilibrium only）

- **Stellar Structure Equations**

$$\frac{\mathrm{d}\ln P}{\mathrm{d}m} = -\frac{Gm}{4\pi r^4}$$

hydrostatic equilibrium

$$\frac{\mathrm{d}r^2}{\mathrm{d}m} = \frac{1}{2\pi r\rho},$$

Mass continuity

$$\frac{\mathrm{d}\ln T}{\mathrm{d}m} = \frac{\mathrm{d}\ln P}{\mathrm{d}m}\nabla$$

$$\frac{\mathrm{d}L}{\mathrm{d}m} = \epsilon - \epsilon_\nu - C_\mathrm{P}T\left(\frac{\mathrm{d}\ln T}{\mathrm{d}t} - \nabla_\mathrm{a}\frac{\mathrm{d}\ln P}{\mathrm{d}t}\right)$$

Energy equations

- **Equations in the adiabatic mass loss model**

$$\frac{\mathrm{d}\ln P}{\mathrm{d}m} = -\frac{Gm}{4\pi r^4 P},$$

$$\frac{\mathrm{d}r^2}{\mathrm{d}m} = \frac{1}{2\pi r\rho},$$

Adiabatic assumption

$$s' \equiv ds/dt = s(m) - s_0(m) = 0,$$

$$X' \equiv dX/dt = X(m) - X_0(m) = 0.$$

$$\zeta_\mathrm{ad} = \frac{\partial \ln R_1}{\partial \ln M_1}\Big|_\mathrm{ad}$$

$$\zeta_\mathrm{L} > \zeta_\mathrm{ad}$$

Ge+, 2010

Dynamical timescale MT

Response of a 1.00$M_\odot$ star to adiabatic mass loss

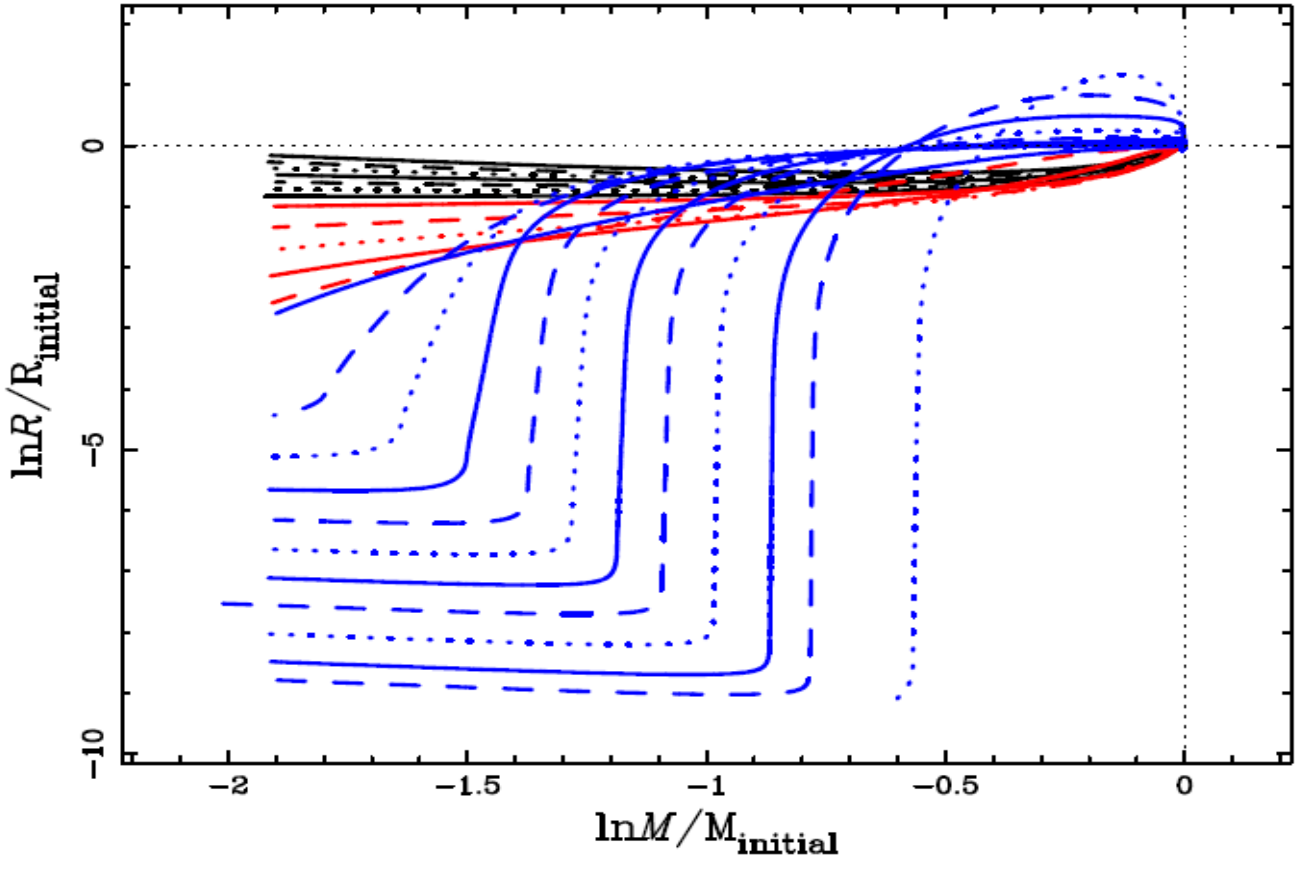

q_c for FGB or AGB donors

Ge+, 2015
Ge+, in prep

Before: qc~1
CE only

Now: from 1.4-5
Both CE and RL(

Non-conservative

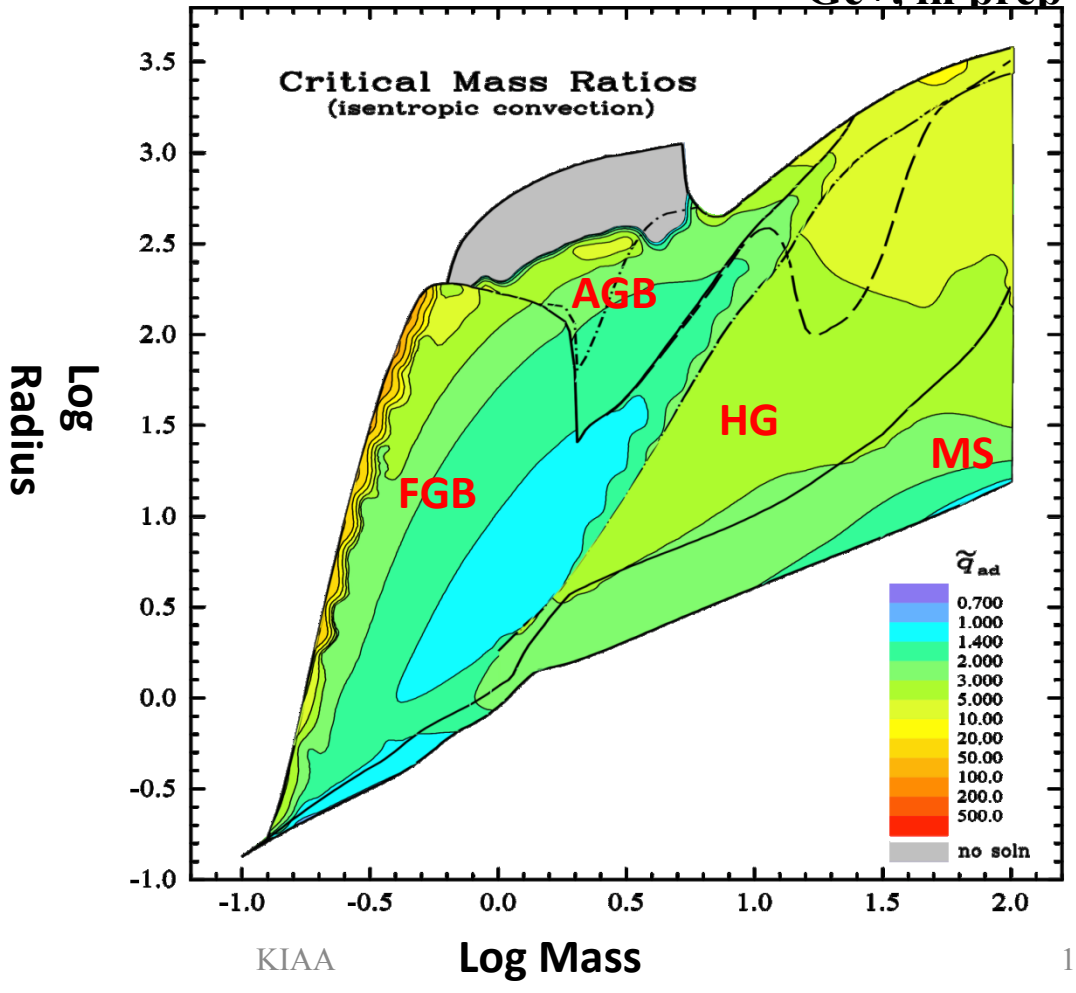

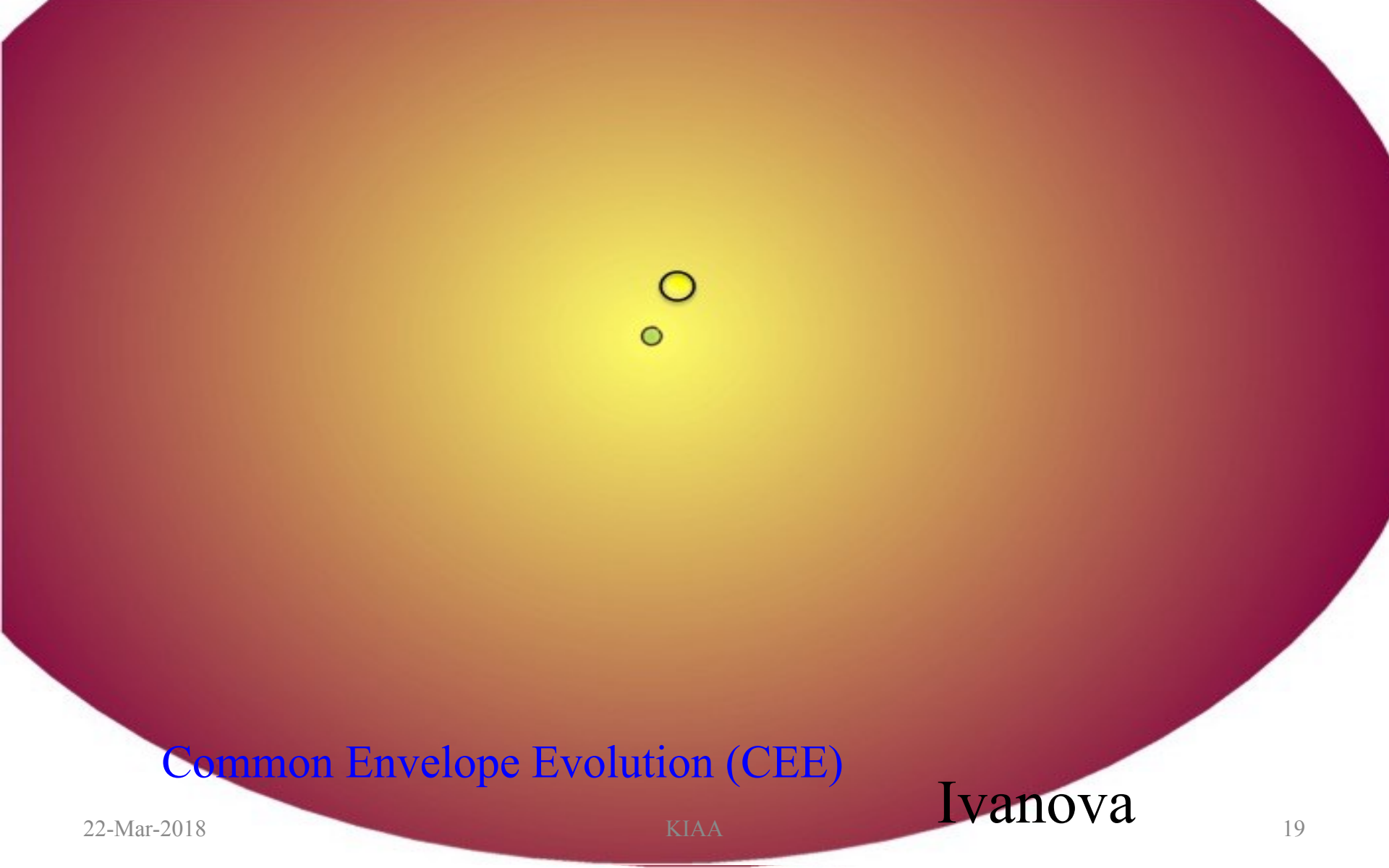

Common Envelope Evolution (CEE)

Ivanova

Common Envelope Evolution

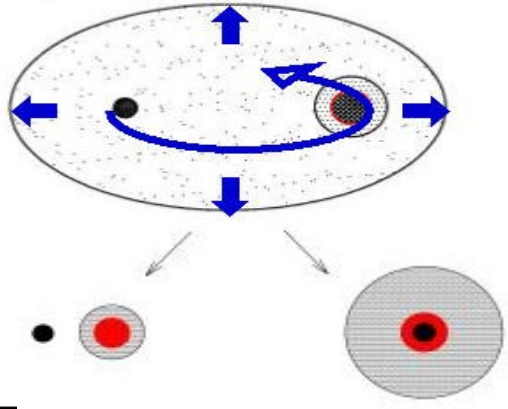

SPH simulations are difficult !

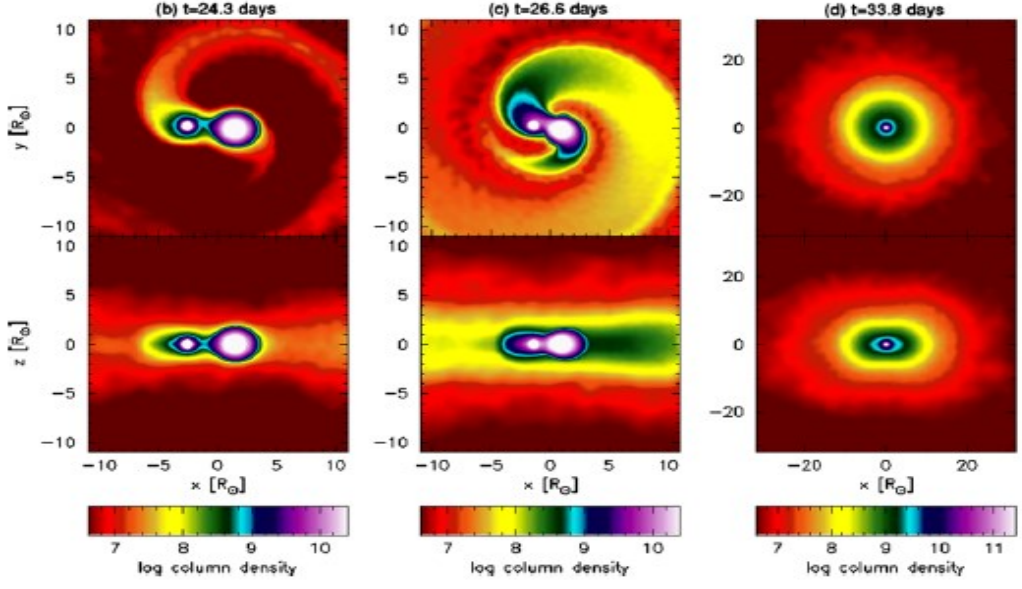

merger

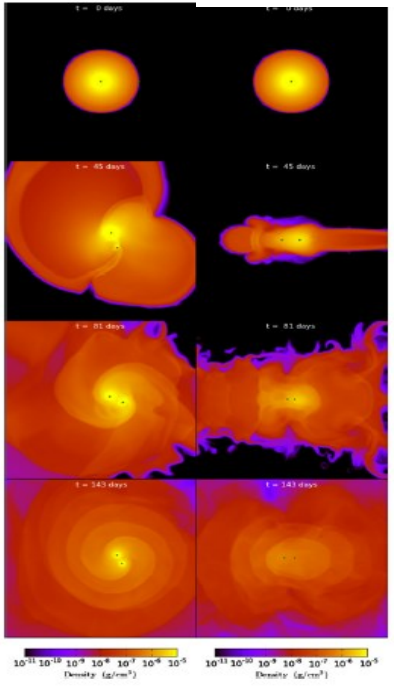

ejection

Common Envelope Evolution

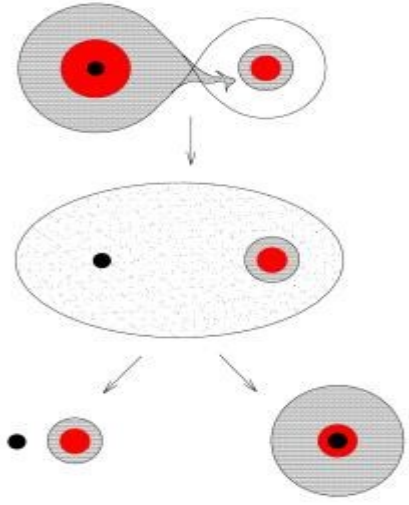

Parameterized !

$$\Delta E_{\rm orb} \simeq \frac{GM_{\rm c}M_2}{2a_{\rm f}} - \frac{G(M_{\rm c}+M_{\rm e})M_2}{2a_{\rm i}}$$

$$\alpha_{\rm CE}\Delta E_{\rm orb} \geq E_{\rm bind} = E_{\rm gr} - \alpha_{\rm th}E_{\rm th}$$

$E_{\rm gr}$ and $E_{\rm th}$ are integrated for the envelope

Outline

- Binary evolution
- Binary-related objects
- Evolutionary population synthesis
- Future perspectives

ELM WDs : Extremely low-mass white dwarfs

Brown+, 2010, ApJ

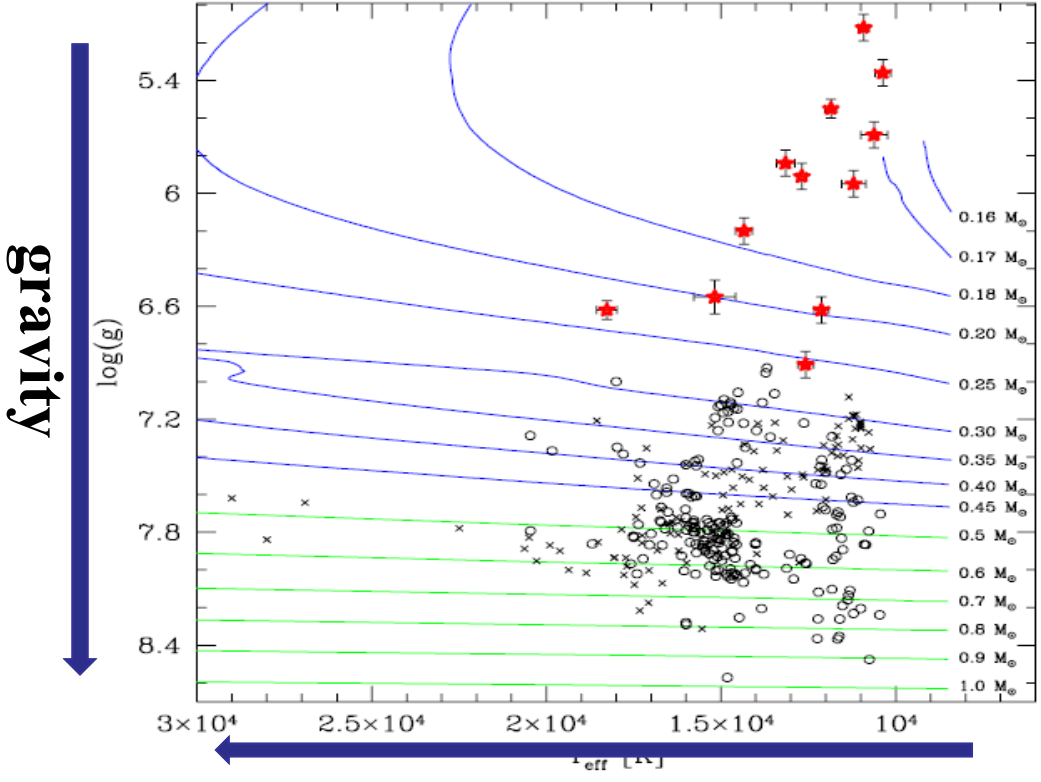

5< log *g* < 7

8000 K < *T*eff <22000 K

***M* < 0.25-0.3 $M_\odot$**

Observations

I.The ELM Survey (Brown, Kilic et al. 2009--, SAO, 6.5 m MMT)

- **88 ELM WDs, of which 76 being in binaries**
- **Half of the observed binaries will merge in less than 6Gyr**

Brown et al. 2016, ApJ

Period distribution

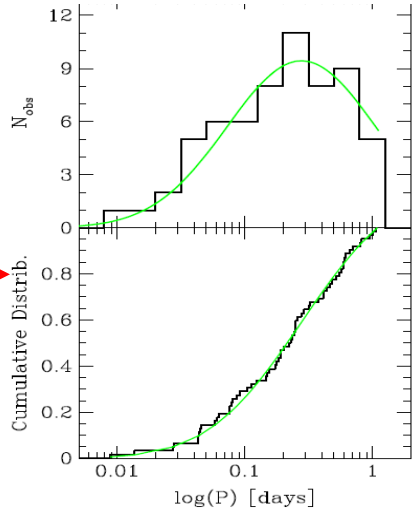

II. The WASP Project Maxted et al.

- **The 1st sample: 1SWASP J024743.37-251549.2 (2011 MNRAS)**
- **Multiple-period pulsations (2013, Nature)**
- **17 EL CVn-type binaries (2014, MNRAS)**

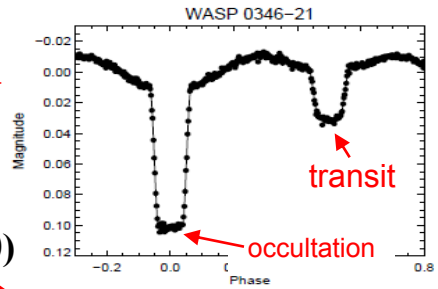

III.Kepler

- **The first two: KOI-74, KOI-81 (van Kerkwijk+,2010)**
- **7 objects in total (Rappaport+.2015. Guo+. 2017)**

Light Curve

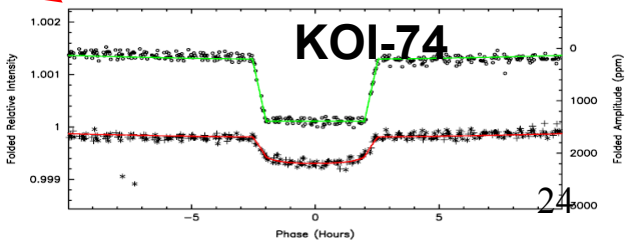

VI. ELM in MSPs (>10)

Istrate+, 2014, 2016

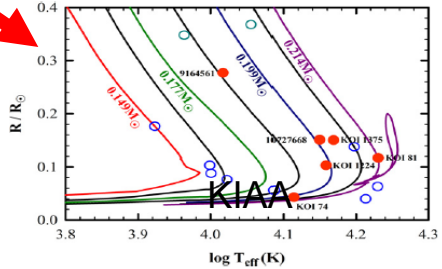

The pre-ELM WD instability strip

Diven by He++,He+, H+

1SWASP J024743.37-251549.2

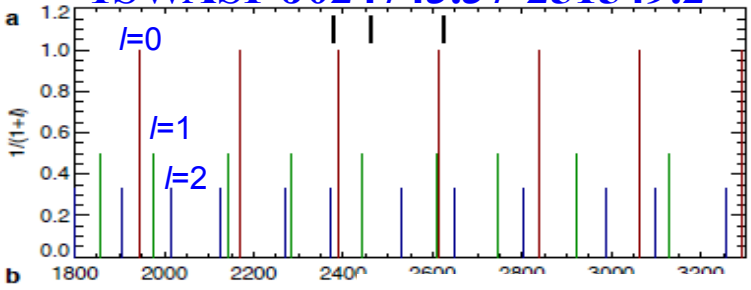

Maxted+, 2013, Nature

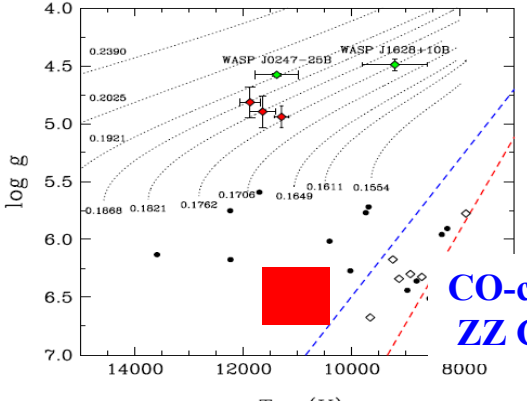

Corsico+, 2016, A&A

CO-core
ZZ Ceti stars

KIC 9164561

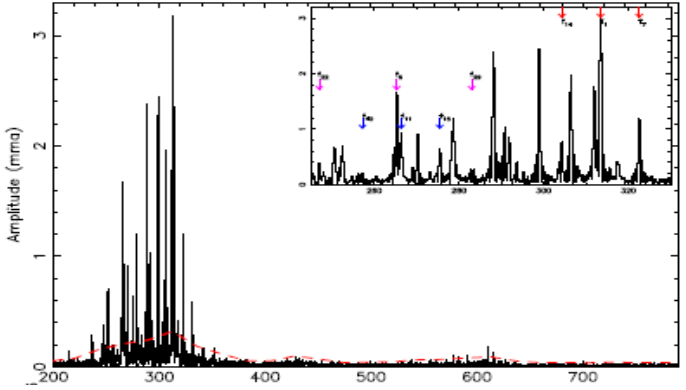

Zhang,X.+, 2016, ApJ

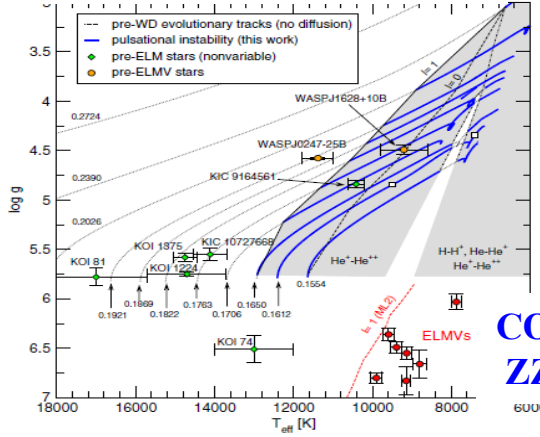

CO-core
ZZ Ceti stars

Gianninas+, 2016, ApJ

Formation of extremely low-mass WDs

Binary Evolution

common envelope ejection

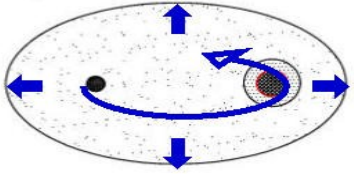

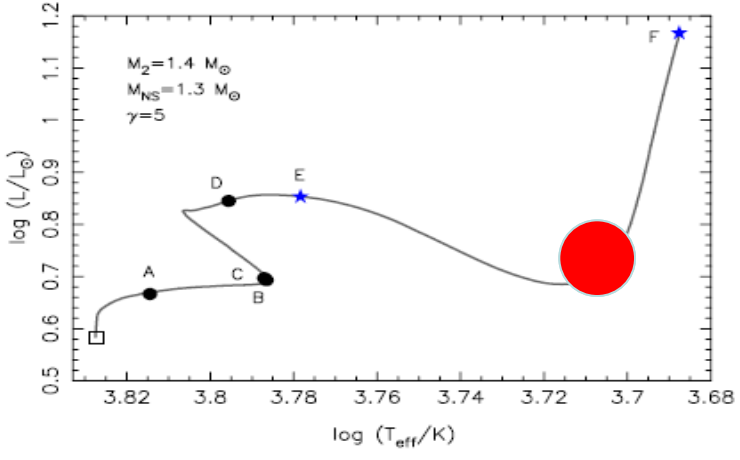

stable mass transfer

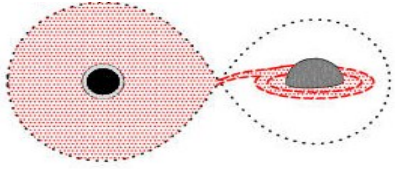

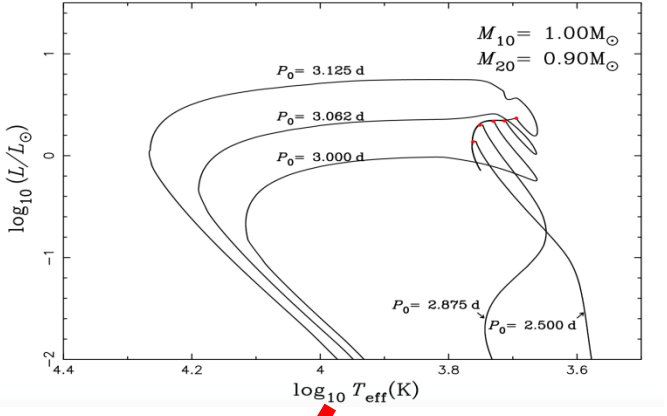

Beyond but very close to the bifurcation period

ELM WD mass VS orbital period

(for 62 double degenerates)

Z. Li,+

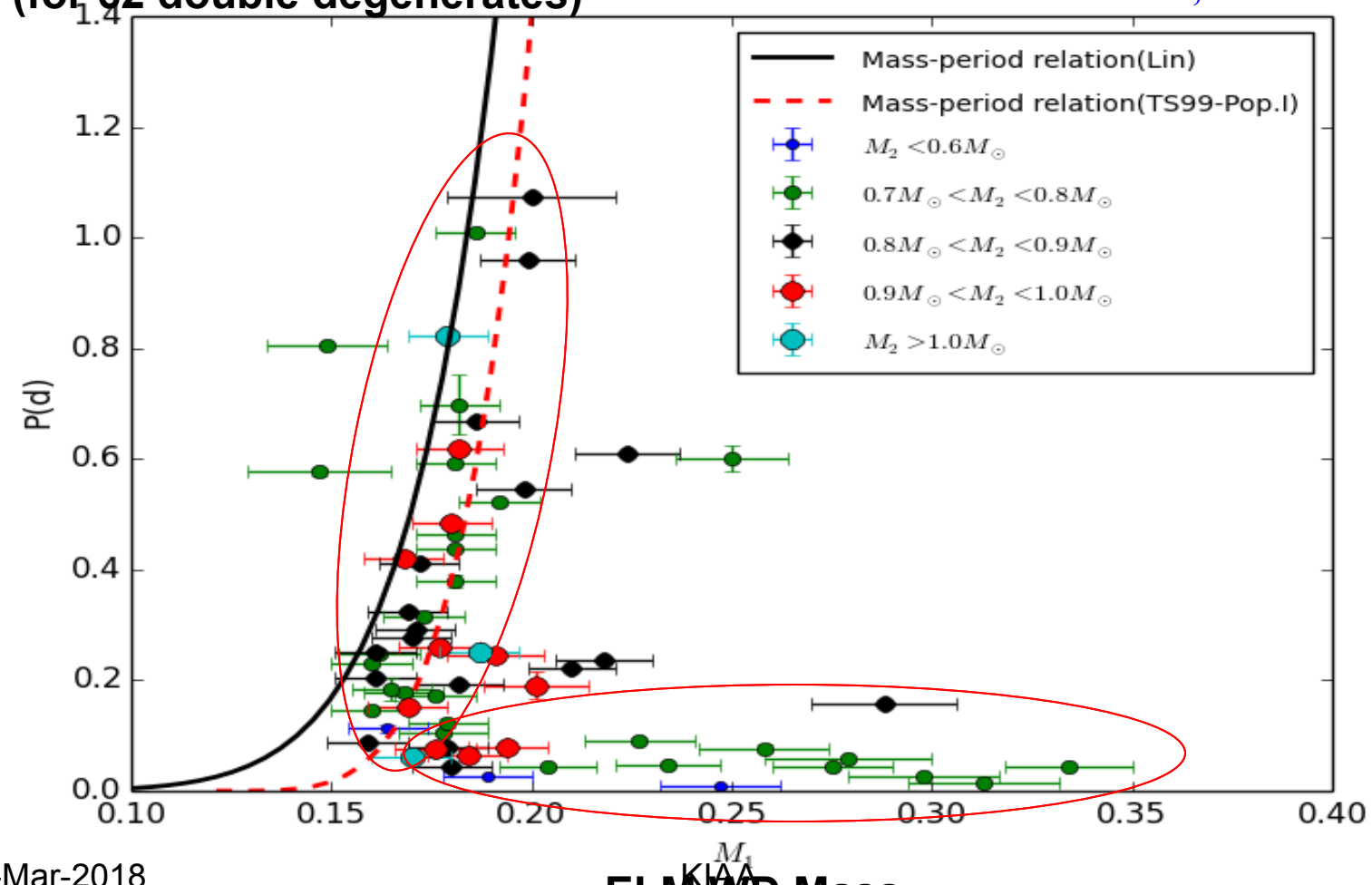

ELM WD Mass

EL CVn-type Binaries

A/F dwarf star + proto-He WD

Maxted et al. 2014 , MNRAS

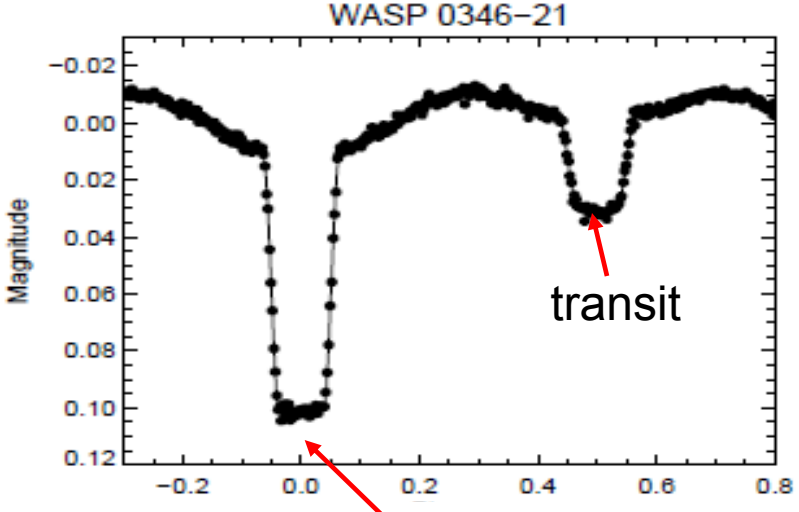

The hot small companion has been occulted.

The hot small companion:

- **extremely low mass （~0.2Msun)**
- **in an evolutionary phase that should be rare observed**

17 EL CVn-type binaries have been found by Maxted et al. from the WASP observations.

The formation of EL CVn-type binaries

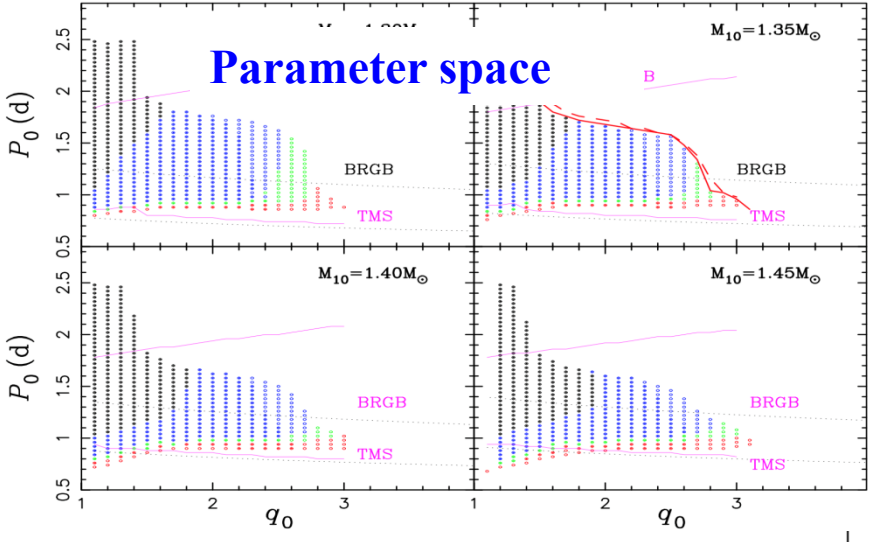

Chen X. et al 2017 , MNRAS, 464, 187

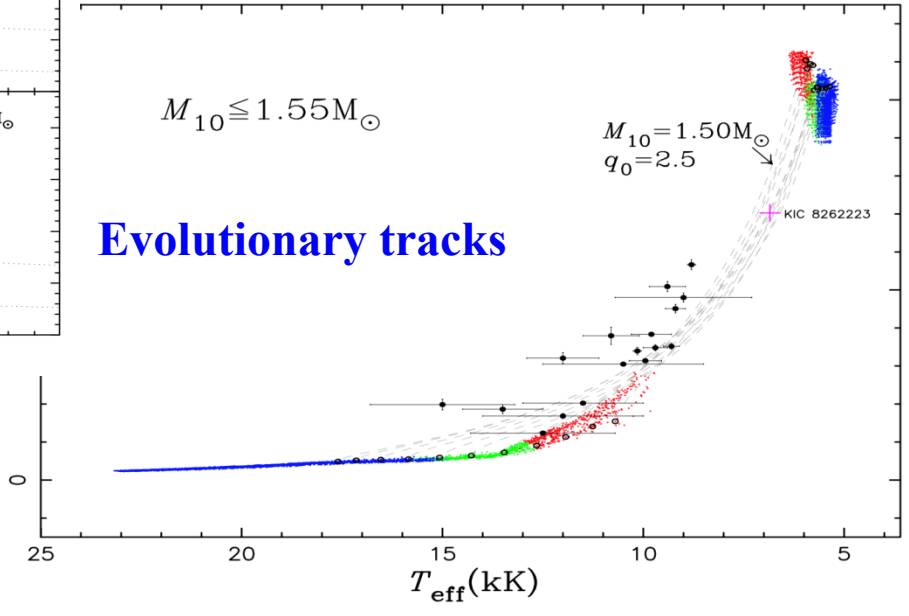

Predictions:

- **More EL CVn-type binaries will be found in the Galaxy.**
- **The are more likely in the thin disk.**

(The peak mass for the progenitors is in ~1.1-1.3Msun)

Monthly Notices
of the
ROYAL ASTRONOMICAL SOCIETY

MNRAS **475,** 2560–2590 (2018)
Advance Access publication 2018 January 31

doi:10.1093/mnras/stx3291

Discovery of 36 eclipsing EL CVn binaries found by the Palomar Transient Factory

J. van Roestel,[1]★ T. Kupfer,[2] R. Ruiz-Carmona,[1] P. J. Groot,[1] T. A. Prince,[2] K. Burdge,[2] R. Laher,[3] D. L. Shupe[4] and E. Bellm[5]

Introduction for the model

In the canonical formation channel of EL CVn binaries (e.g. Chen et al. 2017), two main-sequence stars of similar mass are born at a short orbital period of a few days. The more massive star evolves faster and increases in radius. Before it ascends the red giant branch (RGB), it fills its Roche lobe and starts stable mass transfer to the lower-mass secondary star. This process continues until almost the complete outer envelope is transferred (identified as R CMa-type binaries; e.g. Lee et al. 2016). The remnant of the initially more massive star has become a pre-WD with a helium core and a thick hydrogen envelope (≈0.01–0.04 $M_\odot$; see Istrate et al. 2016a; Chen et al. 2017). The accretor has become a rejuvenated main-sequence

Predictions of the model

Using stellar evolution and population synthesis codes, Chen et al. (2017) predict a space density of 4–10 × 10^{-6} pc^{-3} for EL CVn binaries (including non-eclipsing ones) with orbital periods less than 2.2 d. In addition, they predicted that EL CVn binaries should mainly be found in young stellar populations, and therefore should be more abundant in the thin disc. We use the Galaxy model based

Space density : in line with Chen et al.

systems contain small pre-He-WDs (<0.05 $M_\odot$) and, as a consequence, their light curves feature shallow eclipses only detectable from space. The fact that 10 EL CVn-like systems are found in the Kepler field suggests that there should be many more in our Galaxy, in line with an estimate of the local space density from stellar evolution and population synthesis models, 4–10 × 10^{-6} pc^{-3} (Chen et al. 2017).

Transient Factory (PTF), combined with Sloan Digital Sky Survey (SDSS), Panoramic Survey Telescope and Rapid

ambiguous cases are from the thin disc, this probability drops well

of EL CVn systems. We do find tentative results that EL CVn systems occur more often in the thin disc, as was predicted by Chen et al. (2017). We also find that the space density is at the lower bound, or even below the prediction of 4–10 × 10^{-6} pc^{-3}. To prop-

elow 1 per cent. This indicates that our model is unlikely to be orrect, and confirms that EL CVn systems are more abundant in he thin disc compared to the average stellar population, as was lready suggested by Chen et al. (2017).

Position : as suggested/predicted by Chen et al.

KIC 8262223 Z. Guo, D. Gies, R. Mstson et al (2017, ApJ)

KIC 8262223: A Post-mass Transfer Eclipsing Binary Consisting of a Delta Scuti Pulsator and a Helium White Dwarf Precursor

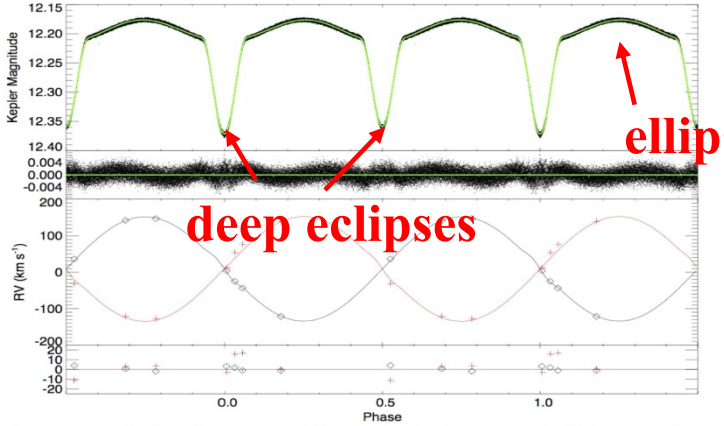

Figure 2. The upper and lower primary and the secondary star a ly. The measured RVs of the re overplotted, with the green li

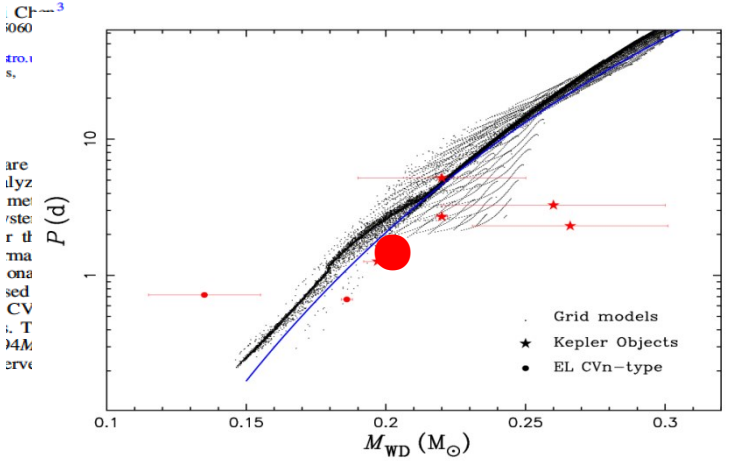

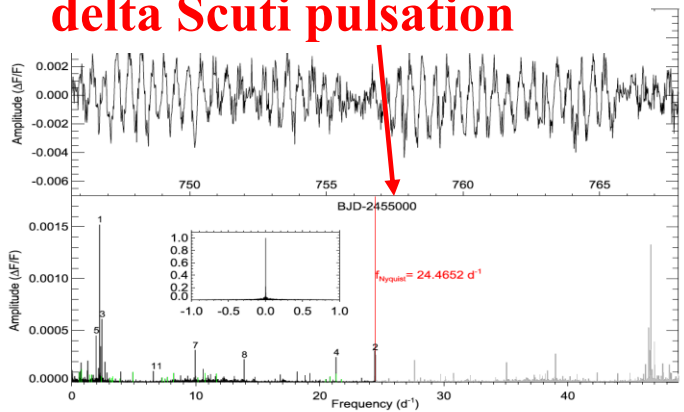

Figure 3. Time series of *Kepler* photometric data of oscillations with the binary light curve subtracted in the time domain (upper) and frequency domain (lower). Several of the strongest pulsation peaks have been labeled by their frequency numbers (Tables 3 and 4). The inset in the lower panel shows the spectral window. The Fourier spectrum in the super-Nyquist region is also shown, with the red vertical line indicating the Nyquist frequency $f_{Nyquist}$ = 24.4652 day^{-1} of *Kepler* long-cadence data. All pulsations in the super-Nyquist region (gray shaded) have lower amplitudes compared to their mirror reflections around the f_{Nquist}, indicating they are not real pulsation peaks, but are aliases.

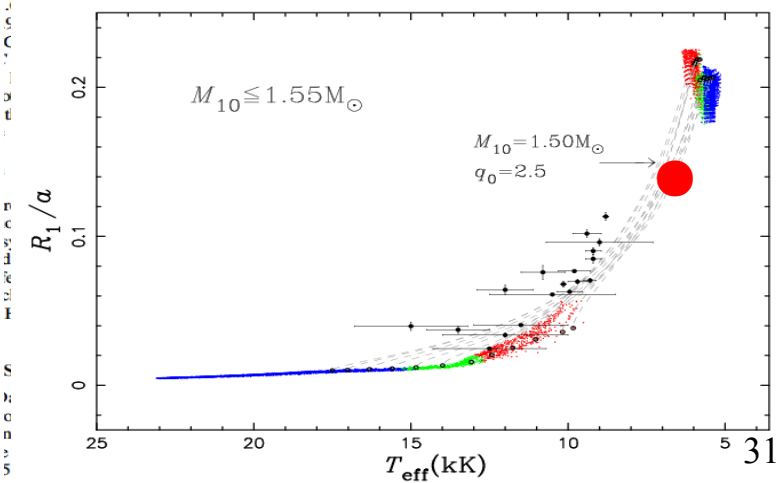

secondary (M = 0.2$M_\odot$, R = 1.15$R_\odot$) and a δ Scuti pulsating primary.

minutes, respectively. Please refer to Caldwell et al. (2016) for more information on the *Kepler* data. The aperture contamination factors (b) reported in the *Kepler* Input Catalog are lower

Eclipsing Binary Millisecond Pulsars

Discovered by Fermi

Two distinct populations

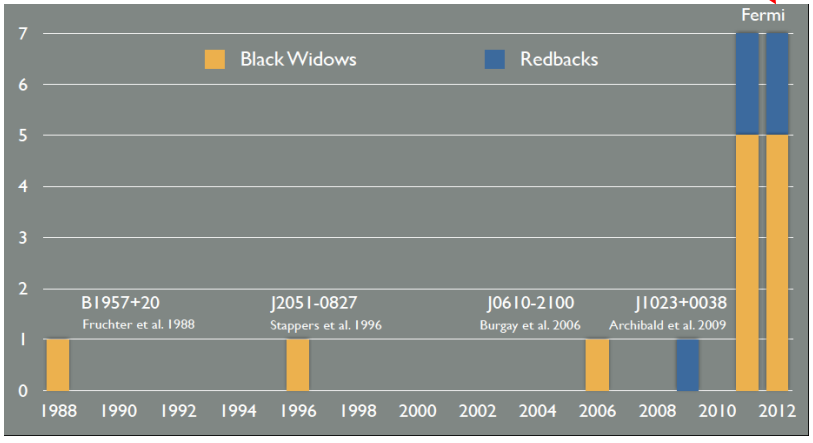

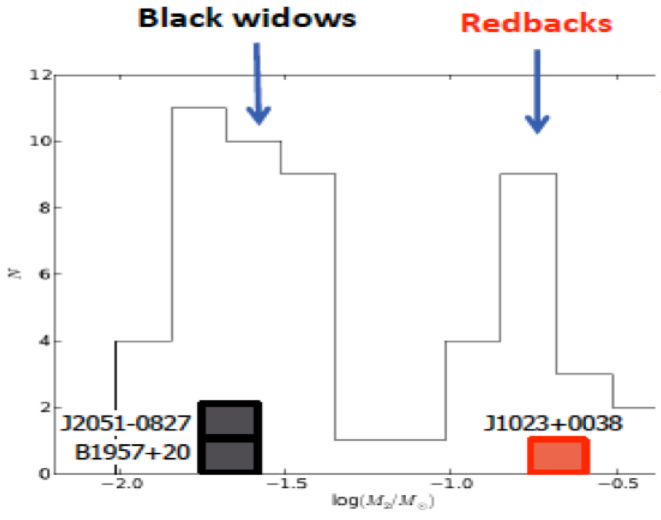

- **The masses of the companions are very low, then they should be small.** **How to produce the eclipses ?**

- **Both populations have orbital periods between 0.1 and 1.0 days, their companion masses differ by an order of magnitude.Why?**

Chen H., Chen X., Tauris, Han, 2013, ApJ, 775, 27

- **Pulsar irradiation and evaporation of the companions are crucial for the formation of eclipsing MSPs**

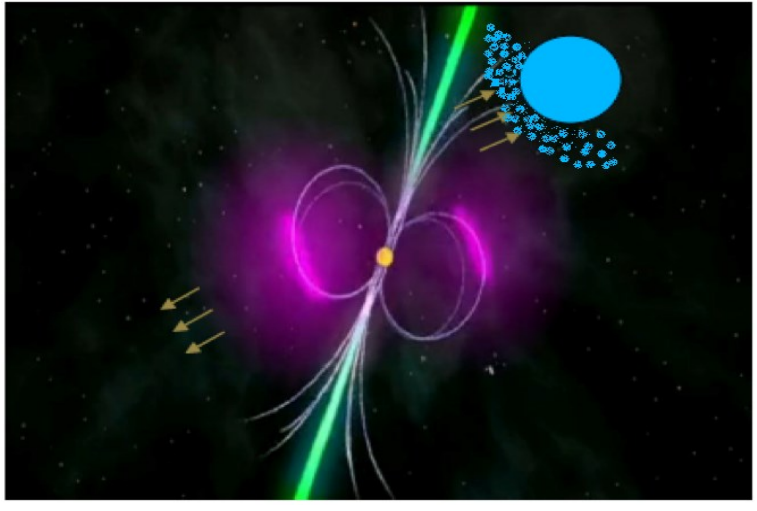

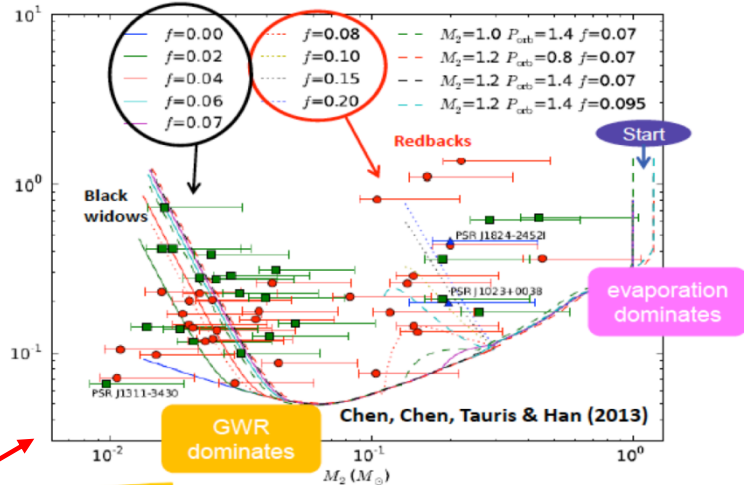

- **The determining factor for the producing the two populations is the efficiency of the irradiation process.**

widely accepted in this field

Dick Manchester

《Physics of neutron stars and Related objects》（2017, JApA, 38, 42）：

Millisecond Pulsars, their Evolution and Applications

R. N. Manchester
CSIRO Astronomy and Space Science, PO Box 76, Eppi
dick.manchester@csiro.au

28 September 2017

ABSTRACT
Millisecond pulsars
mal" pulsars, not
rates and high prob
with MSPs having

Another population of binary systems with very short orbital periods ($P_b < 1$ day) but somewhat larger companion masses, mostly between 0.1 and 0.3 $M_\odot$, can be identified on the $m_c - P_b$ plot. These are the other type of "spider" pulsar known as redbacks (Roberts 2013). The companion is a non-degenerate star that fills its Roche lobe and is losing mass, partly as a result of heating by the pulsar wind, resulting in extended and variable eclipses of the pulsar radio signal – see Chen et al. (2013) for a discussion of the formation processes of black-widow and redback eclipsing binaries. The

any globular cluster and, hence, an origin in a cluster is very unlikely. This showed that such systems could result from evolution of a binary system without the need to invoke exchange interactions; possible evolutionary paths are discussed by Chen et al. (2013). Since then, the *Fermi*-related

e MSPs nearly ideal probes of a wide
, they have been used to detect plan-
tational theories, to set limits on the
the Universe, and to establish pulsar-
ck timescales in long-term stability.
ary evolution, often suggesting exotic
retion-powered MSPs, and especially
MSP and a non-accreting radio MSP,
give important insight into the physics of accretion on to highly magnetised neutron stars.

Key words: pulsars: general—stars: evolution—gravitation

SNe Ia

Thermonuclear Explosions of CO WDs at ~1.4Msun

carbon ignition under degenerate conditions ⟶
thermonuclear runaway ⟶
incineration and complete destruction of the star

10^{51}ergs

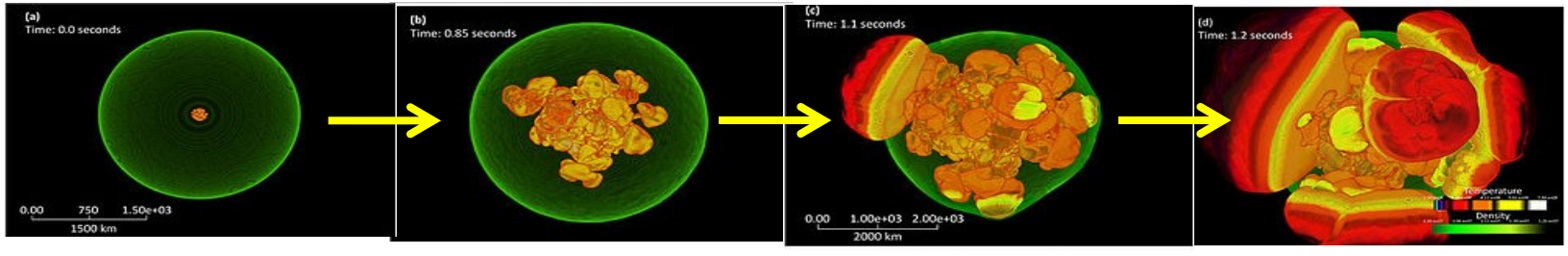

Phillips Relation

(Phillips, 1993): empirical

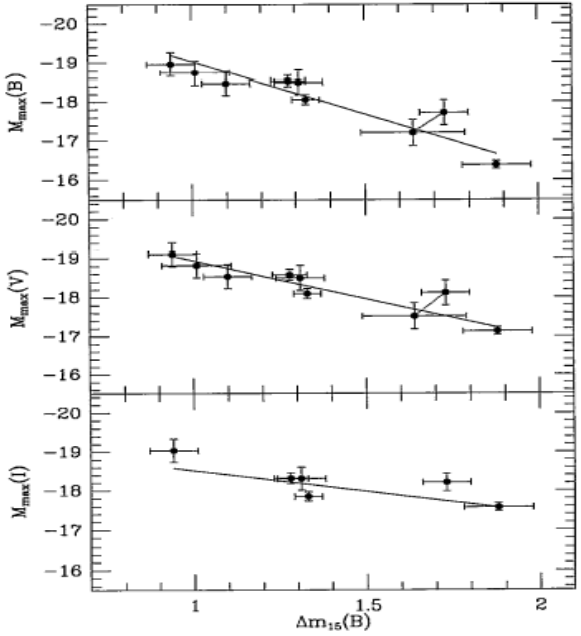

FIG. 1.—Decline rate–peak luminosity relation for the nine best-observed SN Ia's. Absolute magnitudes in B, V, and I are plotted vs. $\Delta m_{15}(B)$, which measures the amount in magnitudes that the B light curve drops during the first 15 days following maximum.

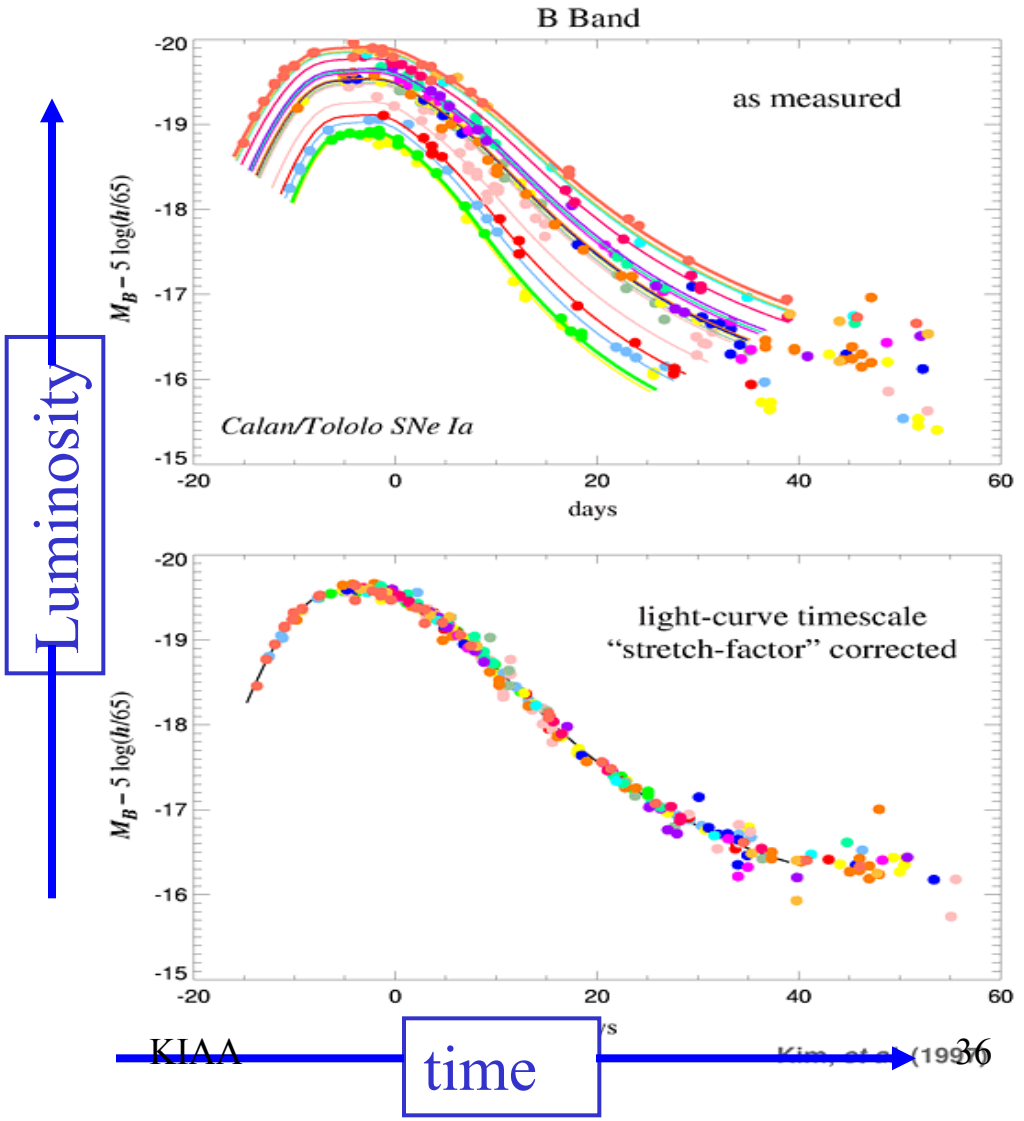

SNe Ia as distance indicators

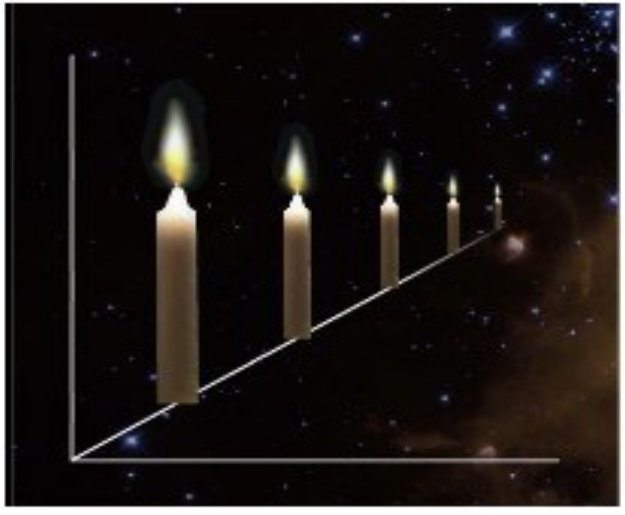

Accretion of WDs

The mass of CO WDs at birth is less than ~1.1Msun .
(~0.6Msun)

Accretion is necessary for final explosions .

How to accrete ?

and when to explode ?

Maximum CO WD mass at birht: 1.1Msol

Chen+ 2014, MNRAS

When does C ignition occur ? Tmax ↑ while keeping ρ constant.

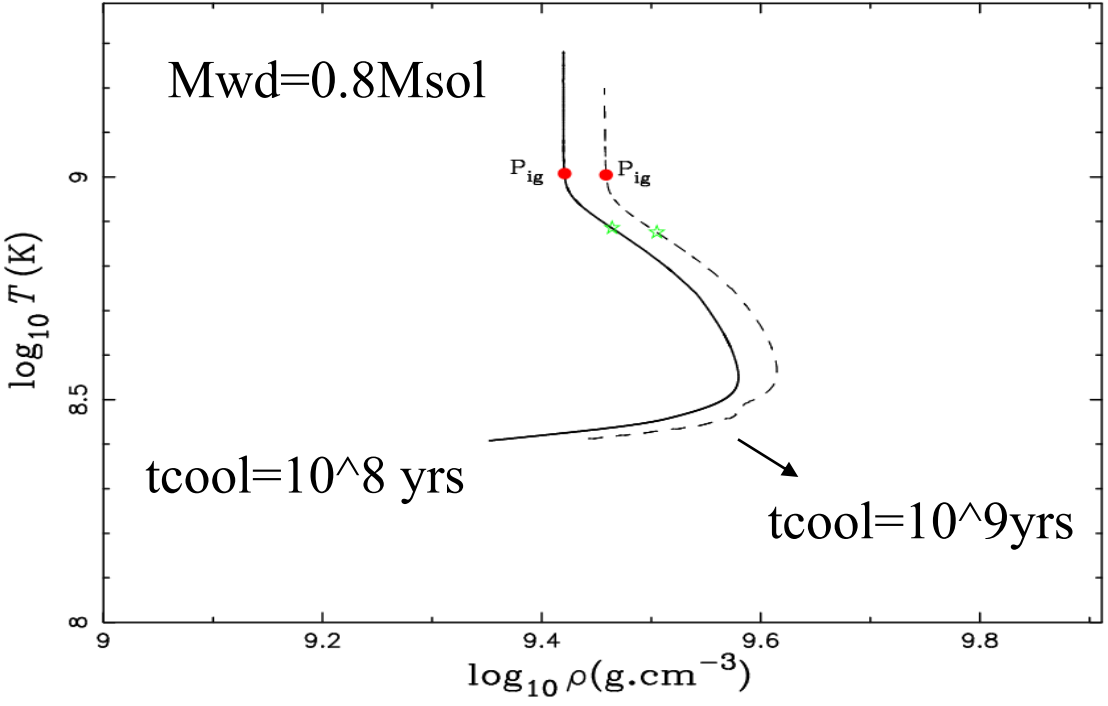

$$t_b = \alpha t_c$$

CO WD structure during accretion

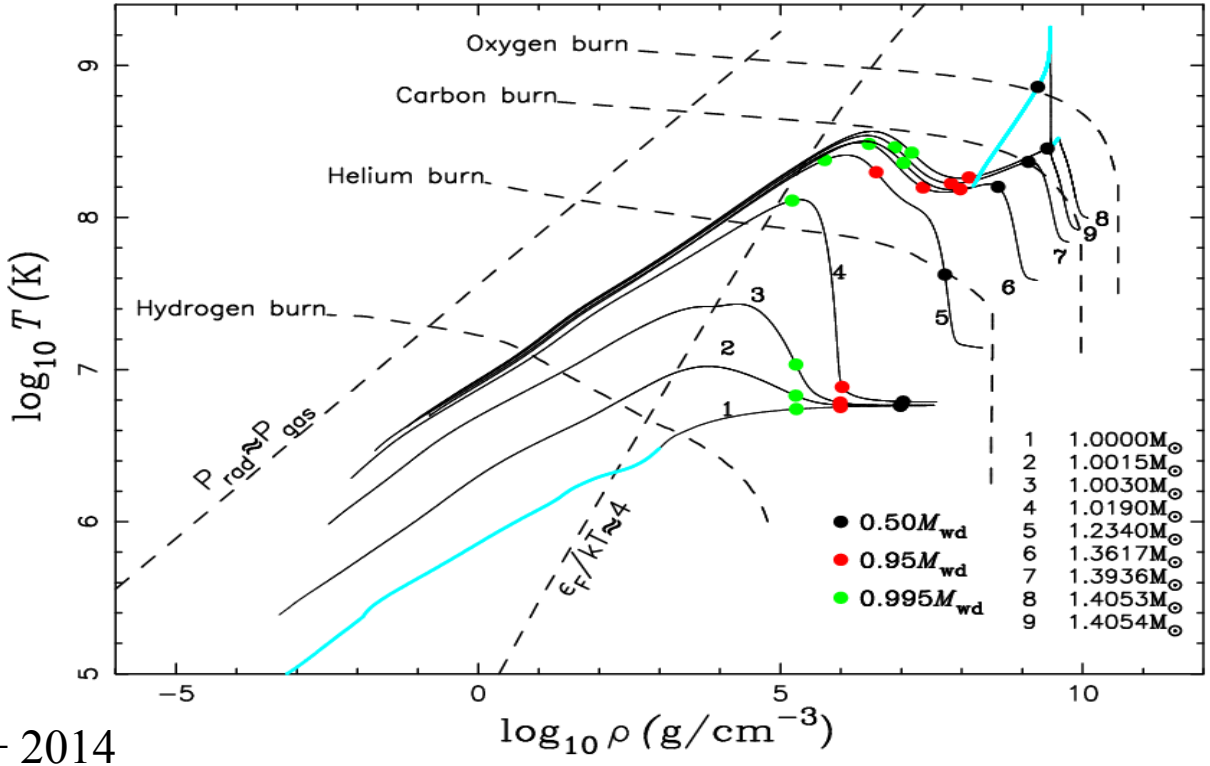

Chen+ 2014

Progenitor models of SNe Ia

Single-degenerate (SD) channel:

accreting from non-degenerate companion

CO WD + MS

CO WD + RG

CO WD + He Star

Double-degenerate (DD) channel:

Two CO WDs with a combined mass greater than 1.4Msun merge

CO WD + CO WD

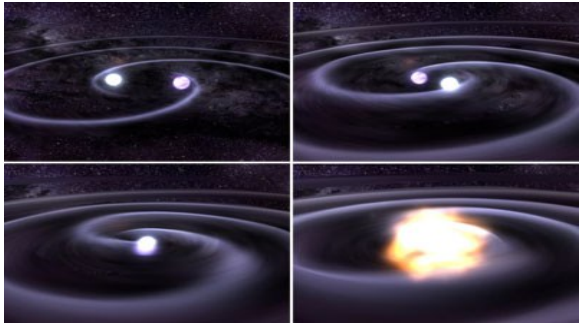

Credit: GSFC/Dana Berry

Helium donor channel (WD+He)

Wang+ 2009, 2010

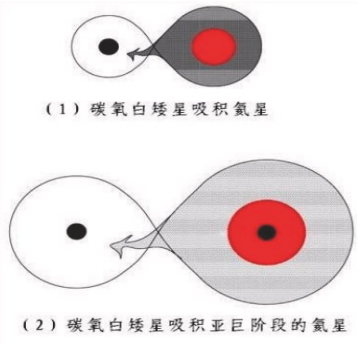

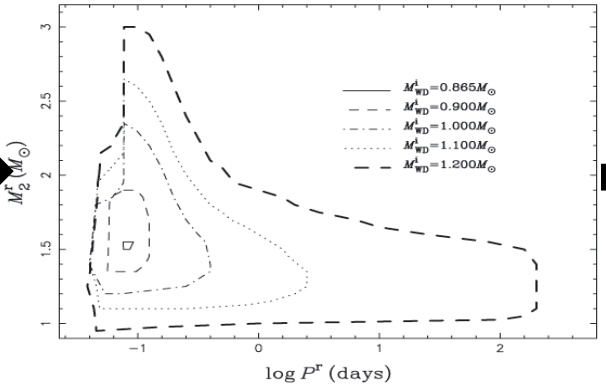

Birthrate
Time delay
Properties of Progenitors
Properties of remnant stars
……

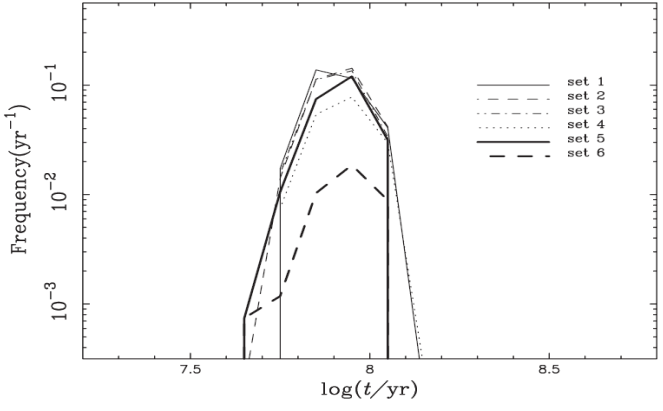

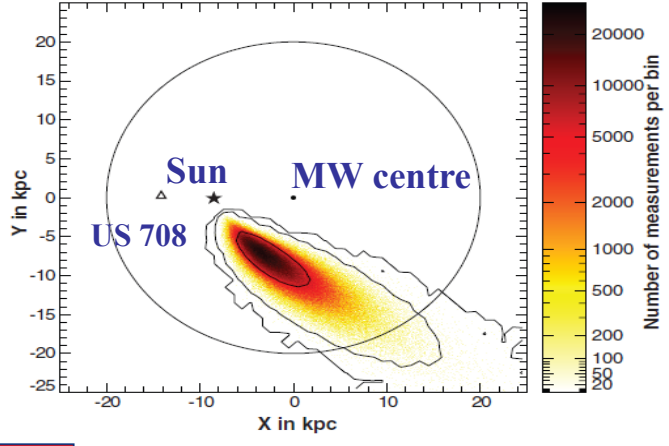

Explain young SNe Ia

Science AAAS

The fastest unbound star in our Galaxy ejected by a thermonuclear supernova
S. Geier *et al.*
Science **347**, 1126 (2015);
DOI: 10.1126/science.1259063

Hypervelocity star
Geier+, 2015, Science

SN Ia rates for single star burst

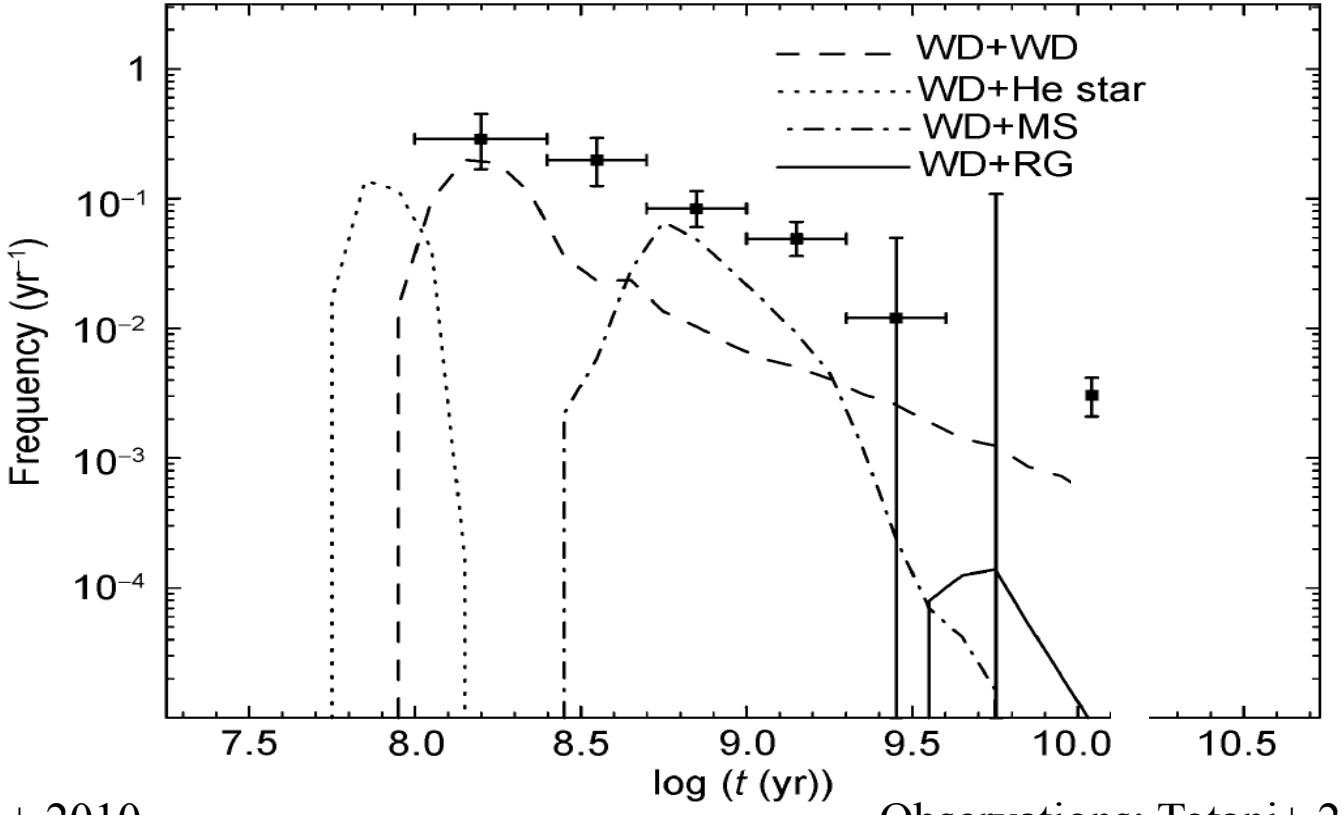

Wang+ 2010

Observations: Totani+ 2008

Stellar mass double BHs

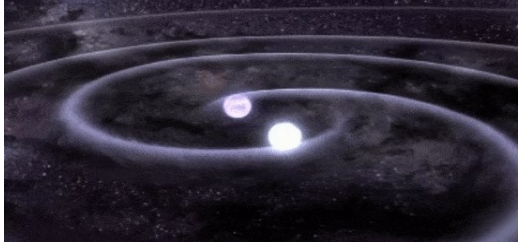

Massive binary evolution is the key scenario for their formation

CE evolution

~218 $Gpc^{-3}yr^{-1}$

~1000 $yr^{-1}$by second LIGO

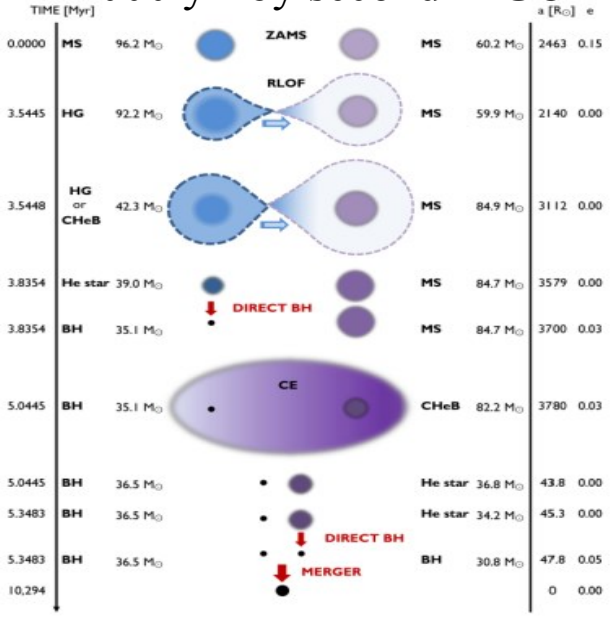

Contact binary evolutin

~10 $Gpc^{-3}yr^{-1}$

~500 yr^{-1} by second LIGO

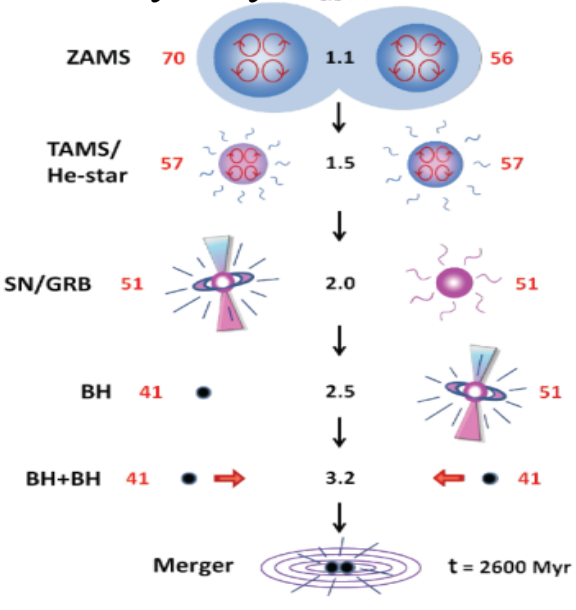

GC dynamics

~6.5 $Gpc^{-3}yr^{-1}$

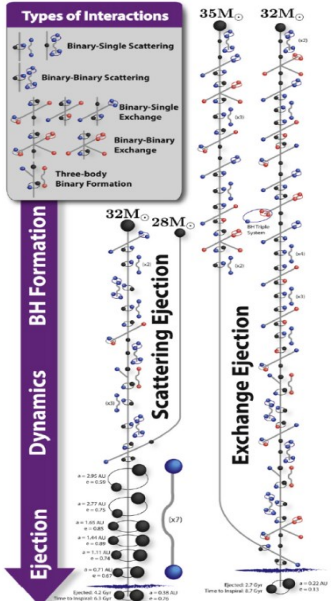

VFTS 352: 29 Msun+29 Msun with P=1.12 d

Mon. Not. R. Astron. Soc. **296,** 1019–1040 (1998)

The formation of double degenerates and related objects

Zhanwen Han[1,2]
[1]*Centre for Astrophysics, University of Science and Technology of China, Hefei, 230026, China*
[2]*Yunnan Observatory, Academia Sinica, Kunming, 650011, China*

Observation

DD	WD number	Name	M_1 ($M_\odot$)	M_2 ($M_\odot$) († for lower limit)	Orbital Period (days)
A	0135–052	L870-2/EG11	0.31	0.35	1.56
a			0.54	0.61	
B	0957–666		0.38	0.33	0.061
C	1101+364	PG 1101+364	0.27	0.31	0.1446
D	1202+608	GD 314/LB 2197	0.486	0.25†	1.49
E	1241–010	PG 1241-010	0.31	0.373†	3.35
F	1317+453	G 177-31	0.33	0.421†	4.8
G	1713+332	GD 360	0.35	0.178†	1.12
H	2032+188	GD 231	0.36		2-10 (6‡)
I	2331+290	GD 251	0.39	0.322†	0.14-0.20 (0.17‡)

Theory

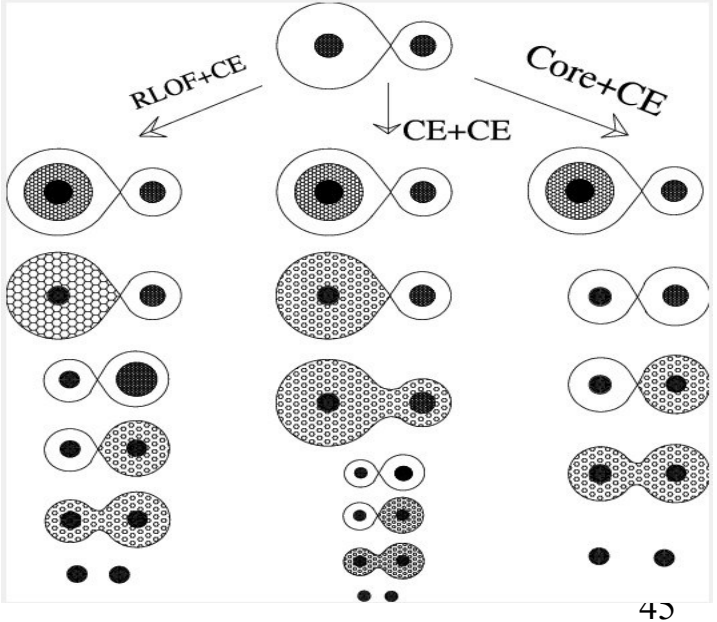

Distributions of masses, mass ratios, orbital periods of Galactic DWDs with BPS approach

1.762×10^8 double WDs

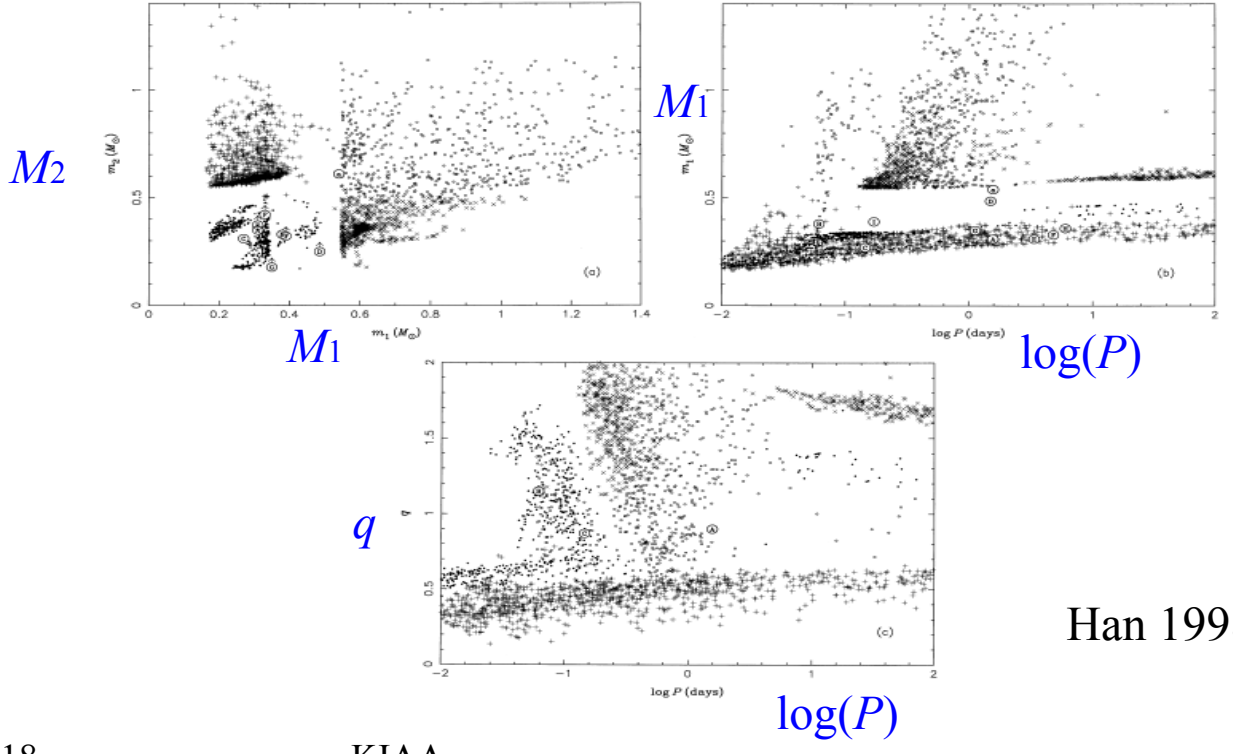

Han 1998

Gravitational Radiation from Close Double White Dwarfs

Ronald F. Webbink* and Zhanwen Han†

*Department of Astronomy, University of Illinois, Urbana, Illinois 61801, U.S.A.
†Centre for Astrophysics, University of Science and Technology of China, Hefei, 230026, China
and Yunnan Observatory, Academia Sinica, Kunming, 650011, China

CP456, *Laser Interferometer Space Antenna*
edited by William M. Folkner
 1-56396-848-7/98/$15.00

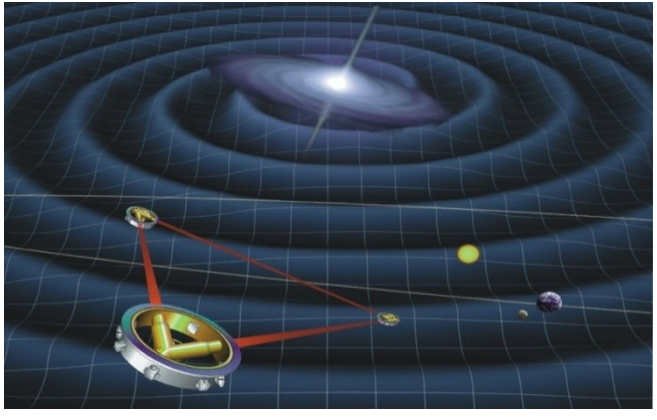

LISA

Spectral density of GW amplitude

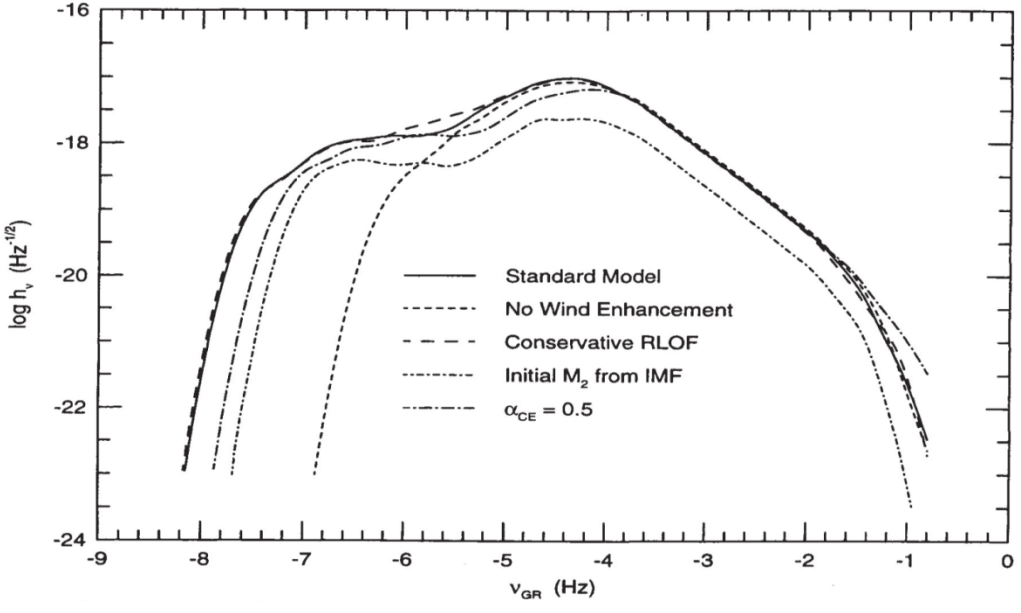

Resolvable DWDs with LISA

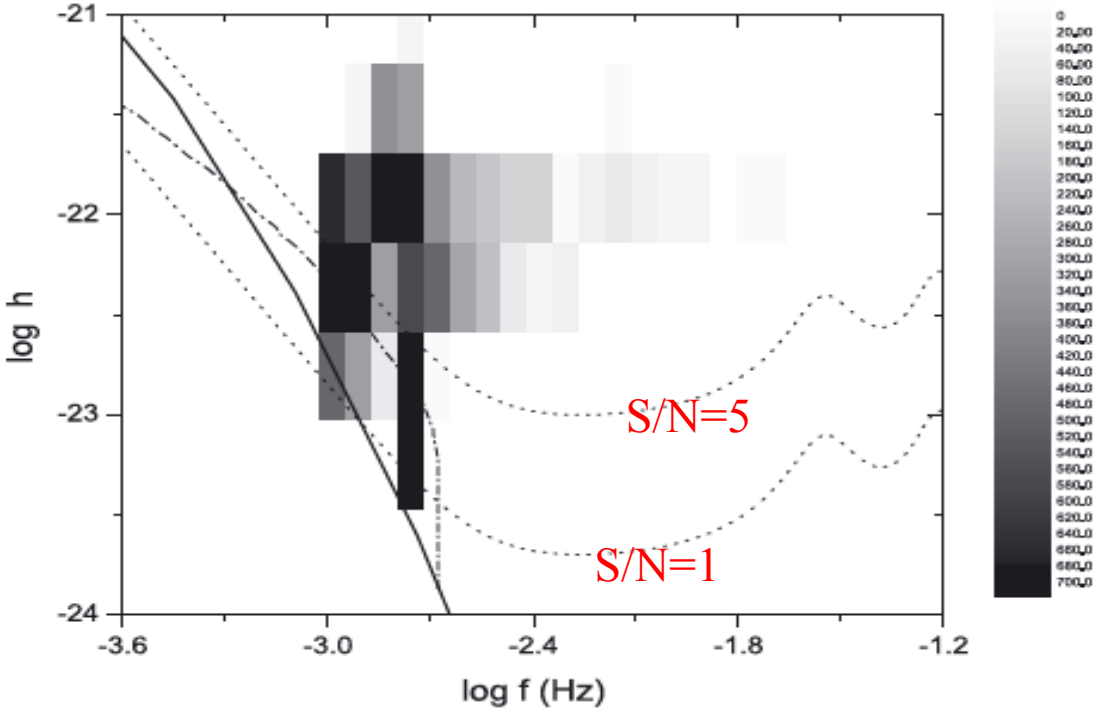

Liu+ 2009, ApJ

Resolvable NS+WD,NS+NS, BH+NS,BH+BH with eLISA

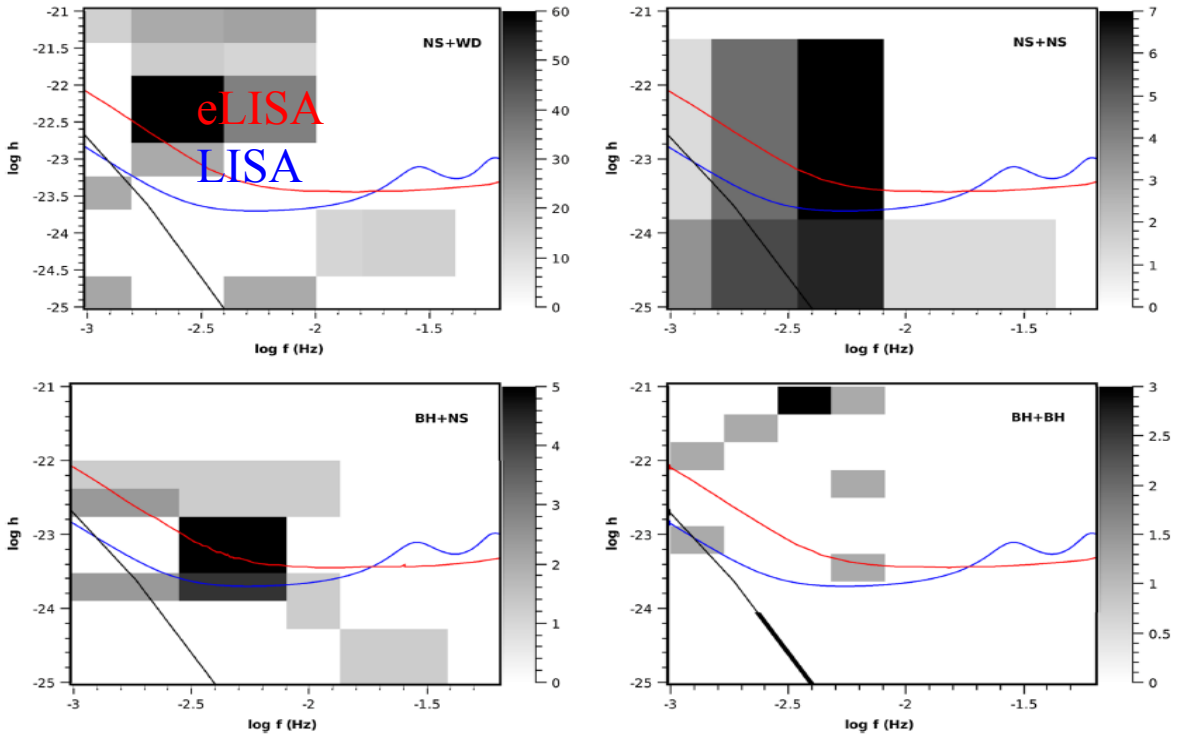

Liu+ 2014

Blue stragglers

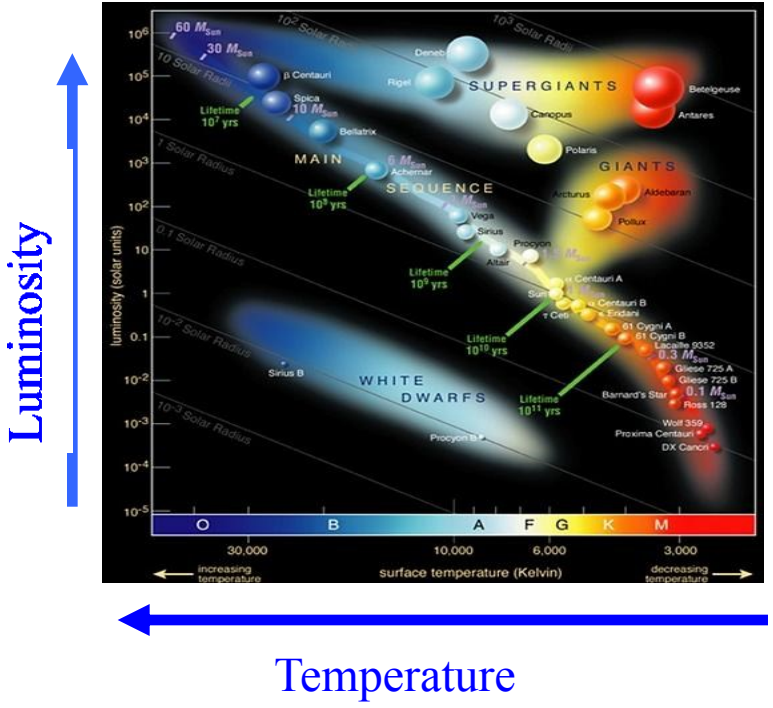

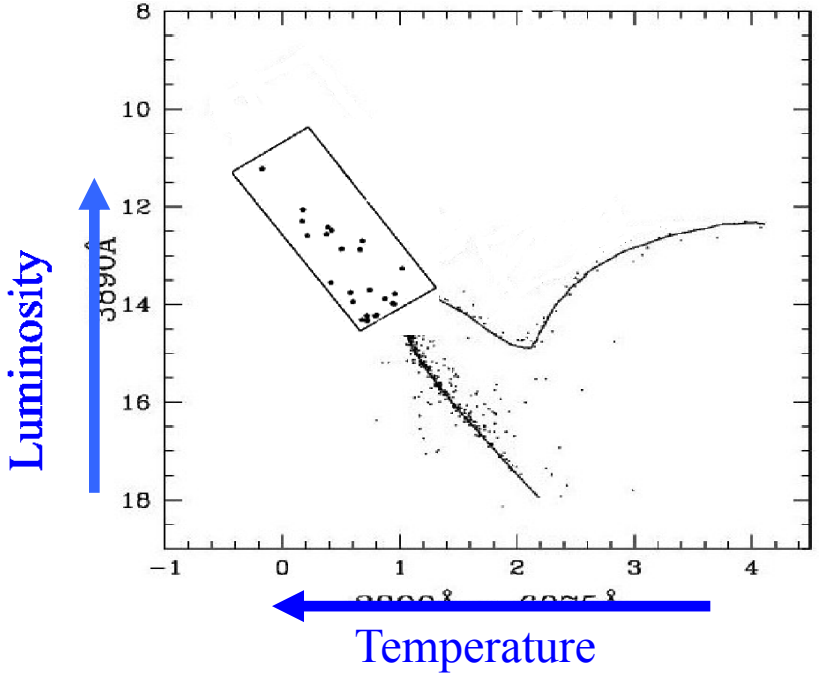

HR diagram

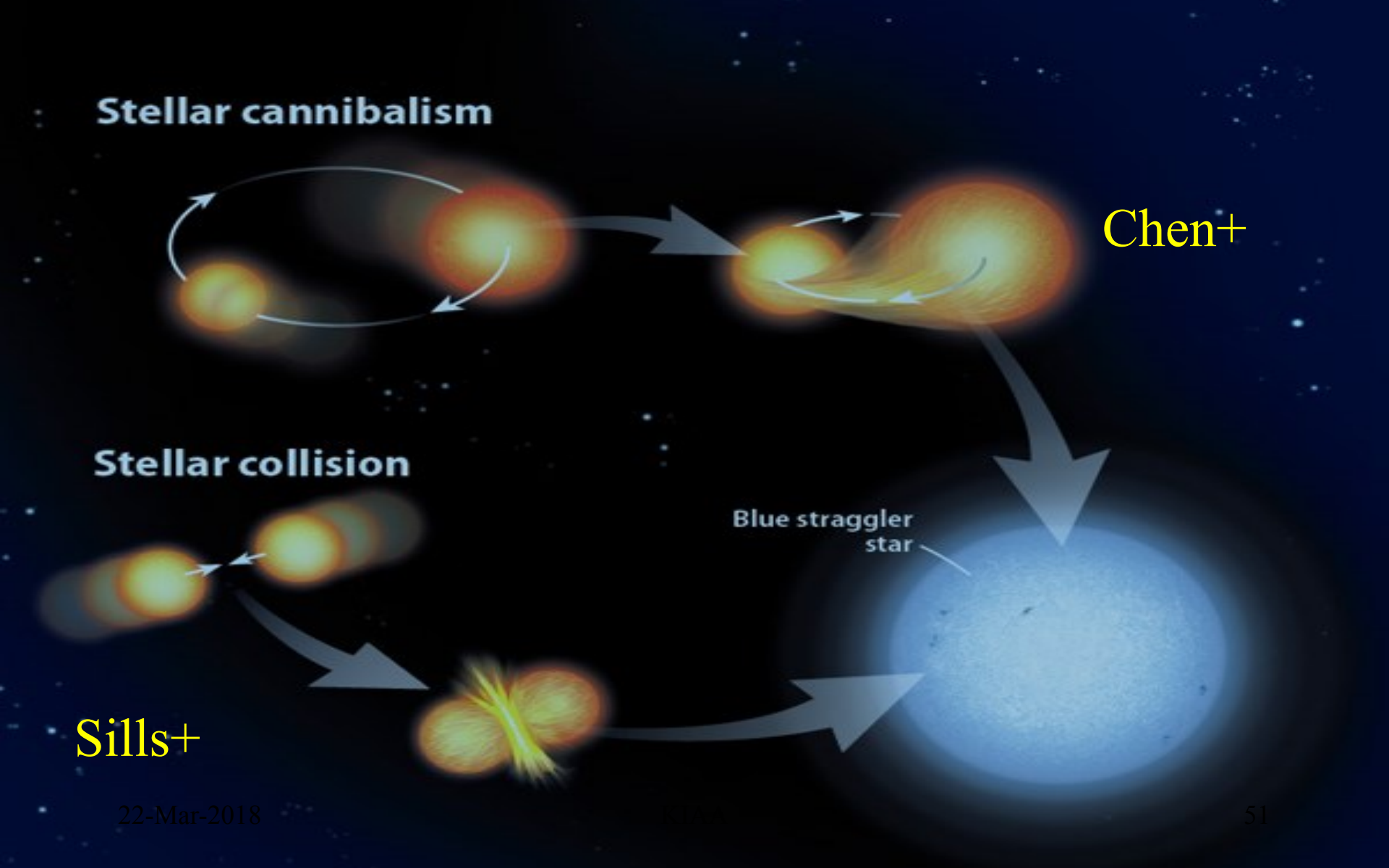
Stellar cannibalism
Chen+
Stellar collision
Blue straggler star
Sills+

Two blue stragglers sequences in M30

Ferraro+, 2009, Nature

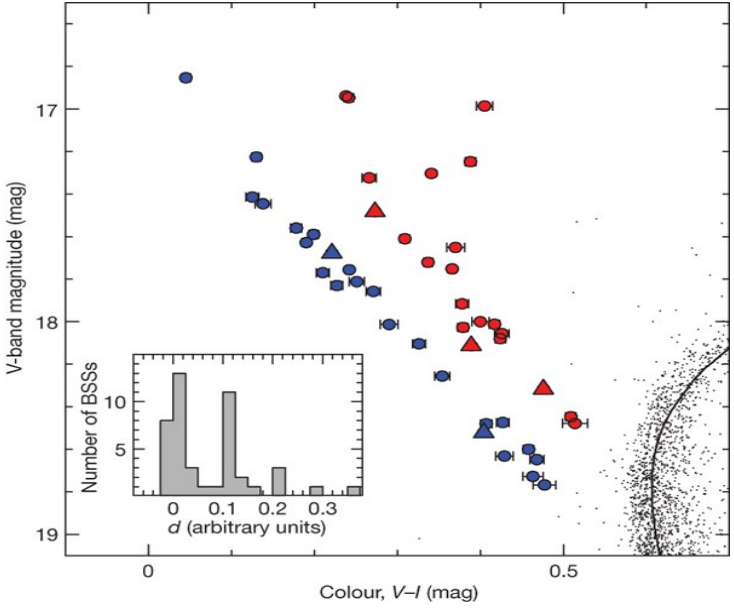

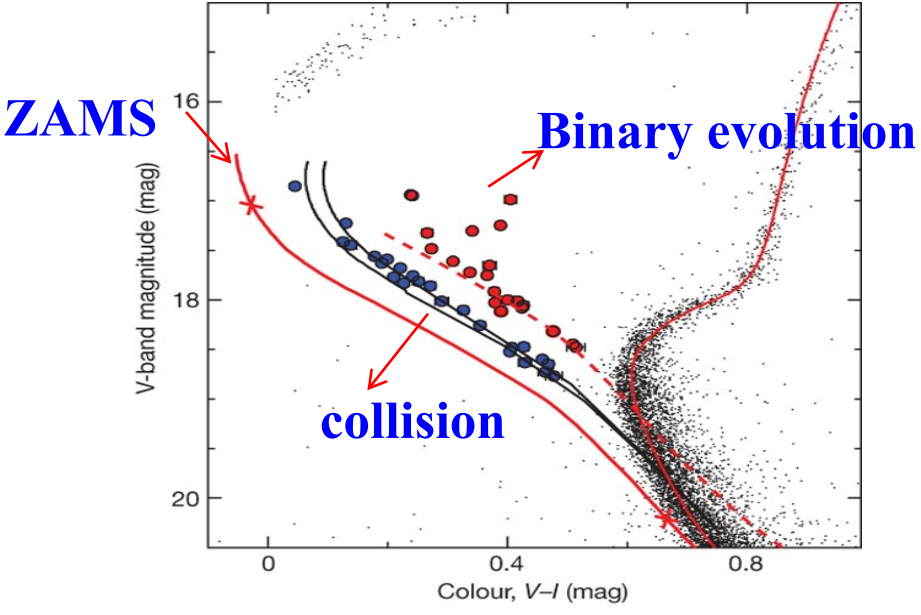

Binary evolution may produce both of the sequences

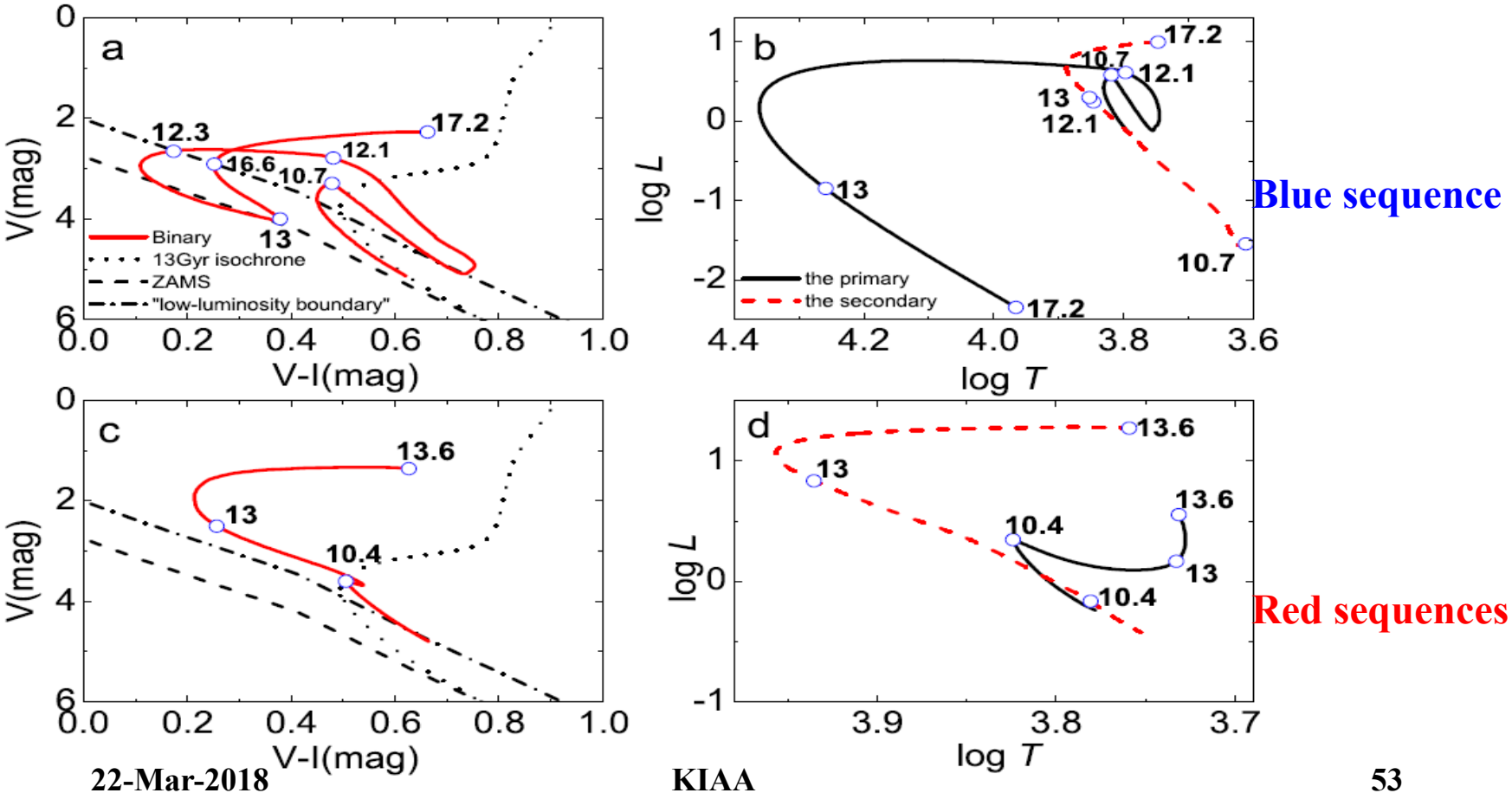

Blue stragglers with BPS

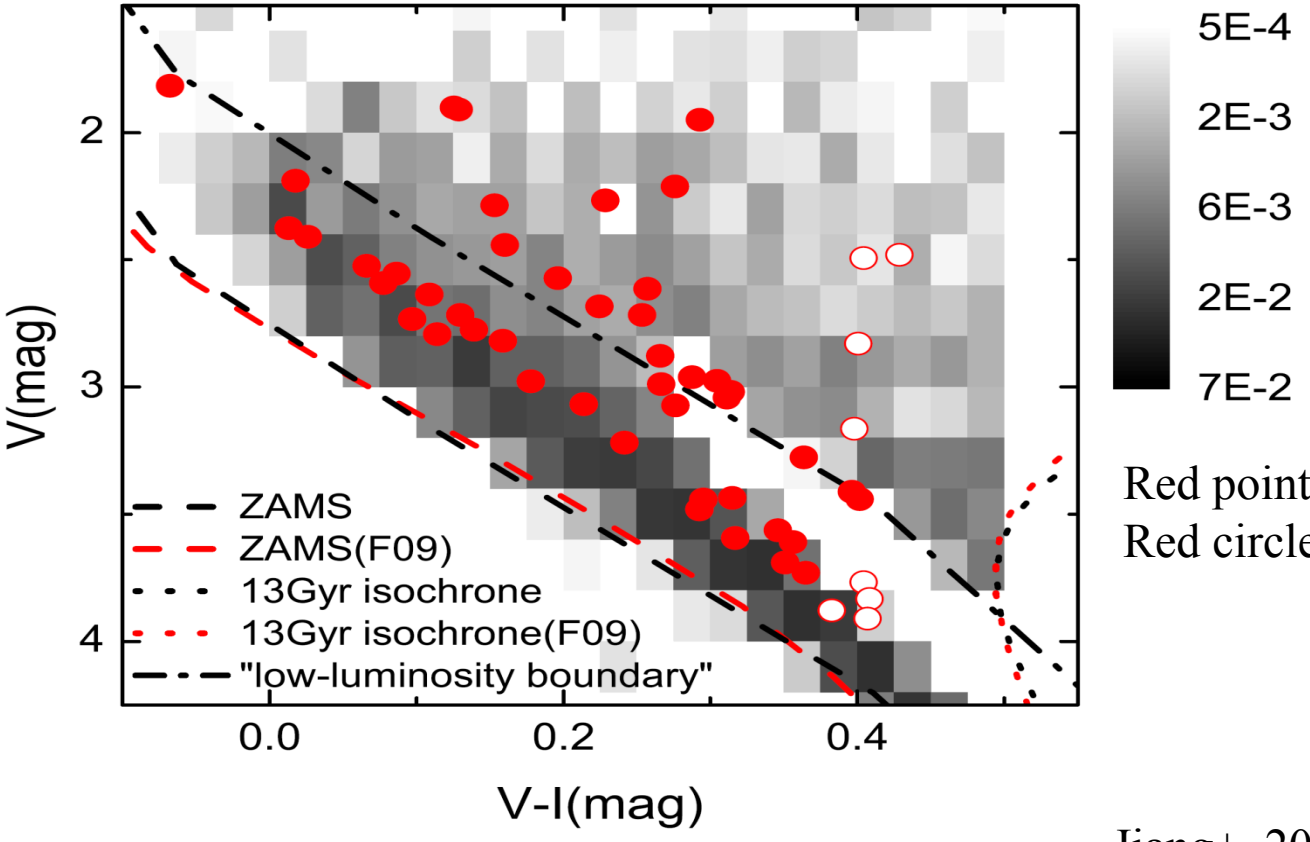

Red points: observed BSs in M30
Red circles: addition BSs

Jiang+, 2017, ApJ

hot subdwarf stars

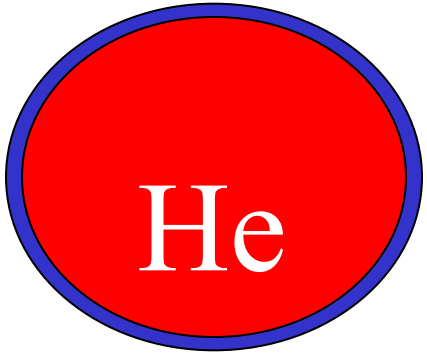

$$M \sim 0.5 M_{\odot}$$

$$M_{\mathrm{env}} \leq 0.02 M_{\odot}$$

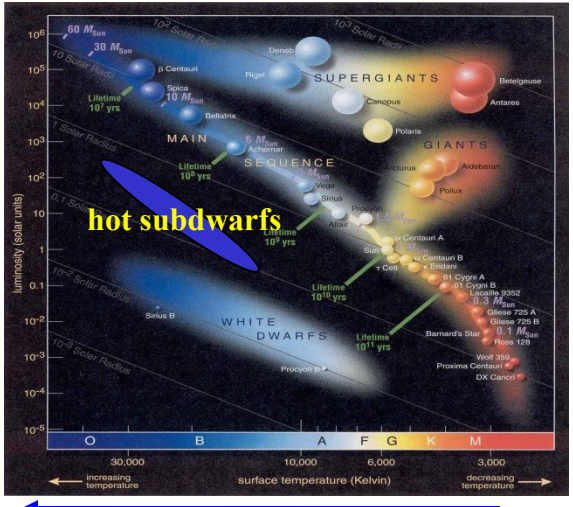

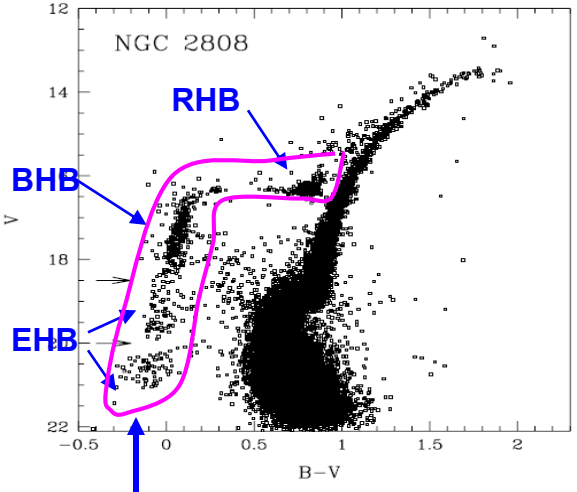

Fig. 4. The V vs. $(B-V)$ CMD from the *HST* WFPC2 data of the inner core of NGC 2808 ($r \leq 100$ arcsec). Only the 35,000 stars with a photometric error less than 0.15 are plotted.

Extreme Horizontal Branch stars

Binary model: stable RLOF

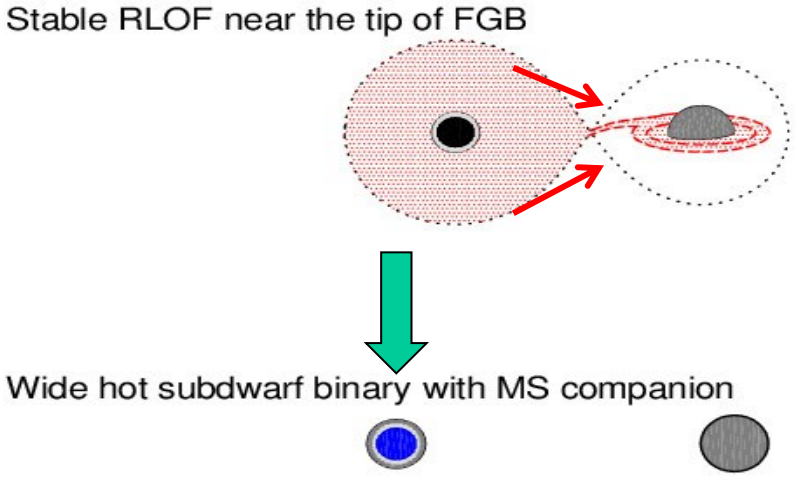

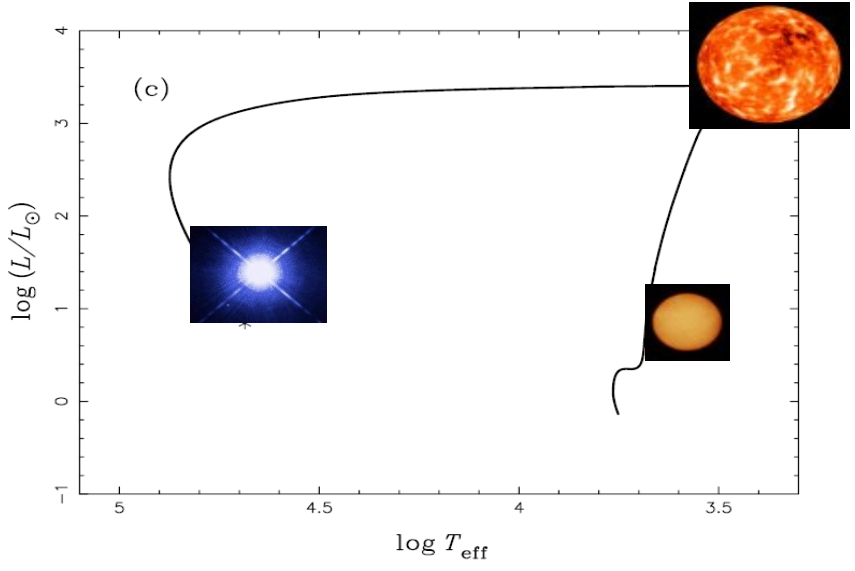

Figure 16. (a) Evolution of mass transfer rate, (b) orbital period as a function of mass, and (c) evolutionary track in the HR diagram, to demonstrate the case of stable RLOF for a binary with a giant donor with an initial mass of 1 $M_\odot$ and a 0.84 $M_\odot$ WD companion (Pop I, with overshooting, one-quarter Reimers' wind). The solid curves in (a) and (b) show the evolution before the onset of RLOF, i.e. due to a stellar wind. No stellar wind was included during and after RLOF.

Binary model: CE ejection

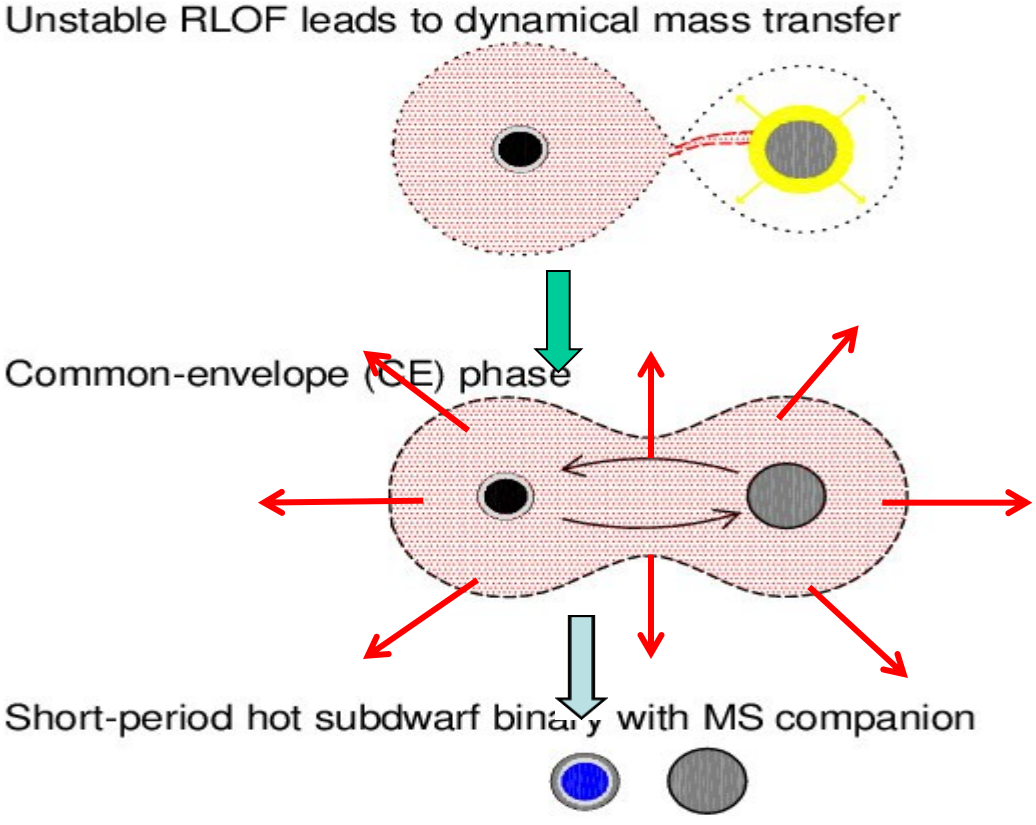

Binary model: He WD merger

He WD merger (1 or 2 CE phases)

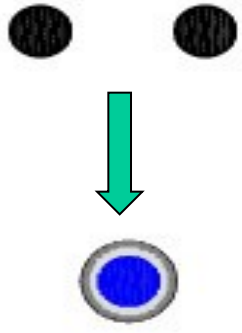

$M_{\rm sdB} = 0.40 - 0.65 M_{\odot}$

The model can reproduce:

- (Log P, Mcomp)
- (Teff, log g)
- P
- Log (g/Teff^4)
- Mass function
- Birthrate
- Number density
- Fraction of sdB+MS
- Fraction of close sdB binaries
- ……

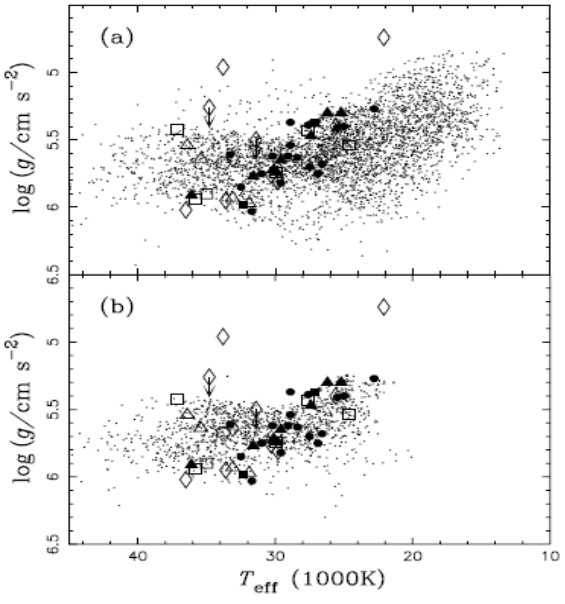

g g diagram for simulation set 2 (the best-fitting model). Dots represent the results of the simulation. Filled circles indicate the position of observed sdB binaries with orbital periods $P_{\rm orb} < 1$ d, solid triangles binaries with $1 < P_{\rm orb} < 10$ d, and solid squares binaries with $P_{\rm orb} > 10$ d. Circles show systems that have radial velocity variations d $V < 10$ km s^{-1}, triangles systems with $20 <$ d $V < 40$ km s^{-1}, squares systems with d $V > 40$ km s^{-1}, crosses systems with $10 <$ d $V < 20$ km s^{-1} and diamonds systems with d $V <$ 10 km s^{-1}, where d V is the maximum difference between radial velocities measured for a particular object. Arrows indicate lower limits for g. (a) does

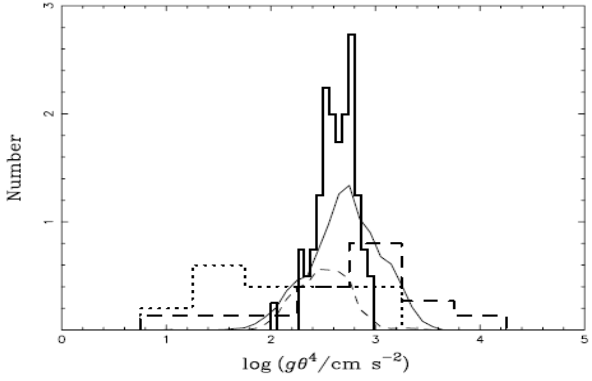

Figure 27. The distribution of log ($g\theta^4$), where g is the surface gravity of an sdB star, and $\theta = 5040$ K $/T_{\rm eff}$. The solid histogram is obtained from the 68 sdB stars observed by Saffer et al. (1994), while the dashed and dotted histograms are based on the observations of 15 sdB stars and 10 sdO stars, respectively, by Ulla & Thejll (1998). The solid curve represents the sdB stars from simulation set 2 (the best-fitting model) without consideration of selection effects, while the dashed curve includes the GK selection effect.

Predictions:

Larger mass range

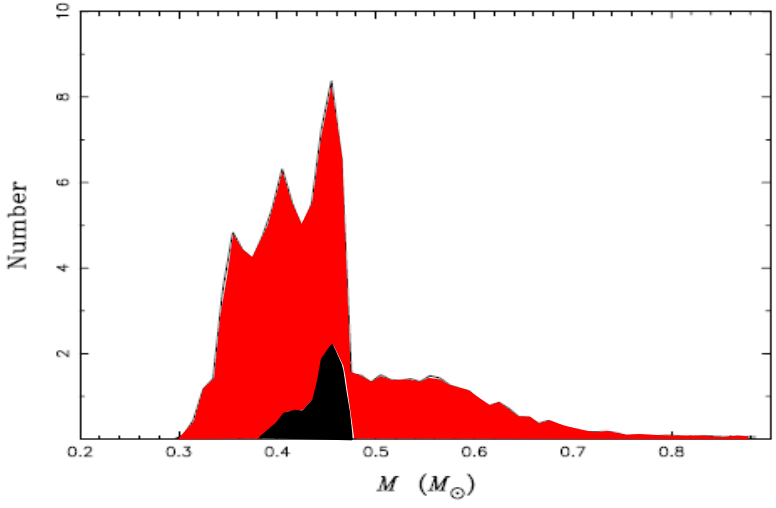

Figure 22. The distribution of masses of sdB stars from all the channels in simulation set 2 (the best-fitting model); solid curve, no selection effects; dashed curve, the GK selection effect; dot-dashed curve, the GK and the strip selection effects; dotted curve, the GK, the strip and the K selection effects.

sdB binaries with long orbital periods

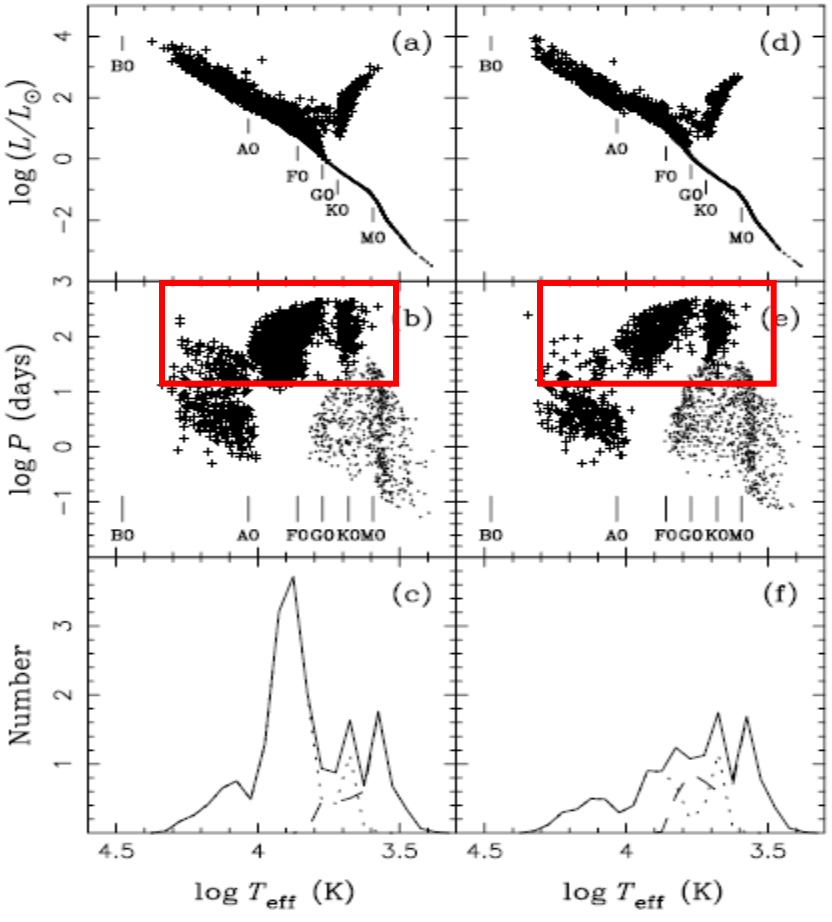

Figure 15. The characteristics of the MS secondaries in sdB binaries from the first CE ejection channel (dots) and the first stable RLOF channel (crosses) for the best-fitting simulations 2 (with $q_{crit} = 1.5$; left-hand panels) and 8 (with $q_{crit} = 1.2$; right-hand panels). (a) and (d), HRD with spectral types indicated along the main sequence (based on Zombeck 1990). (b) and (e), orbital period versus effective temperature. (c) and (f), the distribution of log T_{eff}; solid curves, both channels; dashed curves, the first CE ejection channel only; dotted curves, the first stable RLOF channel.

Outline

- Binary evolution
- Binary-related objects
- Evolutionary population synthesis
- Future perspectives

What is EPS?

Evolutionary Population Synthesis (EPS) is an approach to derive the physical parameters of stellar populations of galaxies from the Spectral Energy Distributions(SEDs) observed.

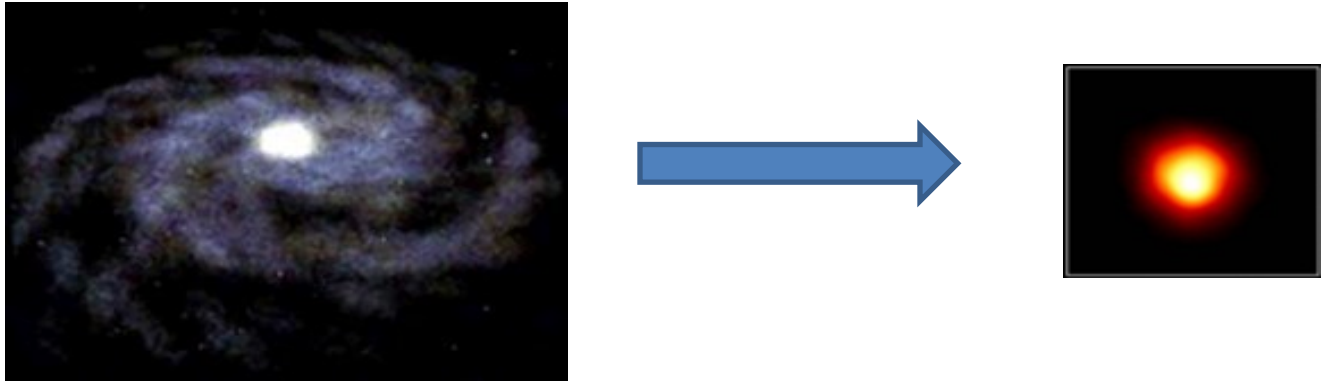

The ingredients of an EPS model:

Star Formation Rate -> how many stars?
Initial Mass Function -> how much mass of each star?
Stellar Evolution Models -> how they evolve?
Model Stellar Atmospheres -> how their spectra?

Integrated SED (the sum of all the spectra of the stars)

Single Stellar Evolution

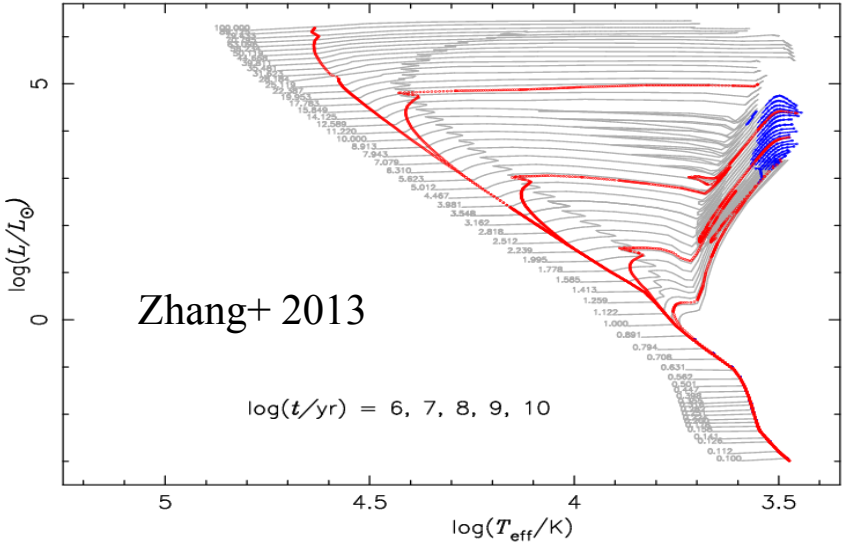

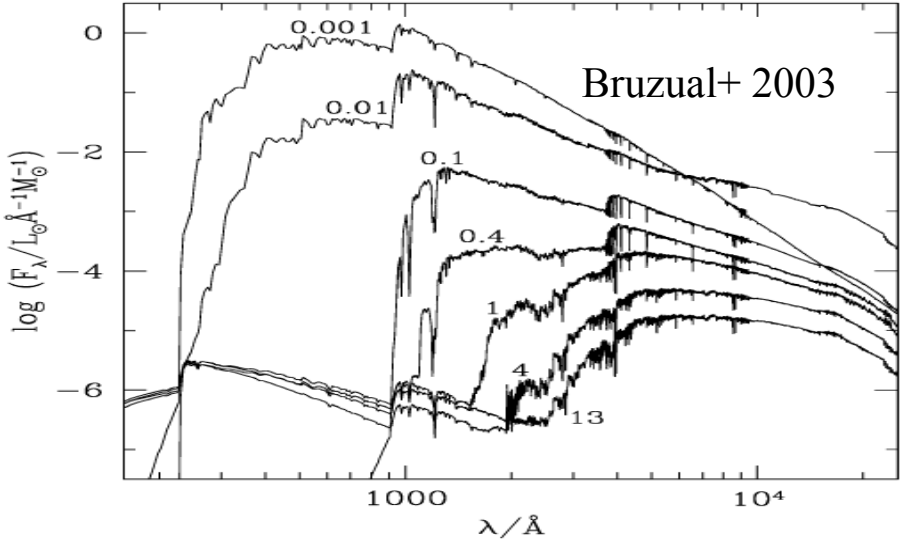

Young stellar population has hot spectra, while old population has cold spectra.

50% are in binaries, how does a binary evolve?

- RLOF removes stellar envelope
  →hot core exposed
  →(core can be ignited)

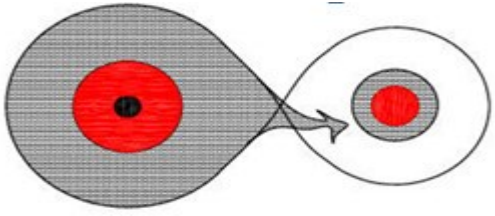

- A star grows in mass via accretion
  →rejuvenation (hotter)

- Coalescence of a binary
  → a more massive star (hotter)

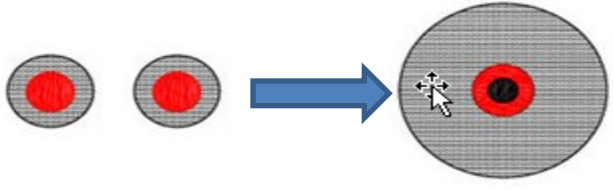

Binary interactions rejuvenate stars!

Binary Contribution to ISED

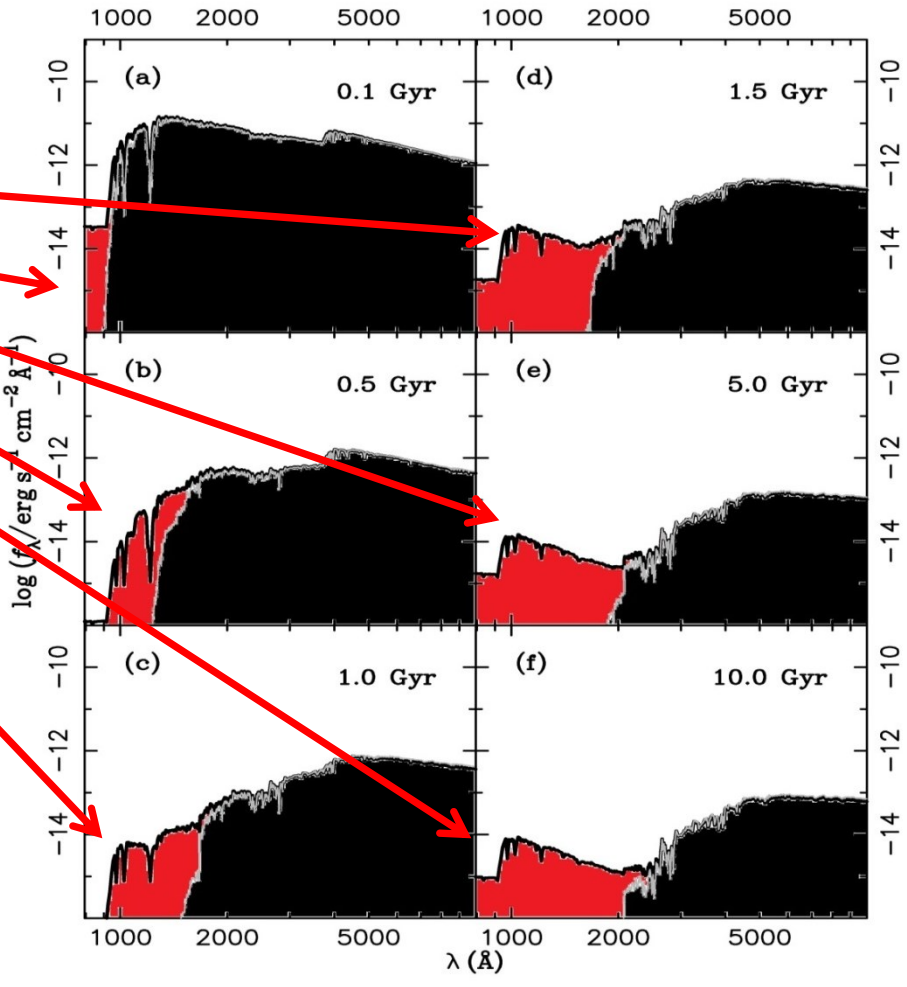

To derive physical parameters properly from a given SED,

we need binaries !

History of EPS studies

- Tinsley (1968)

- Rapid progress since 90's

✓ GISSEL98 or BC03 model (Bruzual+ 1993, 2003)
✓ PopSTAR model (Molla+ 2009)
✓ STARBURST (Leitherer+ 1999)
✓ PEGASE (Fioc+ 1997)
✓ Yunnan model (Zhang+ 2004, Han+ 2007, Chen+ 2015)

The Yunnan Model

- ✓ stellar evolutionary tracks
  (Cambridge stellar evolution code STAR)
- ✓ BaSeL spectral library
- ✓ Binary interactions (blue stragglers, hot subdwarf stars, accreting WDs, rejuvenated stars, ……)

Binaries first included: Zhang+ 2004, A&A, 415, 117

Hot subdwarfs: Han+ 2007, MNRAS, 380, 1098

Blue stragglers: Chen+ 2009, MNRAS, 395, 1822

SFR calibration: Zhang+ 2012, MNRAS, 421, 743

Ionizing sources: Zhang+ 2015, MNRAS, 447, L21

Accreting WDs: Chen+ 2015, MNRAS, 453, 3024

Far-UV Excess of Elliptical Galaxies

There exists a far-UV excess for elliptical galaxies, known since 1969 but unexplained.

Solving the problem is crucial to our understanding of the structure and evolution of early-type galaxies.

Hot subdwarf stars radiate in far-UV, and we applied our binary model of hot subdwarfs to the study of elliptical galaxies and explained their far-UV light

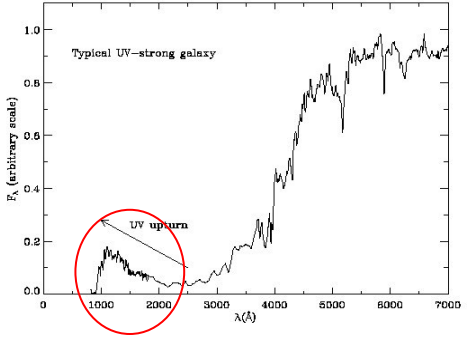

Binary UV model

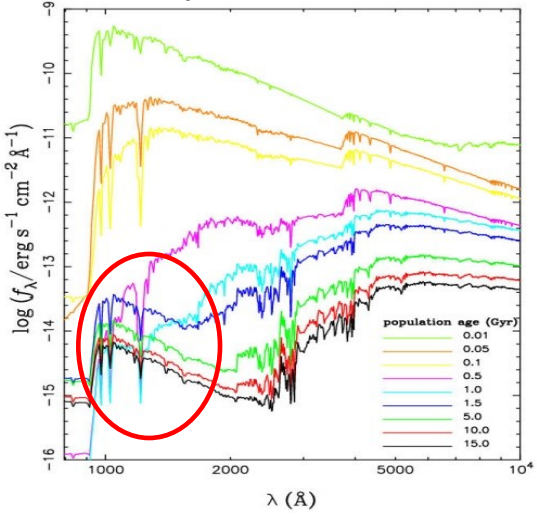

Soft X-ray emission from elliptical galaxies

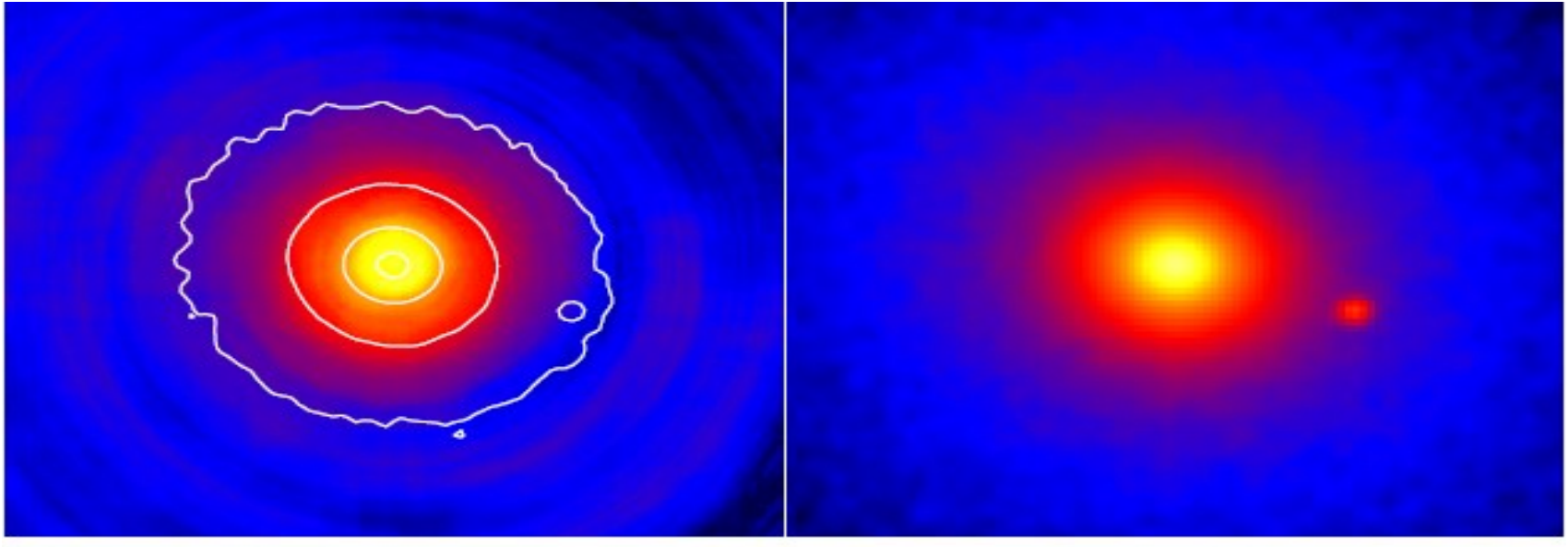

adaptively smoothed image of the unresolved X-ray emission (detected point sour
ared with the near-infrared (K-band) image of the galaxy (right panel). Conto
ically spaced near-infrared brightness isophotes.

Revnivtsev+ 2007

Spectrum of an accreting WD

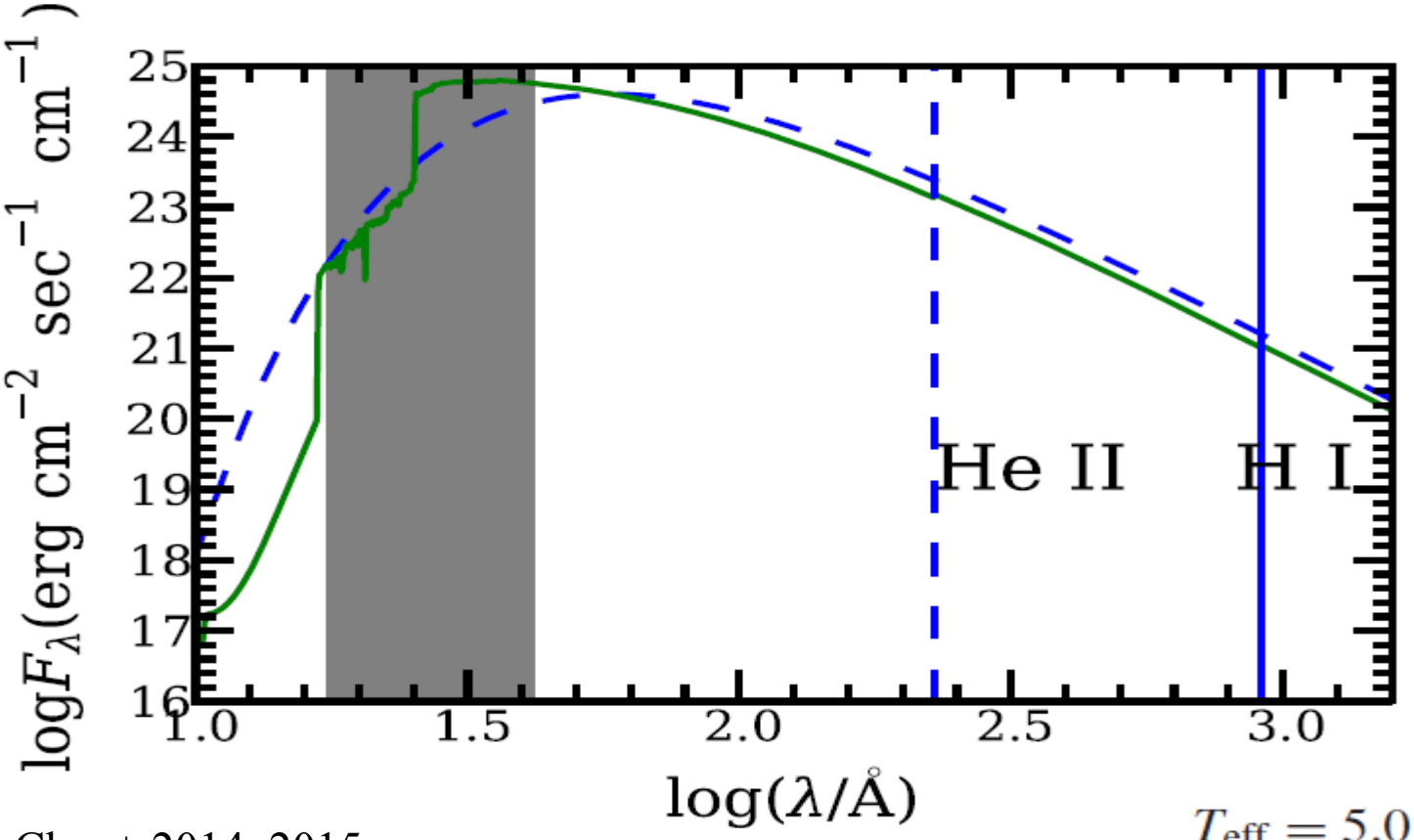

Chen+ 2014, 2015

$T_{\rm eff} = 5.0 \times 10^5$ K.

Evolution of soft X-ray emission

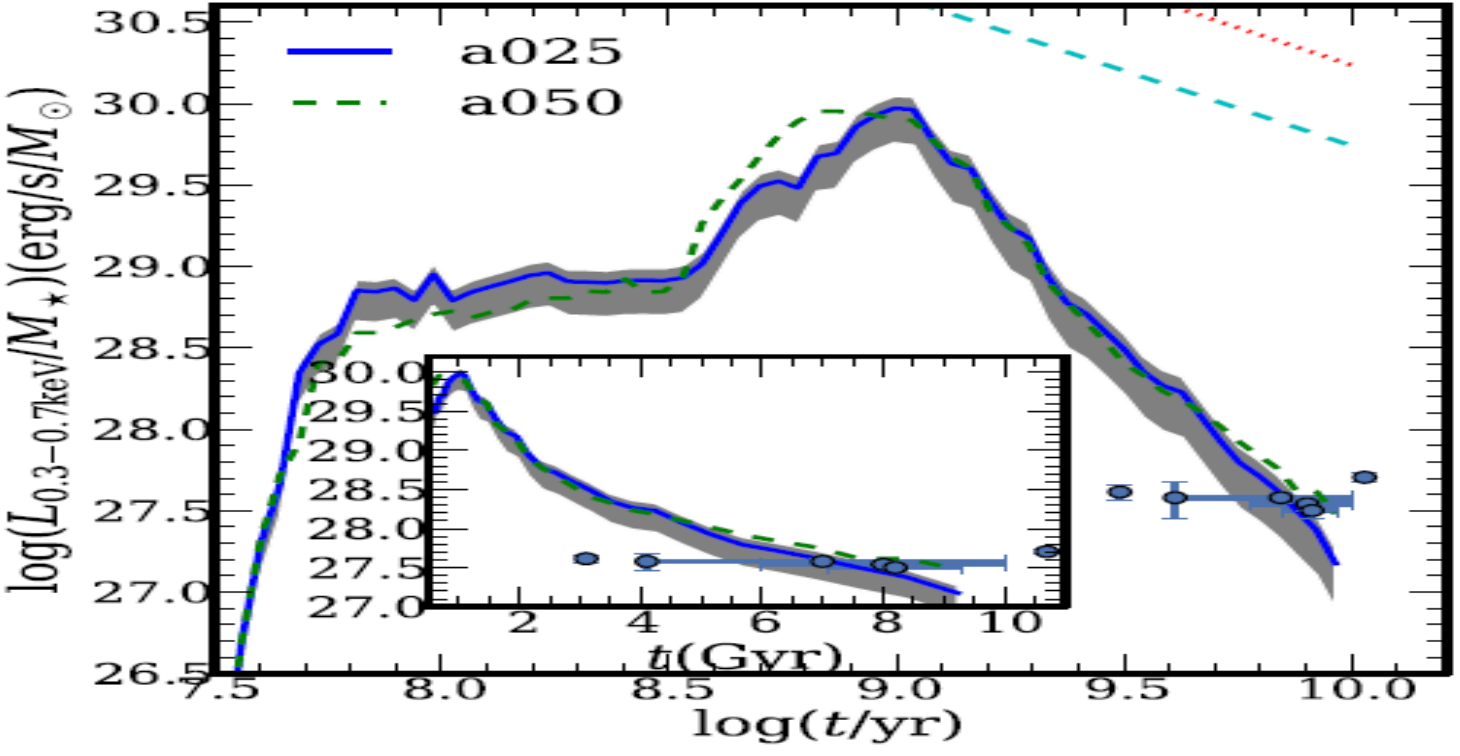

Chen+ 2014, 2015

Observations: Bogdan+ 2010, Zhang+2012

Yunnan Model：

Stellar mass smaller（by 10%）
fainter（by 0.2mag）
bluer（by 0.2-0.4mag）
Mass-light ratio bigger（by 10-20%)
UV flux larger（by 2 orders of mag）
EUV flux larger
X-ray emission

Parameters derived：

Age larger（by 20% to a few times）
Metallicity larger（by 20%）
Photometric redshift (much more accurate for blue-faint-galaxies）
Ionizing sources (middle age）
Far-IR bump（？）
SFR (by 60%, 0.2dex)

Zhang+ 2004, 2010, 2012, 2013, 2014
Chen+ 2014，2015

Binary interactions are important for SEDs of old stellar population (e.g. elliptical galaxies) at short wavelength.

Outline

- Binary evolution
- Binary-related objects
- Evolutionary population synthesis
- Future perspectives

（1）Basic problems of binary evolution

- ✓ Ge's adiabatic mass loss model fully established.
- ✓ Symbiotic channel of SNe Ia with Ge's model.
- ✓ Other RG related objects with Ge's model.

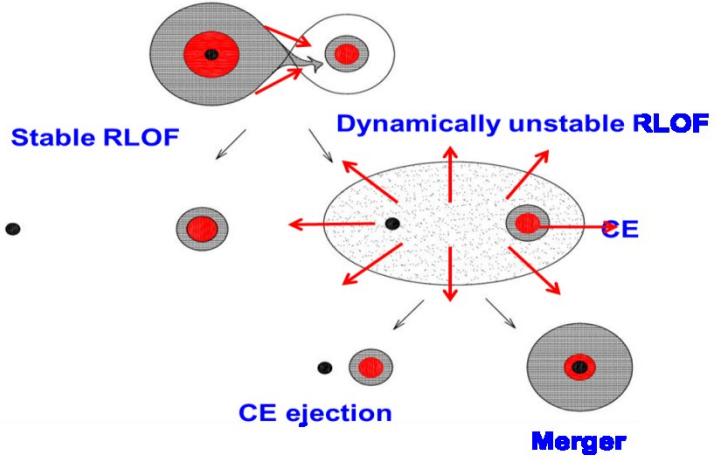

（2）more binary related objects

- ✓ sdB+NS binaris
- ✓ BH+BH, NS+NS
- ✓ WD+WD

.....

（3）evolutionary population synthesis

- ✓ Extends to EUV, X-ray via accreting WDs
- ✓ +phoionization model + galaxy mode
- ✓ BayeSED

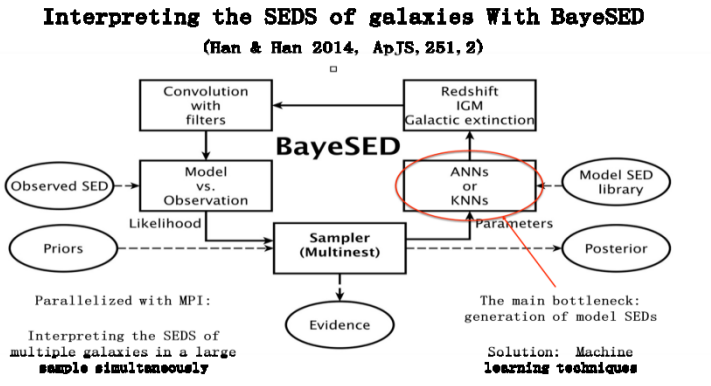

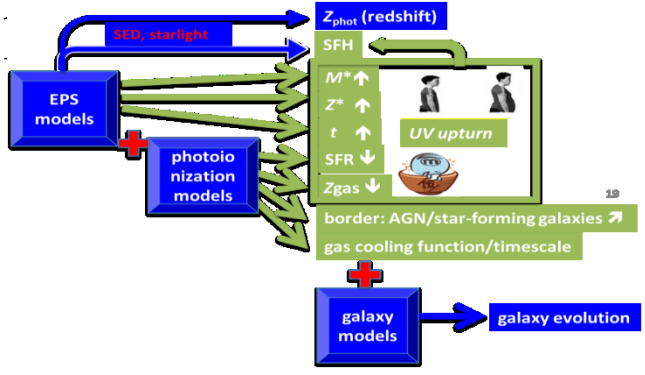


Thanks !

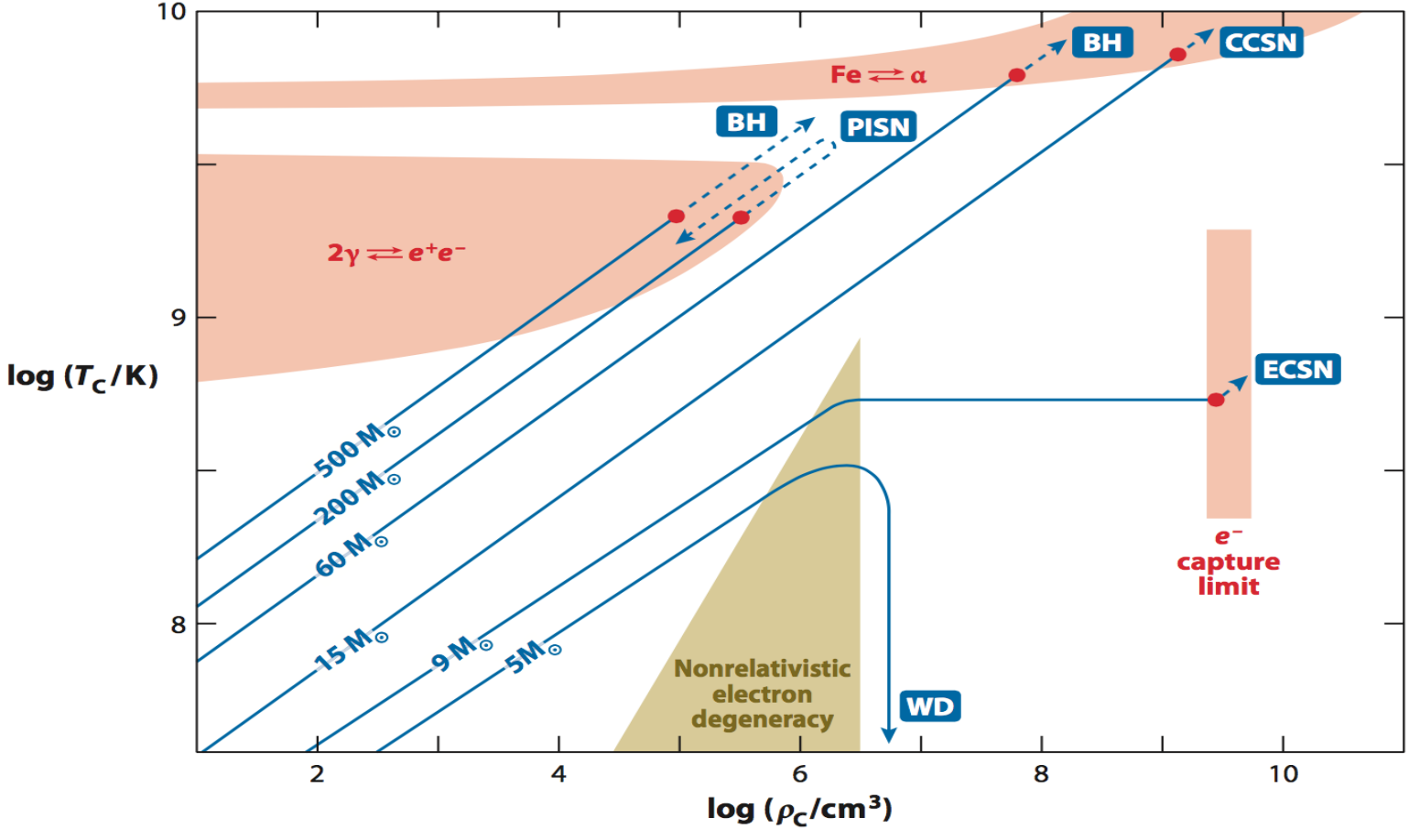
10
9
8
log (T_C/K)
2
4
6
8
10
log (ρ_C/cm^3)
Fe ⇌ α
2γ ⇌ e⁺e⁻
BH
CCSN
BH
PISN
ECSN
e⁻ capture limit
500 M⊙
200 M⊙
60 M⊙
15 M⊙
9 M⊙
5M⊙
Nonrelativistic electron degeneracy
WD

Science with Inspiral Detections: Maximum BH Mass

1) Maximum BH mass depends on:
- extent of Initial Mass Function (IMF)
- stellar models and metallicity -> winds
- SN/core collapse (pair instability)

2) New winds (Vink et al.):

$Z = 1.0\ Z_\odot$: max. BH mass: $\sim 15 M_\odot$
$Z = 0.3\ Z_\odot$: max. BH mass: $\sim 30 M_\odot$
$Z = 0.01\ Z_\odot$: max. BH mass: $\sim 80 M_\odot$

3) Extent of IMF:
- very massive stars found: 200-300 $M_\odot$
- max. BH mass: $\sim$ 100-150 $M_\odot$ (0.1 $Z_\odot$)
- but: pair instability disrupts these stars?

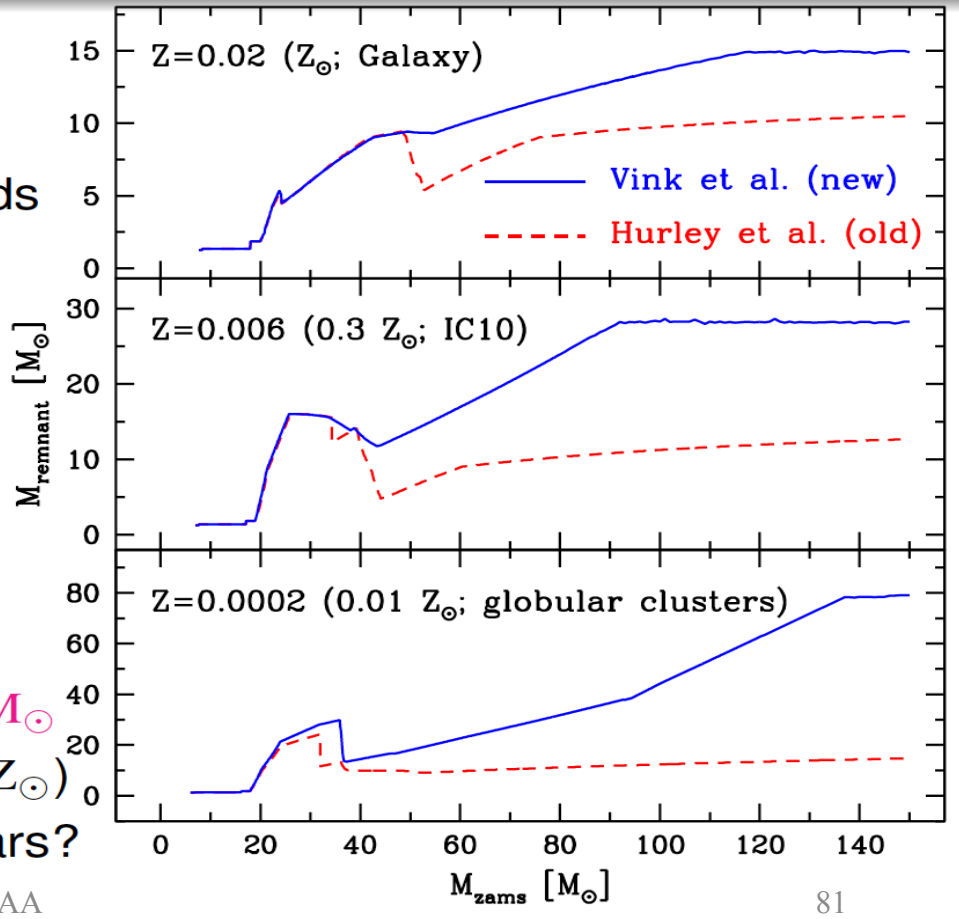

Quasi-chemical homogeneous evolution

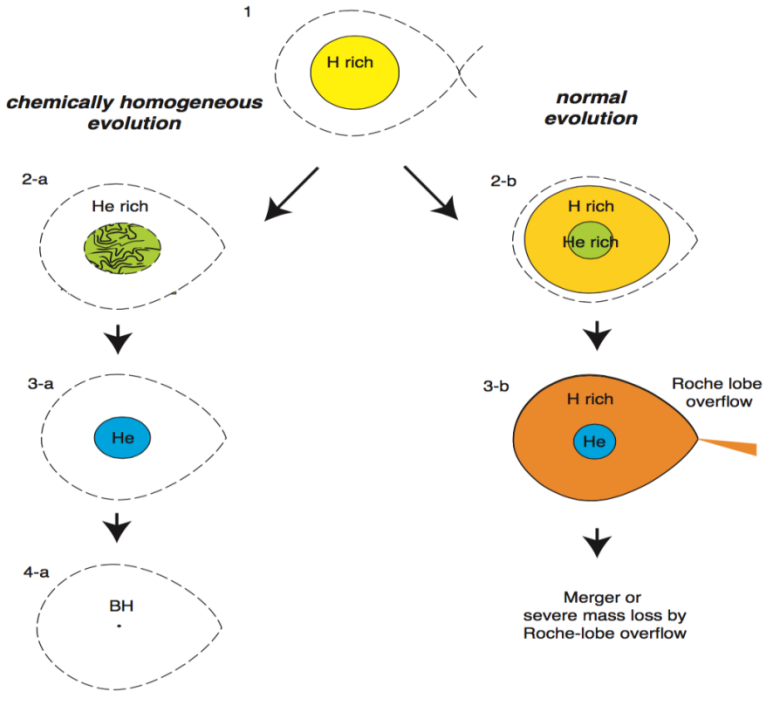

Mandel+, 2016, MNRAS

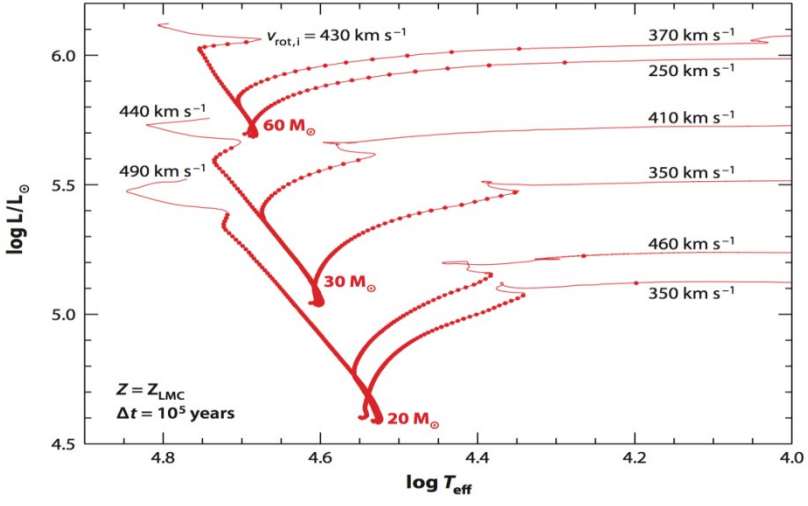

Langer, 2012, ARA&A

Ionizing spectra of stars that lose their envelope through interaction with a binary companion: role of metallicity

Y. Götberg[1], S. E. de Mink[1], and J. H. Groh[2]

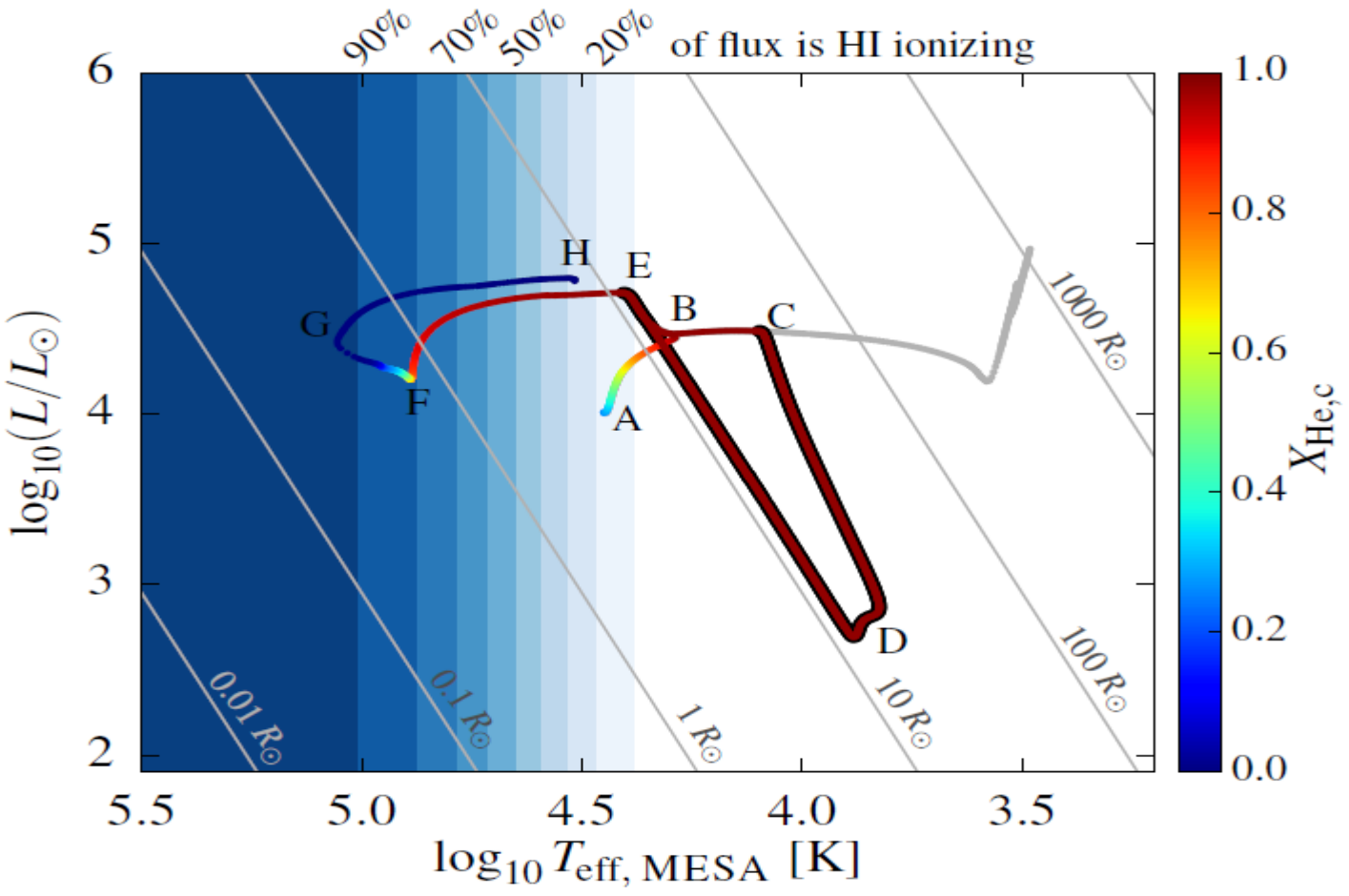

Götberg, De Mink & Groh: Ionizing spectra of stars that lose their envelope through interaction with a binary companion

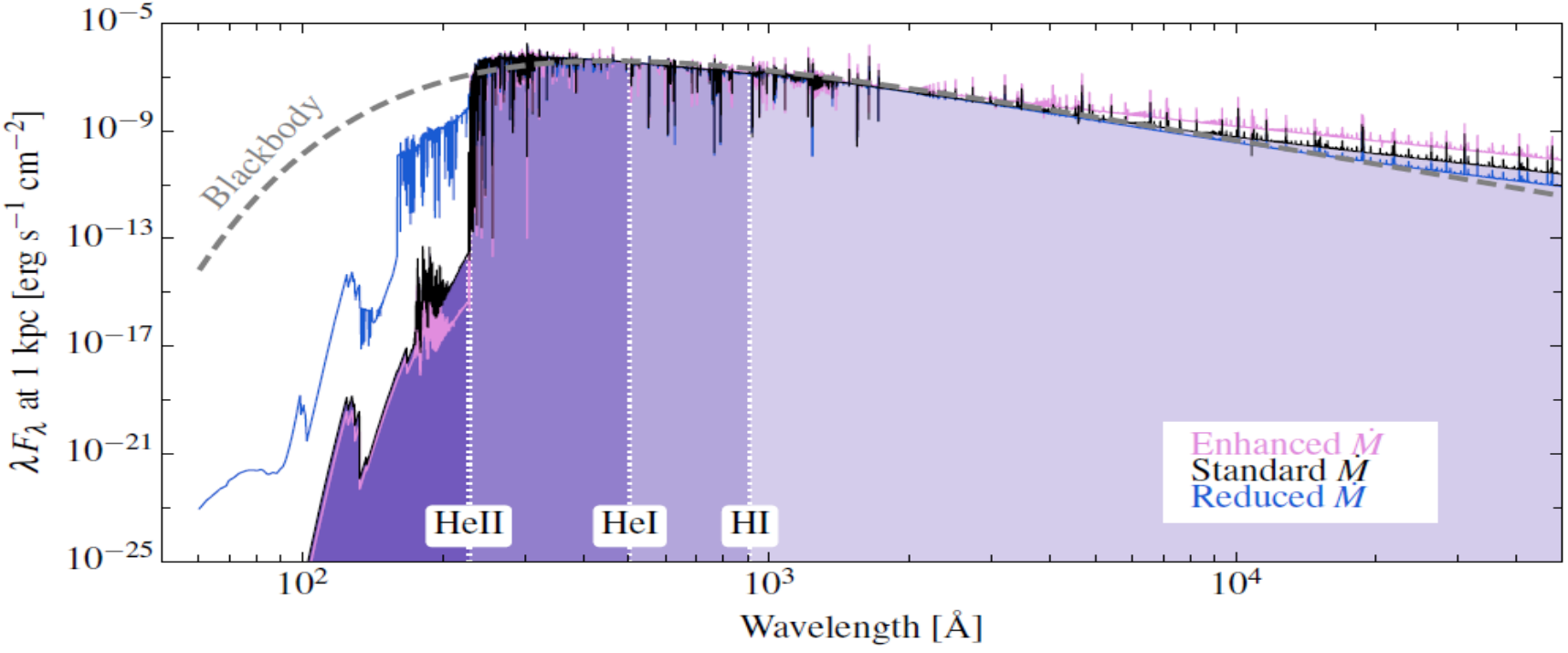

$$\eta = \frac{f_{\rm strip}}{f_{\rm WR,\,60\,M_\odot}} \times \frac{Q_{0,\,\rm strip}}{Q_{0,\rm WR}} \times \frac{\Delta t_{\rm strip}}{\Delta t_{\rm WR}} \times \left(\frac{M_{\rm strip,\,init}}{M_{\rm WR,\,init}}\right)^{-2.35}$$

$$= \frac{0.33}{1.0} \times \frac{1.19 \times 10^{48}\ {\rm s}^{-1}}{2.8 \times 10^{49}\ {\rm s}^{-1}} \times \frac{1.2\ {\rm Myr}}{0.4\ {\rm Myr}} \times \left(\frac{12\ M_\odot}{60\ M_\odot}\right)^{-2.35} \approx 1.8$$

Canonical channels for sdOB formation (Han+ 2002, 2003)

Stable RLOF, CE ejection, merger

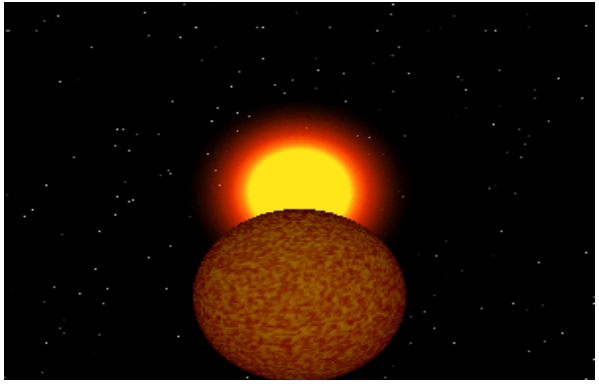

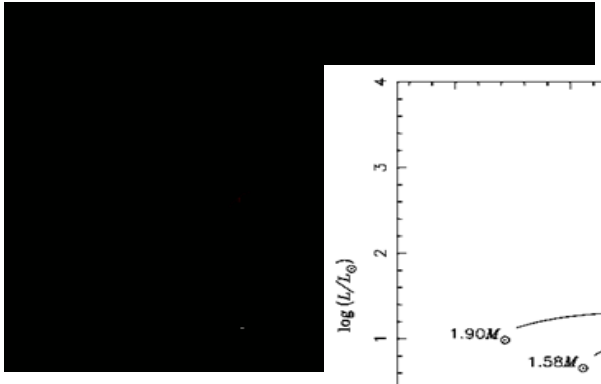

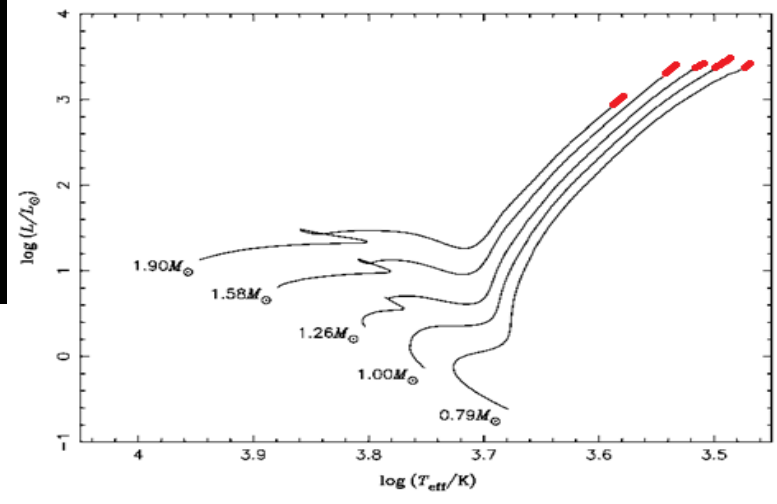

Stable RLOF

During stable RLOF, the donor is Roche-lobe filling.

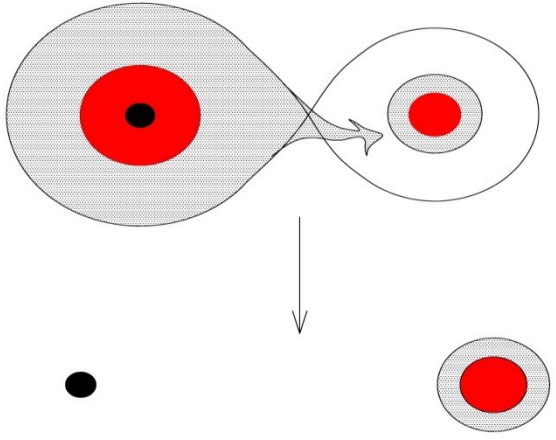

$Mc \rightarrow R, \quad q \rightarrow R_L/A,$
A can be determined，

The RLOF stops when donor's envelope collapses, and we then have a q_f-A relation (Mc is fixed)

The relation does NOT dependent on dJ

To explain the *q*-*A* figure,
we assume that *M*1i=1*M*sun, *R*FGB=0.75AU

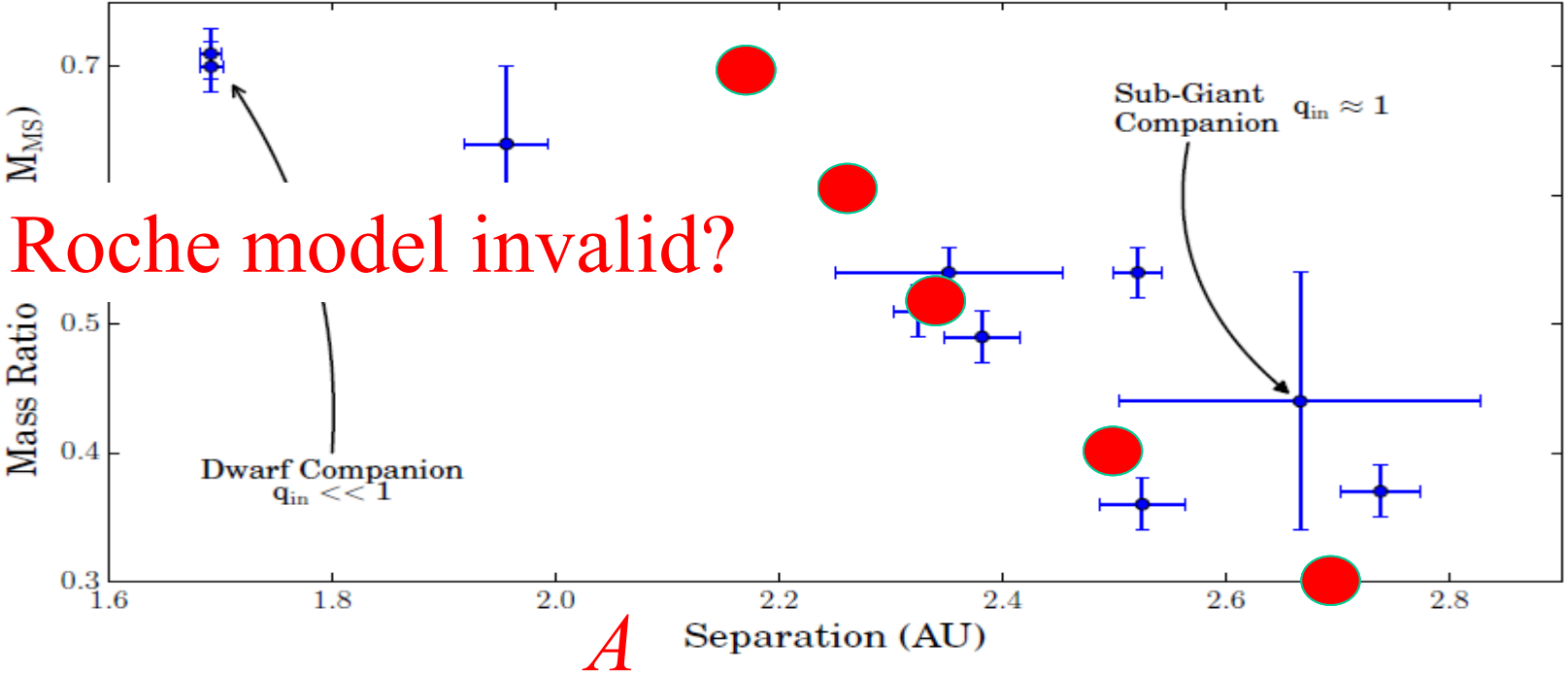

Fig. 2: The separation – mass ratio distribution.

To constrain the stability criterion, q_c ,
we assume that M_{1i}=1Msun, we can derive M_{2i} by assuming 0%, 50%, 100% of the transferred mass is lost from the system during RLOF

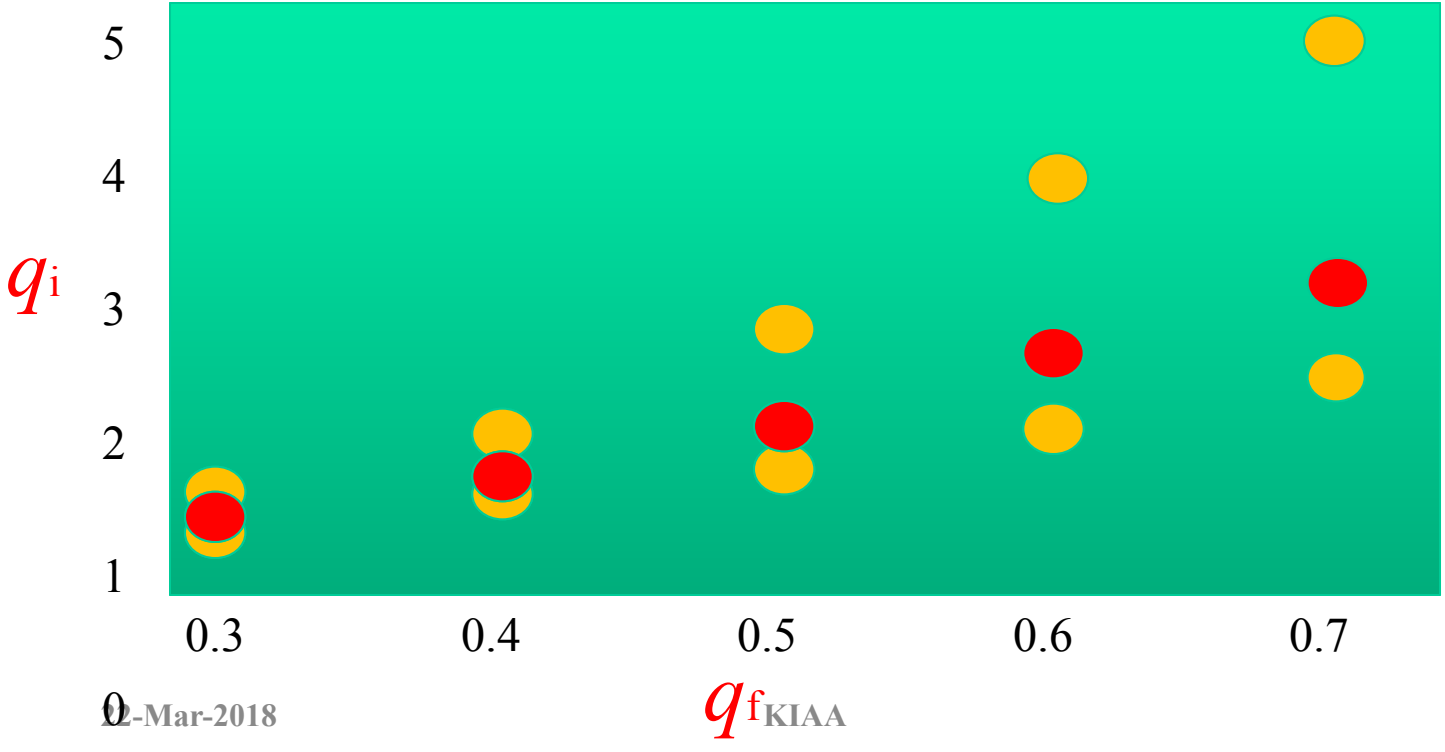

A&A 576, A44 (2015)
DOI: 10.1051/0004-6361/201425213

Astronomy & Astrophysics

Hot subdwarf binaries from the MUCHFUSS project

Analysis of 12 new systems and a study of the short-period binary population⋆

T. Kupfer[1], S. Geier[2], U. Heber[3], R. H. Østensen[4], B. N. Barlow[5], P. F. L. Maxted[6], C. Heuser[3], V. Schaffenroth[3,7], and B. T. Gänsicke[8]

unknown companion

dM companion

WD companion

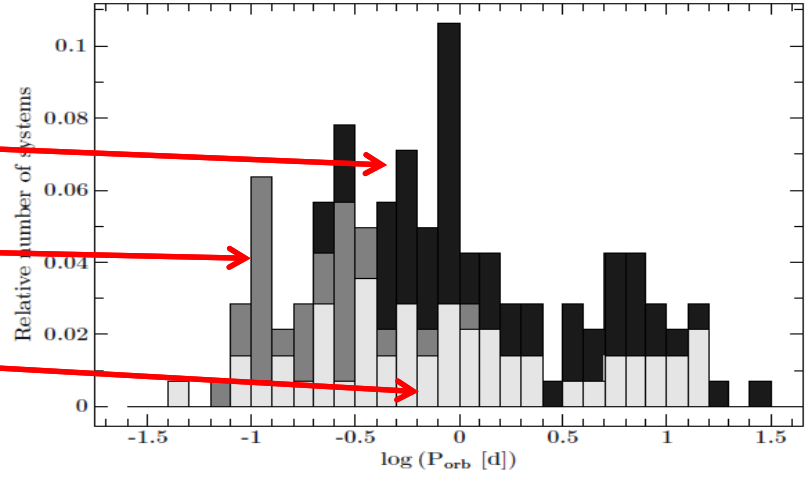

Fig. 7. Period histogram of the full sample. Light grey: WD companions, grey: dM companion, dark grey: unknown companion type.

Chen+, in prep.

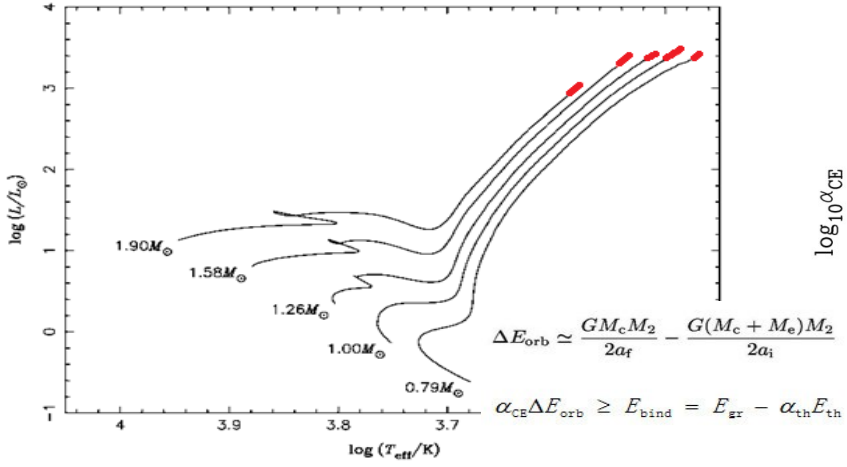

$$\Delta E_{\rm orb} \simeq \frac{GM_{\rm c}M_2}{2a_{\rm f}} - \frac{G(M_{\rm c}+M_{\rm e})M_2}{2a_{\rm i}}$$

$$\alpha_{\rm CE}\Delta E_{\rm orb} \geq E_{\rm bind} = E_{\rm gr} - \alpha_{\rm th}E_{\rm th}$$

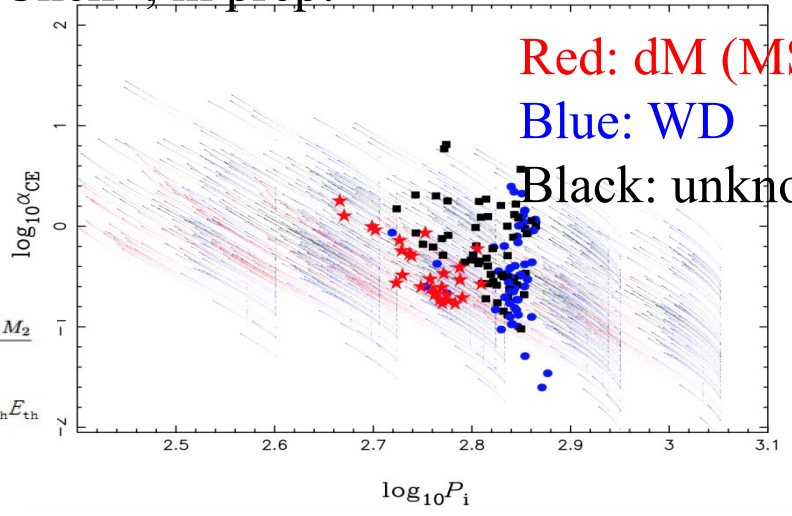

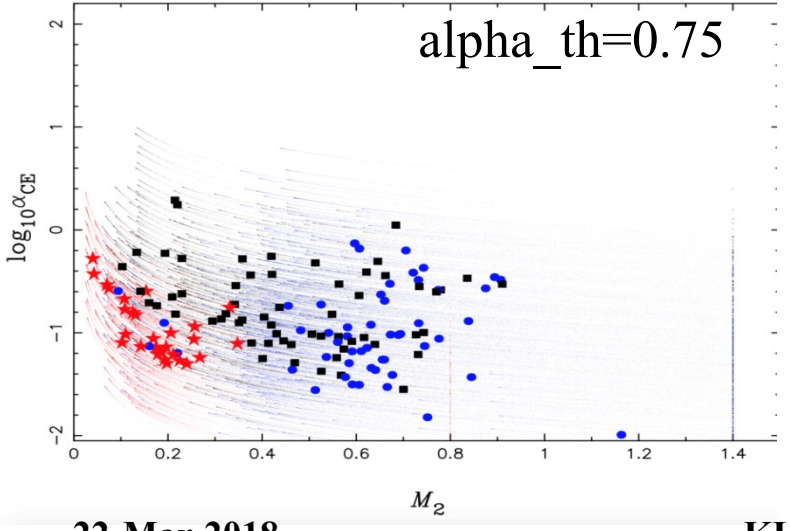

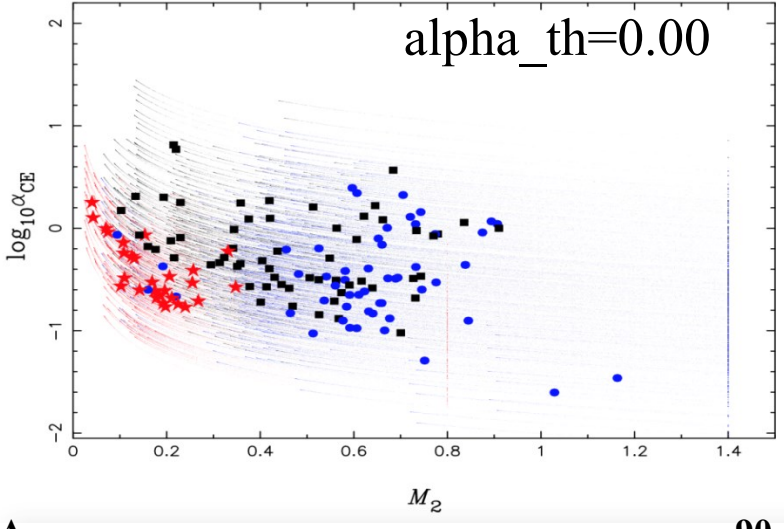

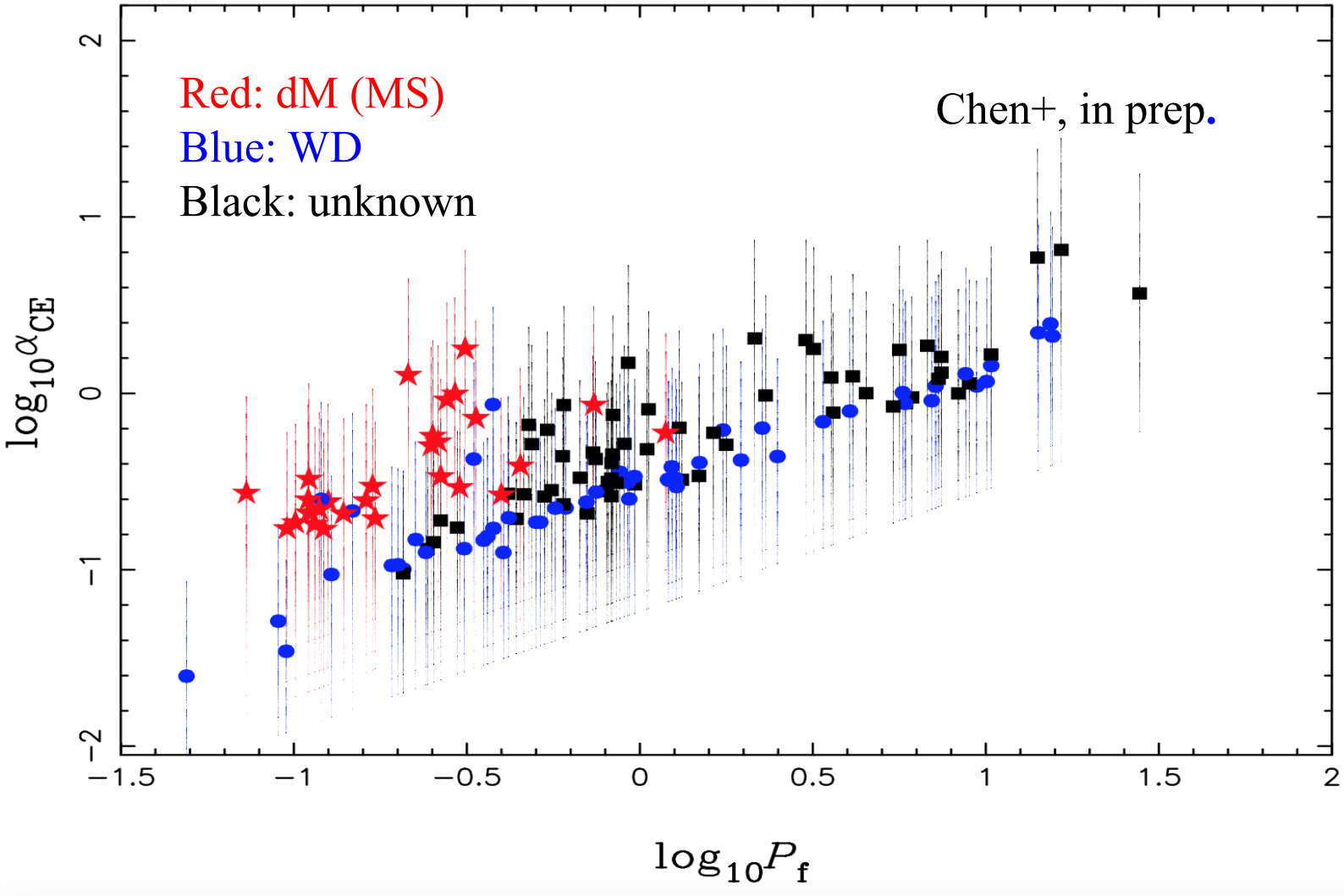
Red: dM (MS)
Blue: WD
Black: unknown
Chen+, in prep.
$\log_{10}\alpha_{\rm CE}$
$\log_{10}P_{\rm f}$
2
1
0
−1
−2
−1.5
−1
−0.5
0
0.5
1
1.5
2